理學博士學位 請求論文

A Dissertation for a Doctor of Philosophy

단백질 티로신 인산가수분해효소1B

억제제로서 barbituric acid

유도체들의 합성과 평가

Synthesis and Evaluation of Barbituric Acid Derivatives as Protein Tyrosine Phosphatase 1B Inhibitors

2012 년 08 월

仁荷大學校 大學院 化學科 (化學專攻)

Department of Chemistry, Graduate School

Inha University

Deegendra Khadka

理學博士學位 請求論文

A Dissertation for a Doctor of Philosophy

단백질 티로신 인산가수분해효소 1B 억제제로서 barbituric acid 유도체들의 합성과 평가

Synthesis and Evaluation of Barbituric Acid Derivatives as Protein Tyrosine Phosphatase 1B Inhibitors

2012 년 08 월

指導敎授 **趙 亨 鎭**

이 論文을 博士學位 論文으로 提出함

仁荷大學校 大學院 化學科 (化學專攻)

Department of Chemistry, Graduate School

Inha University

Deegendra Khadka

이 論文을 Deegendra Khadka 의 博士學位論文으로

認定함

2012 년 08월

주심 ..... 이 건 형 .....(인)

부심 ..... 조 현 진 .....(인)

위원 ..... 소 재 원 .....(인)

위원 ..... 최 은 미 .....(인)

위원 ..... 김 태 현 .....(인)

APPROVAL

I CERTIFY THAT I HAVE READ THIS DISSERTATION AND THAT, IN MY OPINION, IT IS FULLY ADEQUATE IN SCOPE AND QUALITY AS A DISSERTATION FOR THE DEGREE OF DOCTOR OF PHILOSOPHY.

Examining committee

Chairperson: 이 건형

Supervisor: 조 형 진

Member: 소 재 원

Member: 최 은 미

Member: 김 태 현

Date of Approval: **2012/06/27**

This Dissertation Is Dedicated

To

My Parents And Brother

CONTENTS

Appendices

Acknowledgements

In the first place, I would like to record my gratitude to my supervisor Professor HYEONGJIN CHO for his supervisions, advices, and guidances from the very early stage of this research as well as giving me extraordinary experiences throughout the work. Above all and the most needed, he provided me unflinching encouragements and supports in various ways. His truly scientist intuition has made him as a constant oasis of ideas and passions in science, which exceptionally inspire and enrich my growth as a student, a researcher and a scientist want to be. I am indebted to him more than he knows.

Besides my supervisor, I gratefully acknowledge Department of Chemisty, Inha University, Professors of Department of Chemistry, specially, Prof. Lee Keun Hyeung, Prof. Soh Jae Won, Prof. Choi Eun Mi (Incheon University) and Prof. Kim Tae Hyun (Incheon University) for their encouragements, insightful comments and strong questions.

My sincere thanks go to Jungseok International Scholarship, Brain of Korea (BK 21) program and National Research Foundation of Korea (NRFK) for the financial support.

Words fail me to express my appreciation to my family for their unfailing love and supports throughout my life. I am indebted to my late father Kul Bahadur Khadka and late mother Grishma Khadka, maternal and paternal uncles and aunties, brothers (Yogendra, Phadindra and late Gyanendra), sisters (Kalpana, Usha and Kalyani), brothers in law, sisters in law, cousin brothers and sisters and nieces and nephews for their cares and loves.

I would like to acknowledge my senior lab. members Dr. Bhooshan

Kafle for introducing me to this lab and teaching basic but very essential concepts related to chemistry and molecular biology, Dr. Suja Shrestha, Dr. Bharat Raj Bhatatrai and Dr. Nilkantha G. Aher and senior nepali students at Inha University; Dr. Sheila Maskey, Thakur Prasad Subedi, Dr. Sher Bahadur Rawal, Dr. Mrigendra Bir Karmacharya, and friends Dr. Chuda Raj Lohani and Lok Nath Neupane for their unforgettable supports.

It is a pleasure to pay tribute to Dr. Deepak K Khadka, a molecular biologist. His wise suggestions provided such a strange vital energy that really uplifted me from miseries.

Furthermore, my sincere acknowledgements go to Korean, Indian, Chinese, Bangladeshi friends for supporting me in my difficulties.

Finally, I would like to thank everybody who was important to the successful realization of this thesis, as well as expressing my apology that I could not mention personally one by one.

List of Tables

List of Figures

List of Schemes

Schemes

List of Abbreviations

AMPA	α-Amino-3-hydroxy-5-Methyl-4 isoxazole Propionic Acid
CNS	Central nervous system
DFMP	Difluoromethyl phosphate
DIO	Diet induced obese
DUSP	Dual specific phosphatase
DMF	Dimethyl formamide
DMSO	Dimethyl sulfoxide
E. coli	*Escherichia coli*
EDTA	Ethylenediaminetetraacetic acid
ES Complex	Enzyme-substrate complex
GABA	Gamma-aminobutyric acid
^{1}H NMR	Proton nuclear magnetic resonance
Hepes	N-(2-Hydroxyethyl)piperazine-N'-(ethanesulfonic acid)
HeLa cells	Henrietta Lacks cells
HFD	High fat diet

HTS	High-throughput screening
HPV	Human papilloma virus
IBD	Inflammatory bowel disease
IC_{50}	Half maximal inhibitory concentration
IRS	Insulin receptor substrate
IR	Insulin receptor
IZD	Isothiazolidinone
JNK	C-Jun N-terminal kinases
Jak2	Janus kinase 2
LAR	Leukocyte antigen related
LB Medium	Lysogeny broth medium
LepR	Leptin receptor
LB plot	Lineweaver-Burke plot
MAP kinase	Mitogen-activated protein kinase
MKK	Mitogen-activated protein kinase kinase
MES	2-(N-Morpholino)ethanesulfonic acid
oGTT	Oral glucose tolerance test
*p*NPP	*p*- Nitrophenyl phosphate
PTPase	Protein tyrosine phosphatase

PTKase	Protein tyrosine kinase
PKB	Protein kinase B
PI3K	Phosphatidylinositol 3-kinase
PPARγ	Peroxisome proliferator-activated receptor gamma
rpm	Rotations per minute
s, d, t,	Singlet, Doublet, Triplet
q, m, brs,	Quartet, Multiplet, Broad singlet
SH2	Src homology 2
Stat3	Signal transducer and activator of transcription 3
SAPK	Stress activated protein kinase
TLC	Thin layer chromatography
T2DM	Type 2 diabetes mellitus
TC-PTP	T-cell protein tyrosine phosphatase
VHR	Vaccinia virus H1 related
YPTP	Yeast protein tyrosine phosphatase

Abstract

Rapid increase of obesity and diabetes in modern society increases the risk of other complications, such as cardiovascular diseases, blindness, renal failure and even cancer. Orlistat is the only drug approved currently by the US Food and Drug Administration (FDA) for the treatment of obesity. Other drugs previously approved were suspended due to side effects. Sulfonylureas, thiazolidinediones, and meglitinides are available in the market as the drugs for type 2 diabetes mellitus but they are not kept a distance from side effects. Science communities have been focusing attention on the development of novel drugs that are safer and more efficient in treating obesity and diabetes. Protein tyrosine phosphatase1B (PTP1B) is an enzyme closely related with these diseases. PTP1B is a negative regulator of leptin and insulin signaling pathways. Genetic deletion of PTP1B in mice improved both leptin and insulin signaling, resulting in the resistance to diet-induced obesity and the enhancement of insulin sensitivity and glucose tolerance. The enhancement of leptin signaling reduced food intake and increased energy expenditure, resulting in weight loss in mammals. Increased PTP1B expression has also been observed in insulin-resistant states associated with obesity. These results established PTP1B as a target for the treatment of both obesity and type 2 diabetes.

The aim of this research is to develop low molecular weight inhibitors of PTP1B which have a good inhibitory potency, selectivity and favorable pharmacokinetics for the development of antidiabetic and antiobesity drugs. Barbituric acid was selected as a scaffold for the derivatization. A series of derivatives containing a single substitutuent were synthesized and their efficacy to inhibit PTP1B activity was determined. The most potent compound **II-5e** showed IC_{50} of 11 μM against PTP1B and 27 μM against VHR. The

nature of inhibition by compound **II-5e** was investigated by steady-state kinetic experiments with PTP1B, VHR and YPTP1. When the mode of inhibition was examined by the Lineweaver-Burk plot analysis of the kinetic experiments, **II-5e** inhibited PTP1B and YPTP1 noncompetitively and VHR competitively.

초 록

현대 사회에서의 비만과 당뇨의 급속한 증가는 심장질환, 시력상실, 신장질환, 심지어 암과 같은 다른 질병의 발생 가능성을 증가시킨다. 현재 미국 식품의약품청에 의해 비만치료제로 허가된 약품은 올리스탓이 유일하다. 과거에 허가되었던 약들은 부작용 때문에 취소되었다. 설포닐우레아, 싸이아졸리딘다이온, 메글리티나이드는 2형 당뇨의 치료제들인데 이들의 경우에도 부작용이 존재한다. 과학계는 비만과 당뇨 치료를 위해 더 안전하고 효과적인 약품을 개발하는데 관심을 기울이고 있다. 단백질 티로신 가수분해효소 1B (PTP1B)는 이 질병들과 밀접하게 연관된 효소이다. PTP1B는 렙틴 및 인슐린 신호전달과정을 억제하는 작용을 한다. 생쥐에서 PTP1B 유전자를 제거하면 렙틴 및 인슐린 신호전달과정이 개선되어, 식이유발 비만에 대한 저항성과 인슐린 민감성 및 글루코오스 내성이 증가한다. 렙틴 신호전달과정의 증진되면 음식섭취가 감소하고 에너지 소모가 증가하여 포유동물에서 체중이 감소하게 된다. PTP1B 발현이 증가하면 비만과 관련된 인슐린저항성이 발생한다. 이 결과들을 바탕으로 PTP1B는 비만과 2형 당뇨 치료의 표적이 될 수 있다는 사실이 확립되었다.

본 연구의 목적은 PTP1B에 대한 새로운 저분자량 억제제 개발이다. 이들은 억제활성이 좋고, 선택성이 있어야 하며 약으로 개발하기 위한 특성들을 갖추어야 한다. 바비츄릭산을 기본 구조로 하여 단일 치환체를 가지는 유도체들을 제조하여 이들의 PTP1B 억제활성을 측정하였다. 가장 억제활성이 큰 화합물 **II-5e** 은 PTP1B에 대하여 IC_{50} 값이 11 μM 이었고 VHR에 대해서는 27 μM

이었다. 화합물 II-5e에 의한 억제의 특성을 PTP1B, VHR, YPTP1의 세 효소들에 대해 정류상태 반응속도 실험을 통해 연구하였다. 반응속도 실험 결과를 라인위버-버크 도시 방법으로 분석한 결과 II-5e는 PTP1B와 YPTP1를 비경쟁적으로, VHR는 경쟁적으로 억제하였다.

CHAPTER I

1. General Introduction

1.1. Phosphorylation

1.1.1. Reversible Phosphorylation

In both prokaryotic and eukaryotic organisms, reversible phosphorylation is indispensible because of its regulatory mechanism in a myriad of cellular functions.[1] Contribution of kinases (phosphorylation) and phosphatases (dephosphorylation) makes this processes balanced. Many enzymes and receptors are activated or deactived by the conformational changes in their structure induced by reversible phosphorylation. Addition of phosphate moieties to side chains of amino acid residues makes significant changes in local charge and hydrophilicity of proteins.

1.1.2. Types of Phosphorylation

Phosphorylation usually occurs on serine, threonine, tyrosine and histidine residues in eukaryotic proteins. Histidine phosphorylation of proteins appears to be much more frequent than tyrosine phosphorylation in eukaryotic cell.[2] In prokaryotes, protein phosphorylation occurs on serine, threonine, tyrosine, histidine, arginine, and lysine residues.[3,4] Histidine and aspartate phosphorylations occur in prokaryotes as part of two-component signaling and in some cases in eukaryotes in some signal transduction pathways.[4]

1.1.3. Importance of PTKases and PTPases

Reversible phosphorylation controls a diverse of cellular functions including cell growth, tissue differentiation, mitogenesis, gene transcription,

inter and intracellular communications.[5] Kinases and phosphatases are mutual partners in regulating signaling responses; kinases often control the amplitude of a signaling response, and phosphatases play a role in controlling the duration of response.[6] Among them, protein tyrosine kinases (PTKases) and protein tyrosine phosphatases (PTPases) are often considered more critical in signaling pathways because they are in most cases involved in the upstream of the pathways. Protein tyrosine phosphorylation can create novel recognition motifs for protein interactions and cellular localization, affects protein stability, and regulates enzyme activity. Proper control of phosphotyrosine (pTyr) phosphorylation is critical for maintaining cellular functions. Above all, abnormal functionalities of PTKases and PTPases are associated with numerous diseases in human.

1.2. Protein Tyrosine Phosphatases

All together 107 PTPase genes were identified in human genome, and 81 of them was known to encode active phosphatases.[7] All the PTPases are characterized by a conserved active site sequence $(H/V)C(X)_5R(S/T)$, termed as PTPase signature motif, in which the cysteine residue functions as a nucleophile and is essential for catalysis.[8]

1.2.1. Diverse Family of PTPases

Most of the PTPases have approximately 250 amino acid long catalytic domain which is also a characterization of PTPases. PTPases can be divided into three subfamilies; classical tyrosine-specific PTPases, dual-specific PTPases and low molecular weight PTPases.[9,10] Compared to the other two PTPases which are specific to pTyr residues, dual-specific PTPases (DUSPases) are capable of dephosphorylating phosphoserine (pSer) and phosphothreonine (pThr) residues as well as pTyr residues. Tyrosine-

specific PTPases can be further divided into two groups: transmembrane receptor-like and cytosolic PTPases (Figure **I-1**). Receptor-like PTPases (RPTPases) have an extracellular putative ligand-binding domain, a single transmembrane segment, and a cytoplasmic domain. The cytosolic domain contains one or, less frequently, two catalytic domains.

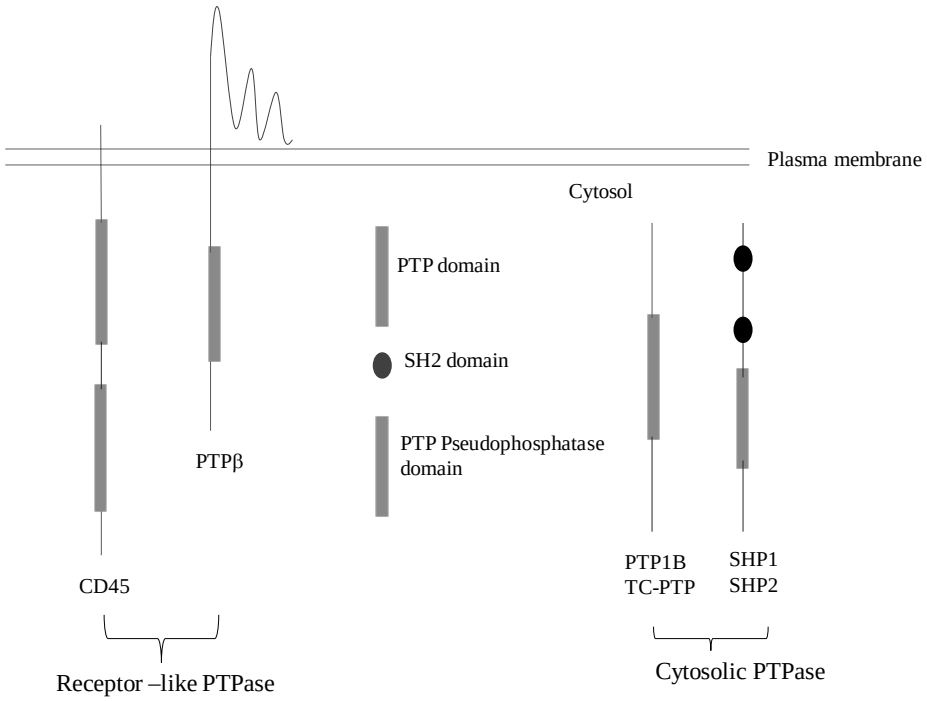

Figure I-1: Diverse family of PTPase

On the other hand, cytosolic PTPases contain single catalytic domain and additional flanking regions with roles in regulation of catalytic activity, protein-protein interactions and subcellular targeting.[11]

1.2.2 PTPases as Potential Targets for Human Diseases

About 4% of 'druggable genome' is thought to be phosphatases. Among those, numerous PTPases are implicated in a variety of human diseases (**Table I-1**).

Table I-1 Examples of PTPases as Potential Therapeutic Targets

Human Diseases	PTPases
Obesity and diabetes	PTP1B [7]
Infectious diseases	SHP-1, SHP-2 [12, 13]
Autoimmune diseases	CD45[14]
Cancer	PTP- α, PTP- ε, Prl-3, Cdc25[15, 16]
Inflammation	PTP-β (VE-PTP), PTP- ε [17]
Neurodegeneration	PTP 1B, PTP- σ [18,19]
Osteoporosis	GLEPP-1 (PTP-oc), PTP- ε [20, 21]

1.2.3 Catalytic Mechanism of PTPases

The cleft in the active site of PTPases is surrounded by four loops, which contain residues essential for catalysis and substrate recognition. The cleft depth ensures the specificity towards pTyr by preventing the shorter side chain of pSer and pThr residues reach the bottom of the cleft.[22]

The role of cysteine is critical in the catalytic mechanism of PTPases. The cysteine residue takes phosphate moiety from pTyr residues and forms a phosphocysteine intermediate. The latter is then hydrolyzed to release water molecule and to form free cysteine for another cycle of catalysis. As such, the common catalytic mechanism by PTPases involves two steps. Details are described in **1.3.2.**

1.3. Protein Tyrosine Phosphatase 1B

Protein-tyrosine phosphatase 1B (PTP1B) is a founding member of the PTPase family. In humans, it is encoded by the *PTPN1* gene. PTP1B is a negative regulator of the insulin signaling pathway and is considered as a

promising potential therapeutic target for the treatment of type 2 diabetes.

1.3.1. Structure of PTP1B

PTP1B is a 50 kD protein which is the first PTPase to be isolated in a pure form from human placental tissue.[23] PTP1B is a cytosolic PTPase and composed of 435 amino acids. The catalytic domain contains 249 amino acid residues (amino acid number 30-278) and the 35 carboxyl terminus residues target the enzyme to the cytosolic face of the endoplasmic reticulum.[24] The structure of PTP1B was first elucidated as a tungstate ion bound form by X-ray crystallography in 1994.[25] PTP1B has the most, if not all, of the conserved structural features that are common to classical PTPases. Catalytic active site, the WPD loop and the P-loop are the main structural features of PTP1B.

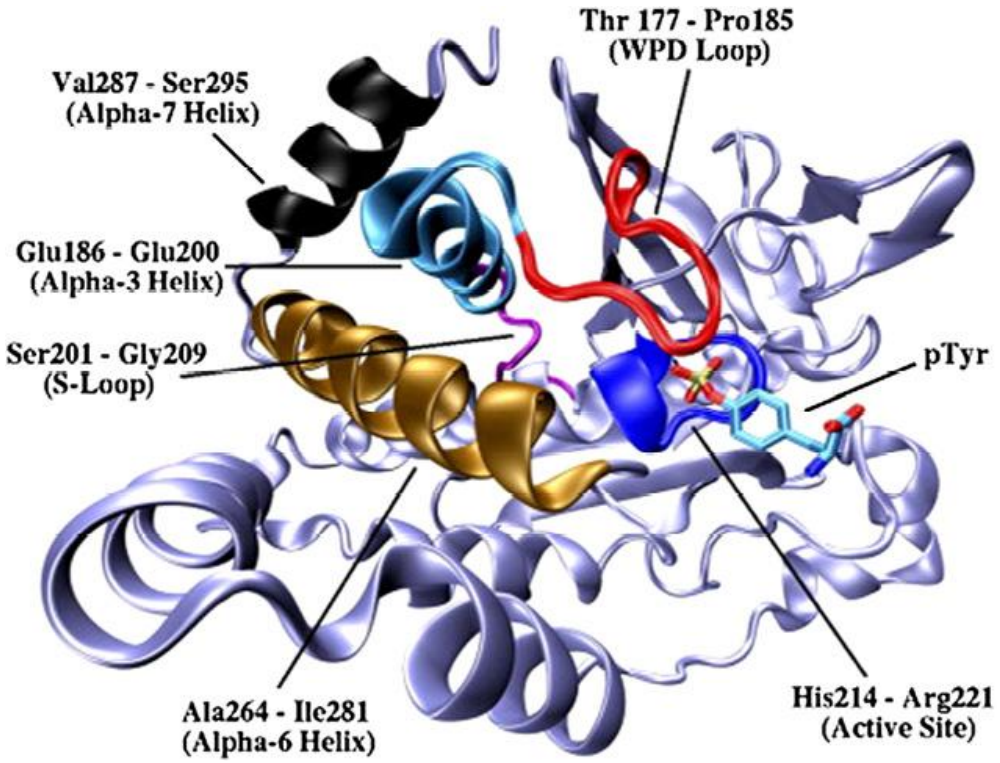

Figure I-2: Structural Features of PTP1B. The active site His214–Arg221 lies within the pTyr substrate binding pocket. The essential reduced Cys215 lies within this sequence. The WPD loop is a flexible region which is in an 'open' conformation in the absence of substrate and closes once the pTyr substrate binds. Closure is required for catalysis, and a hydrogen bond appears to form between the amino acids Trp179 in the WPD loop and Arg221 in the active site. Inhibitors which reduce the mobility of the WPD loop may block substrate binding and/or decrease catalytic activity. The S-loop, Ser201–Gly209, also influences WPD loop mobility and may itself also be inhibited by inhibitor binding.[26]

Active site: A loop of eight amino acid residues from 214-221 forms the active site of PTP1B (P-loop, His-Cys-Ser-Ala-Gly-Ile-Gly-Arg). The loop forming cradle-like structured coordinates to the aryl-phosphate moiety of the substrate and contains the catalytic Cys215. Nucleophilic attack of Cys215 results in cleavage of the P-O bond and formation of a phosphocysteine intermediate which is hydrolyzed to give the final products. Asp181, Phe182, Tyr46, Val49, Lys120 and Gln262 form the sides of the catalytic cleft assist catalysis and structure recognition. The active site is located within a crevice (8-9 Å) on the protein surface. The much deeper active site pocket in the PTPases selects exclusively pTyr-containing substrates[22,27] while the shallower active site cleft for the dual specificity phosphatases (DUSP) may accommodate both pTyr and pSer/pThr.[28,29]

Second aryl-phosphate-binding site: Second aryl-phosphate-binding site is located just next to the catalytic site on PTP1B.[30] The second site is catalytically inactive, and provides weaker binding interactions compared with the primary site. Nevertheless, it has important implications

for inhibitor design. It opens the possibility of using the strategy of finding molecules that bind to each site independently, then linking them together to get more potent inhibitors.[31]

The WPD loop: The WPD loop (amino acid residue numbers 79–187) moves up to 12 Å to close down on the phenyl ring of the substrate, which maximizes hydrophobic interactions. Asp181 moves into a position where it can act as a general acid to protonate the tyrosyl leaving group. Arg221 also reorientates into a position to optimize salt-bridge interactions with the substrate phosphate. In this conformation, Cys215 is in a position to undergo a nucleophilic attack on the substrate phosphorous atom. As there are two conformations of PTP1B (open and closed) inhibitors could be designed to target either conformation.[32]

1.3.2. Catalytic Mechanism of PTP1B

A. Formation of Cysteinyl-phosphate Intermediate

The catalytic cysteine residue makes a nucleophilic attack on the phosphate moiety resulting in a cysteinyl-phosphate intermediate. Protonated form of an invariant aspartic acid in the flexible loop acts as a general acid catalyst providing a proton to the leaving phenolic group of the substrate.

B. Hydrolysis of Cysteinyl-phosphate Intermediate

The same aspartic acid in step A now acts as a general base by abstracting a proton from the water molecule in the active site for the hydrolysis of cysteinyl-phosphate intermediate. In this step, a hydrogen bond between Ser222 and the Cys215 compensates the negative charge developing on the S atom of the cysteine.

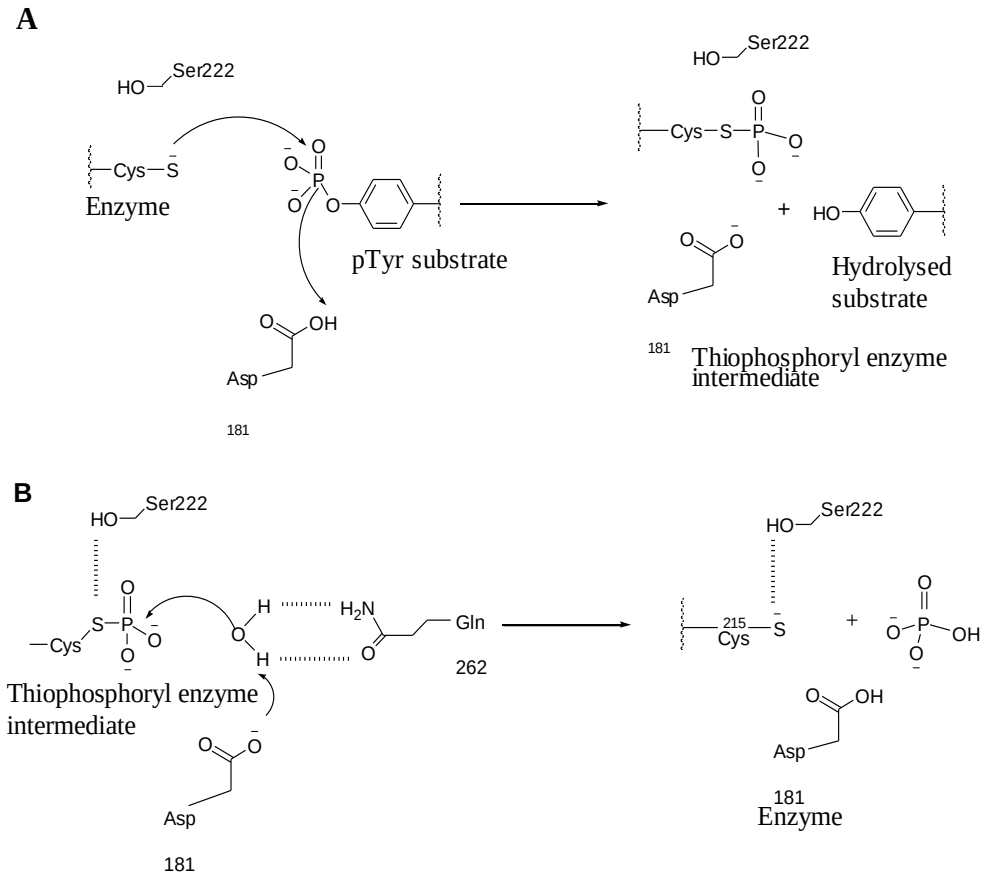

Figure I-3: Catalytic Mechanism of PTP1B.

1.3.3. PTP1B as a Negative Regulator in Insulin Signaling

The insulin receptor is a transmembrane receptor that is activated by insulin.[34] Two alpha subunits and two beta subunits make up the insulin receptor. The alpha subunits are involved in ligand binding while the two intracellular tyrosine kinase beta-subunits participate in transducing the signal into the cell. The alpha subunits are linked by disulphide bonds to the beta subunits.[34,35] Activation of the insulin receptor (IR) after ligand binding is a multi-step process involving structural changes in both the ligand and the receptor. The binding of insulin to IR results in autophosphorylation of the receptor on a number of crucial tyrosine residues. This causes activation of

the insulin receptor tyrosine kinase, followed by phosphorylation of various insulin receptor substrate (IRS) proteins to propagate the insulin-signaling event further downstream and mediate various biological effects. The phosphorylation on tyrosine residues in IR and IRS proteins develops docking sites for other enzymes and effector molecules containing SH2 or phosphotyrosine-binding (PTB) domains to propagate insulin signal.[35,36]

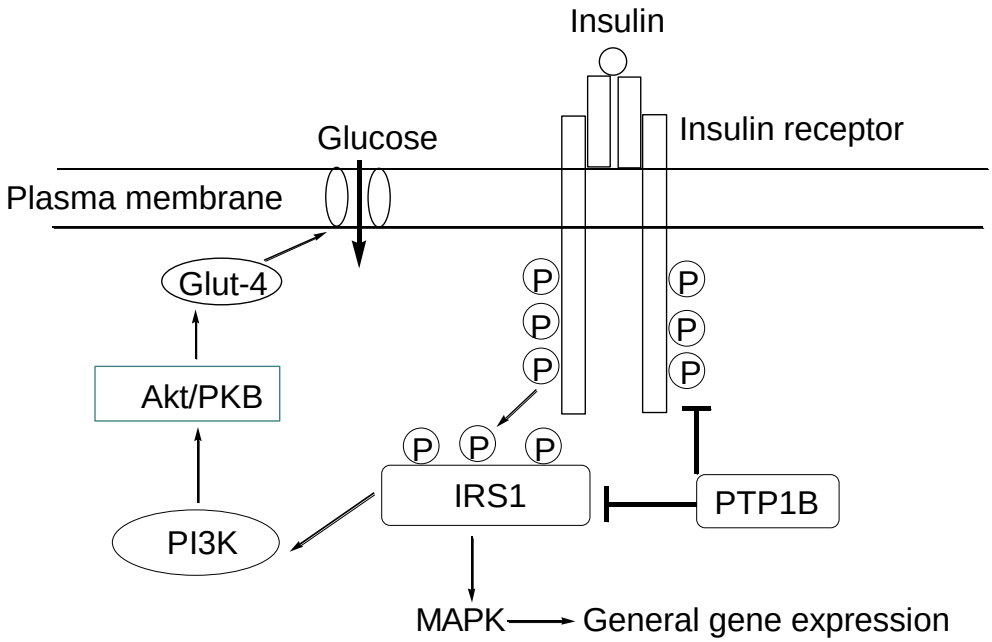

Figure I-4: View of the Role of PTP1B in Metabolic Insulin Signaling Pathway. IRS1: Insulin receptor substrate 1; PI3K: phosphatidylinositol 3-kinase; PKB: Protein kinase B; MAPK: Mitogen-activated protein kinase.

Insulin signaling is known to be attenuated through dephosphorylation by PTPases. Among those, PTP1B is a key player that negatively regulates insulin signaling. Several *in vivo* and *in vitro* experiments revealed the relationship of PTP1B and insulin receptor.[37,38]

Insulin stimulates cells to take up glucose and store it as glycogen,

and to inhibit hepatic glucose production. The effect of PTP1B on the metabolic arm of the insulin signaling pathway is thought to be mediated upstream of phosphatidylinositol 3-kinase (PI3K)[38,39] and is capable of interacting with and removing tyrosine phosphates from both IR and IRS proteins.[37,40,41] The schematic view of role of PTP1B in metabolic insulin signaling pathway is represented in **Figure I-4**.

At the cellular level, insulin resistance is manifested either as reduced capacity or reduced sensitivity to promote glucose transport and metabolism.[42] The mice lacking PTP1B gene have enhanced insulin sensitivity and are resistant to diet–induced obesity.[43] In addition, several studies have depicted that increased expression of PTP1B results in insulin-resistant states associated with obesity. The insulin resistance observed in type 2 diabetes and obesity is due to the disequilibrium in enzyme activity between IR and PTPases.[24,42] As a fascinating phosphatase for the treatment of obesity and type 2 diabetes, PTP1B has been a subject of keen interest to the researchers for numerous screenings and development of specific inhibitors.

1.3.4. PTP1B Functions as a Negative Regulator of Leptin Signaling

Leptin is a 16 kD protein hormone that plays a key role in regulating energy intake and energy expenditure, including appetite and metabolism. It is one of the most important adipose derived hormones. It is produced in white adipose tissue throughout the body, including epididymal, parametrical, perirenal and inguinal but lesser extent in brown adipose tissue.[44] Hypothalamus is known as the primary site of action of leptin where it signals to inhibit feeding.[45] Leptin receptor (LepR) is a type I cytokine receptor that associates with Jak2.[46] Upon leptin binding, Jak2 becomes activated and phosphorylates itself and LepR. LepR then recruits signal relay

molecules such as Stat3.[47] The transcription of target genes is regulated when tyrosylphosphorylated Stat3 is dimerised and translocated into the nucleus.

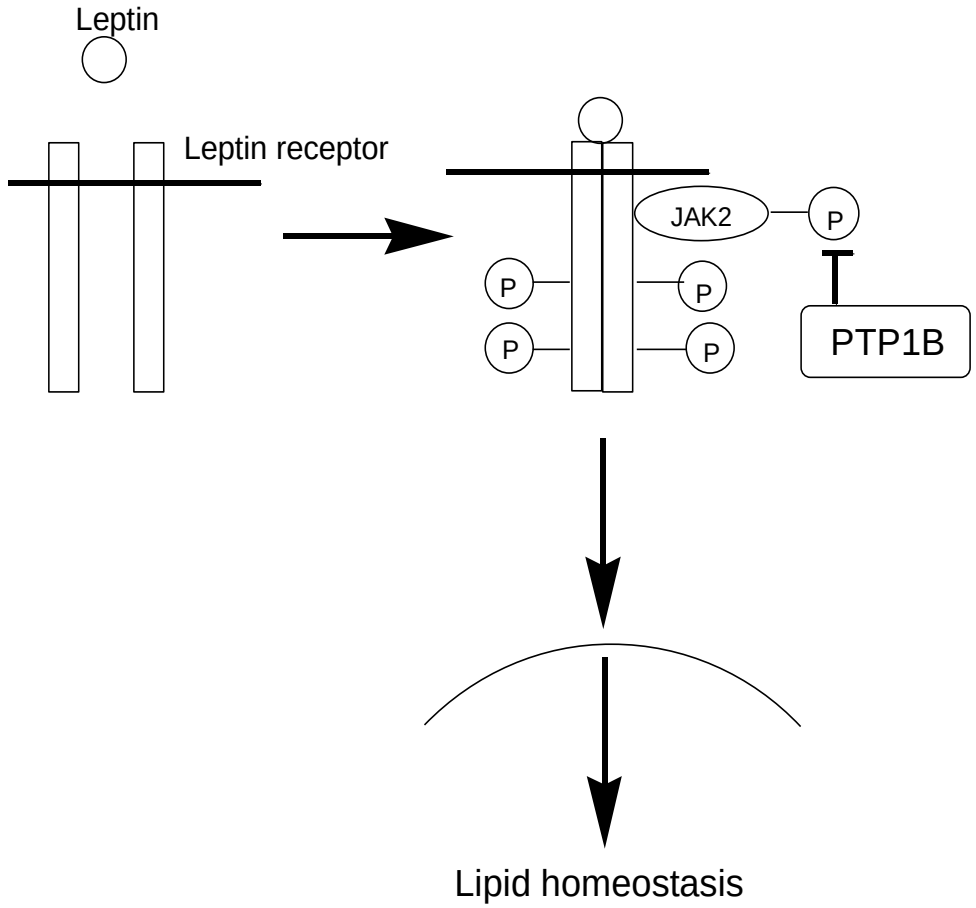

Figure I-5: View of Role of PTP1B in Leptin Signaling Pathway. JAK2: Janus kinase 2.

An important cause of obesity is improper leptin signaling which would ultimately results in leptin resistance. Leptin levels acutely depend on feeding. Leptin cuts food intake, heightens energy expenditure and thus results in weight loss in mammals. Chronic intake of high fat diets without compensatory increase in energy expenditure causes obesity. Treatment of leptin deficient mice with leptin significantly reduces food intake and body

weight gain and corrects metabolic defects. Mice with mutations of the leptin receptor genes have elevated levels of circulating leptin and experience hyerphagia and obesity.

Dephosphorylation of Jak2 by PTP1B blocks the phosphorylation of LepR and Stat3. Dephosphorylated form of Stat3 is unable to exert transcriptional control over its target genes. It is widely known that PTP1B knockout mice display resistance to high fat diet-induced obesity. This could be due to increased energy expenditure.[44] PTP1B deficient mice show enhanced sensitivity for exogenous leptin to suppress food intake.[48] Inhibitors of PTP1B augment the beneficial effects of leptin on food intake, body weight regulation and metabolism in normal and leptin resistant individuals. These observations indicate that PTP1B is a potential target for the prevention of obesity. PTP1B action in leptin signaling pathway is depicted in **Figure I-5**.

1.3.5. PTP1B is a Potential Target for the Treatment of Obesity and Type 2 Diabetes

Solely in the United States, nearly 3 hundred thousand individuals die per year because of obesity and most of these deaths are due to the effect of obesity promoting diseases like hypertension, cardiovascular disease and varieties of cancer.[49] In 2003, 194 million populations were diagnosed with diabetes worldwide and assumed to extend up to 333 million by 2025.[50] Ninety percent of diabetic patients are victims of type 2 diabetes (T2DM) caused by a disturbance in insulin signaling. In medical field, obesity is defined as a condition of gaining body weight by depositing adipose tissues. Deposition of adipose tissues creates type 2 diabetes,[51-54] hypertension,[54] coronary heart disease,[55] certain type of cancer,[56] bone joint disease,[57] sleep apnea,[58] nonalcoholic fatty liver disease,[59] and psychological problems.[60]

However, both diabetes and obesity are currently difficult to cure completely. Thus, a research associating obesity is important to relieve a large population from a health calamity.

Biological role of PTP1B as a regulator of body weight and glucose homeostasis was studied by genetic ablation of PTP1B in mice and the experiments with the PTP1B-knockout mice established the rationale for PTP1B inhibition as one of the therapeutic target for obesity and diabetes. Both homozygotic ($PTP1B^{-/-}$) and heterozgyotic ($PTP1B^{+/-}$) mice were born and grew healthy reducing the worry for the toxicity.[61] PTP1B knockout mice exhibited enhanced insulin sensitivity in skeletal muscle and liver, and resistance to diet induced obesity.[43,44] Genetic deletion of PTP1B in mice did not affect normal development, fertility, and the risk of cancer. This result was surprising because PTP1B is expressed in all tissues and controls a number of growth factor signaling pathways. Excessive energy obtained by PTP1B-deficient mice was apparently dissipated as heat, rather than being stored as fat. The lower metabolic efficiency was not due to the increase of UCP expression, a most common mechanism of heat production. In PTP1B-deficient mice, leptin levels in serum were maintained low, consistent with their decreased adiposity. Interestingly, $PTPB^{-/-}$ mice on a HFD had leptin levels much lower than those of the wild type control on a chow diet. In addition to the resistance to diet-induced obesity, enhanced insulin sensitivity was observed in $PTP1B^{-/-}$ mice, but not in $PTP1B^{+/-}$ mice.

Numerous companies and academic laboratories have been working to develop a potent cell permeable inhibitor for the control of obesity and type 2 diabetes.

1.4. PTP1B Inhibitors

Among PTPases, PTP1B is the most exploited phosphatase as a drug target. Numerous screening and structural studies were carried out to develop specific PTP1B inhibitors. There are two major hurdles in the development of PTP1B inhibitors as drugs;

1) Highly conserved active site and

2) The regulation of multiple signaling pathways by a single PTPase as well as the regulation of single pathway by diverse PTPases.

To defeat aforementioned difficulties, different research groups tried to find additional structural features of PTPases.

1.4.1. PTP1B Inhibitors Reported in Literature

1.4.1.1. Vanadium-Based PTP1B Inhibitors

Vanadium (VO_4^{-3}) in a proper oxidation state acts as a non specific phosphatase inhibitor. Vanadium-containing compound[62,63] has been shown in human clinical trials to be potentially useful for treating insulin and non insulin-dependent diabetes mellitus.[64,65] Bis(maltolate) oxovanadium (IV) compound **I-1** has been reported as a potent PTP1B inhibitor with a blood glucose lowering effect in diabetic animal models.[66] For the vanadium-based inhibitors to be used as therapeutic agents, improvements should be made in their selectivity, bioavailability and toxicity. [67]

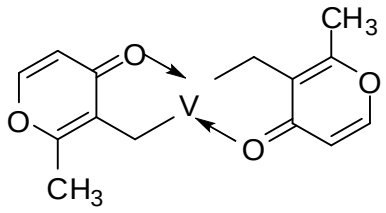

I-1

1.4.1.2 Natural Products and Their Derivatives as PTP1B Inhibitors

Some of the natural products acting as PTP1B inhibitors are shown below.

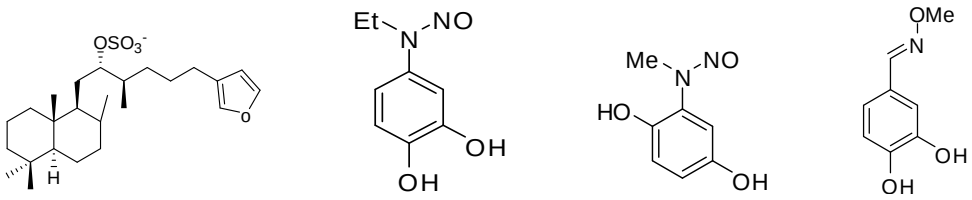

I-2 **I-3** **I-4** **I-5**

Figure I-6: Natural Products as PTP1B Inhibitors

Table I-2. IC_{50} of Natural Products Inhibitors of PTP1B [67]

Compound No.	IC_{50} (μM)
I-2	29.8
I-3	~580
I-4	580
I-5	5800

Sulfircin **I-2,** a compound isolated from water sponge is a moderate inhibitor against PTP1B as well as other PTPases (VHR, cdc25A) with slightly better potencies.[68]

1.4.1.3. DFMP-containing Peptides as PTP1B Inhibitors

Zhang *et al.* reported a highly potent (Ki = 2.4 nM for PTP1B) and selective (10-fold selectivity over TC-PTP) peptide **I-6** with two DFMP moieties.[30] Even being a highly potent inhibitor, the bis-anionic DFMP compounds exhibit poor physiochemical properties like low oral bioavailability and poor cell permeability.

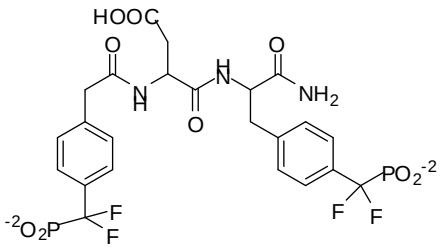

I-6

Figure I-7: Peptide-based PTP1B Inhibitor Containing Two DFMP Moieties

1.4.1.4. Nonhydrolyzable pTyr Mimics

Research has been emphasized on the development of non-peptide low molecular weight inhibitors than the peptide backbone. The peptide backbone inhibitors are inadequate for the development of effective drugs due to lack of bioavailability and cell permeability.[30] Typical nonhydrolyzable pTyr mimetics used in PTP1B inhibitors are described below.

1.4.1.4.1. DFMP as pTyr Mimics

DFMP-containing PTP1B inhibitors were reported by Merck Frosst, including napthyl **I-7** (IC_{50} = 120 nM), benzotriazole **I-8** (IC_{50} = 5 nM) and aryketone **I-9 (**IC_{50} = 120 nM).[69-71] Compound **I-7** and **I-9** exhibited an antidiabetic effect in an oral glucose tolerance test (oGTT) with diet induced obese (DIO) mice. These inhibitors revealed the modest degree of cell permeability and oral bioavailability in rodents.

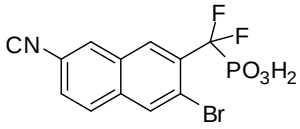

I-7

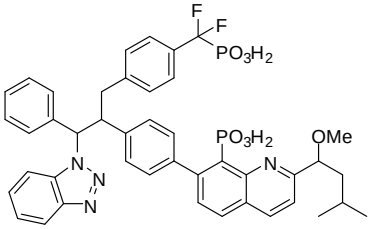

I-8

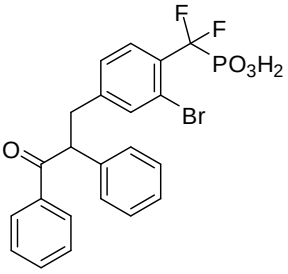

I-9

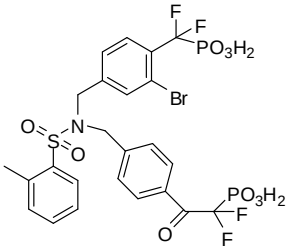

I-10

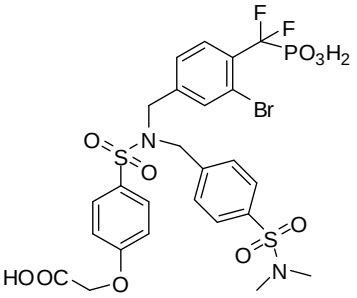

I-11

Figure I-8: Nonhydrolyzable DFMP as pTyr Mimics

A ketophosphonate scaffold as in **I-10** (IC_{50} = 600 nM) and a sulfonamide scaffold as in **I-11** were also reported as PTP1B inhibitors[72] without the selectivity data.

1.4.1.4.2. Sulfamic Acid as a Phosphate Mimic

A high throughput screening (HTS) identified a sulfamic acid compound as a pTyr mimic. On optimization these compounds showed extremely good inhibitory potency against PTP1B but the membrane permeability was not reported.

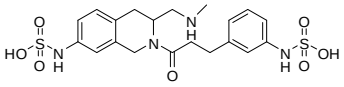

I-12

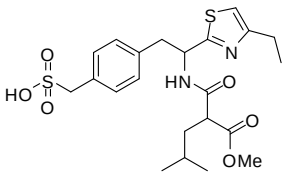

I-13

Figure I-9: Sulfamic Acid as a Phosphate Mimic

Table I-3. IC_{50} of Some Sulfamic Acid Phosphate Mimic

Compound No.	IC_{50} (μM)		PTP1B Selectivity over TC-PTP	Research group
	PTP1B	TC-PTP		
I-12	4.8	9.4	1.9	Proct.&Gamble[73]
I-13	0.007	NA	NA	Proct.& Gamble[74]

1.4.1.4.3. Carboxylic Acid as a Phosphate Mimic

PTP1B inhibitors containing dicarboxylic acid were reported potent but poorly cell permeable. Some of the examples are shown below.

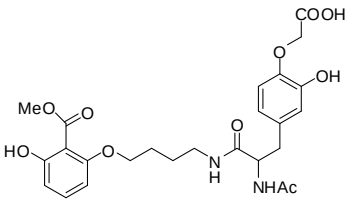

I-14

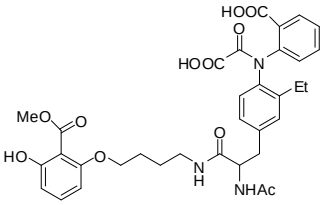

I-15

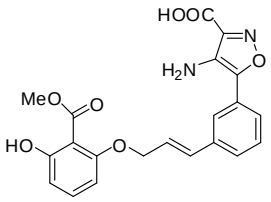

I-16

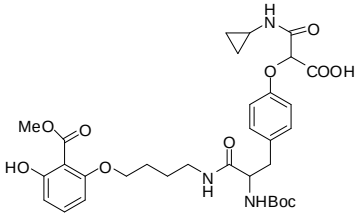

I-17

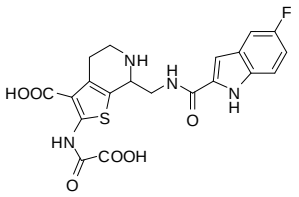

I-18

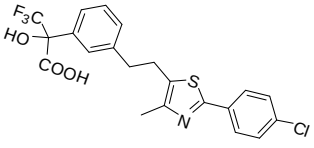

I-19

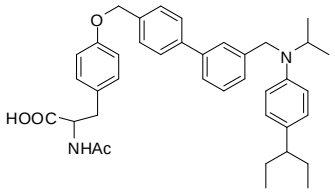

I-20

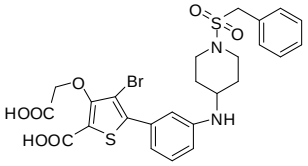

I-21

Figure I-10: Carboxylic Acid as a Phosphate Mimic

Table I-4. IC_{50} of Carboxylic Acid as a Phosphate Mimic

Compound No	IC_{50} (μM)		PTP1B Selectivity over TC-PTP	Research Group
	PTP 1B	TC-PTP		
I-14	0.018	0.065	3.6	Abbott [75]
I-15	9.0	182	20	Abbott [76]
I-16	8.4	>200	>23	Abbott [62]
I-17	2.1	>30	>15	Abbott [63]
I-18	0.081	NA	NA	Novo Nordisk[77]
I-19	3.2	NA	NA	Kyorin Pharma[78]
I-20	0.016	NA	NA	Inst. Pharm. Dis.[79]
I-21	0.004	0.005	1.0	Wyeth [80]

1.4.1.4.4. TZD and IZD as pTyr Mimics

The discovery of the TZD and isothiazolidione (IZD) heterocycle as effective pTyr mimics provided additional scaffolds for the development of novel inhibitors of PTP1B. A *de novo* structure-based design derived TZD and IZD that mimic pTyr and bind competitively to the active site of PTP1B. TZD and (S)-IZD were efficient pTyr mimics for PTP1B inhibition with better membrane permeability compared to the carboxylic acid and DFMP containing inhibitors. These mimetics still requires improvements in oral bioavailability and cellular penetration to increase *in vivo* efficacy.

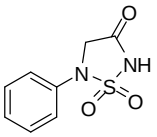

I-22

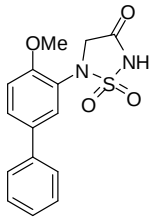

I-23

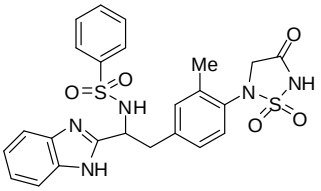

I-24

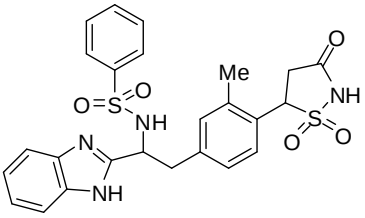

I-25

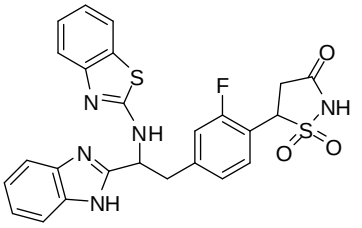

I-26

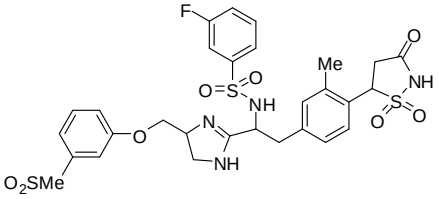

I-27

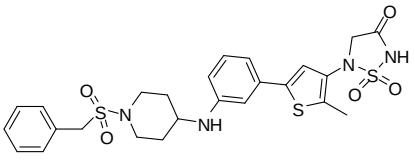

I-28

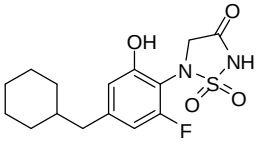

I-29

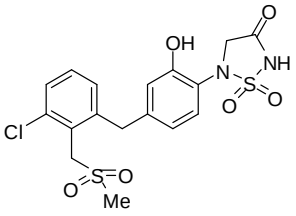

I-30

Figure I-11: TZD or IZD-containing PTP1B Inhibitors

Table I-5. IC_{50} of Some of the TZD or IZD Containing PTP1B Inhibitors

Compound No.	IC_{50} (μM)		PTP1B Selectivity over TC-PTP	Research Group
	PTP1B	TC-PTP		

I-22	6.0	NA	NA	Astra Zeneca[81]
I-23	2.50	NA	NA	AstraZeneca[82]
I-24	0.14	0.5	1.0	Incyte[83]
I-25	0.02	0.5	0.8	Incyte[84]
I-26	0.27	NA	1.0	Incyte[85]
I-27	0.023	NA	1.0	Incyte[86]
I-28	4.30	NA	NA	Incyte[87]
I-29	0.104	NA	NA	Novartis[88]
I-30	0.126	NA	NA	Novartis[89]

1.5. PTP1B Inhibitors Reported from our Laboratory

To find lead compounds for the development of PTP1B inhibitors, 1120 molecules in 'The Prestwick chemical library' were examined in our laboratory. Among the 1120 small molecules, 90% were drugs and 10% were bioactive alkaloids or related compound.[90] Nine novel inhibitors of PTP1B were identified through a computer-aided drug design protocol involving structure-based virtual screening with docking simulations process. Effects of ligand solvation were considered in the scoring function. These inhibitors were structurally diverse and revealed potencies with IC_{50} values ranging 10-50 μM. The initial hits thus obtained from the Prestwick library could be used as starting points for structural optimization to improve the potency.[91]

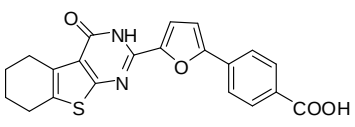

I-31

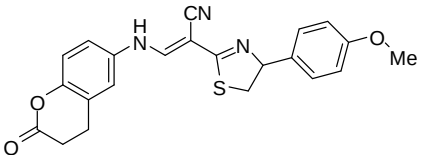

I-32

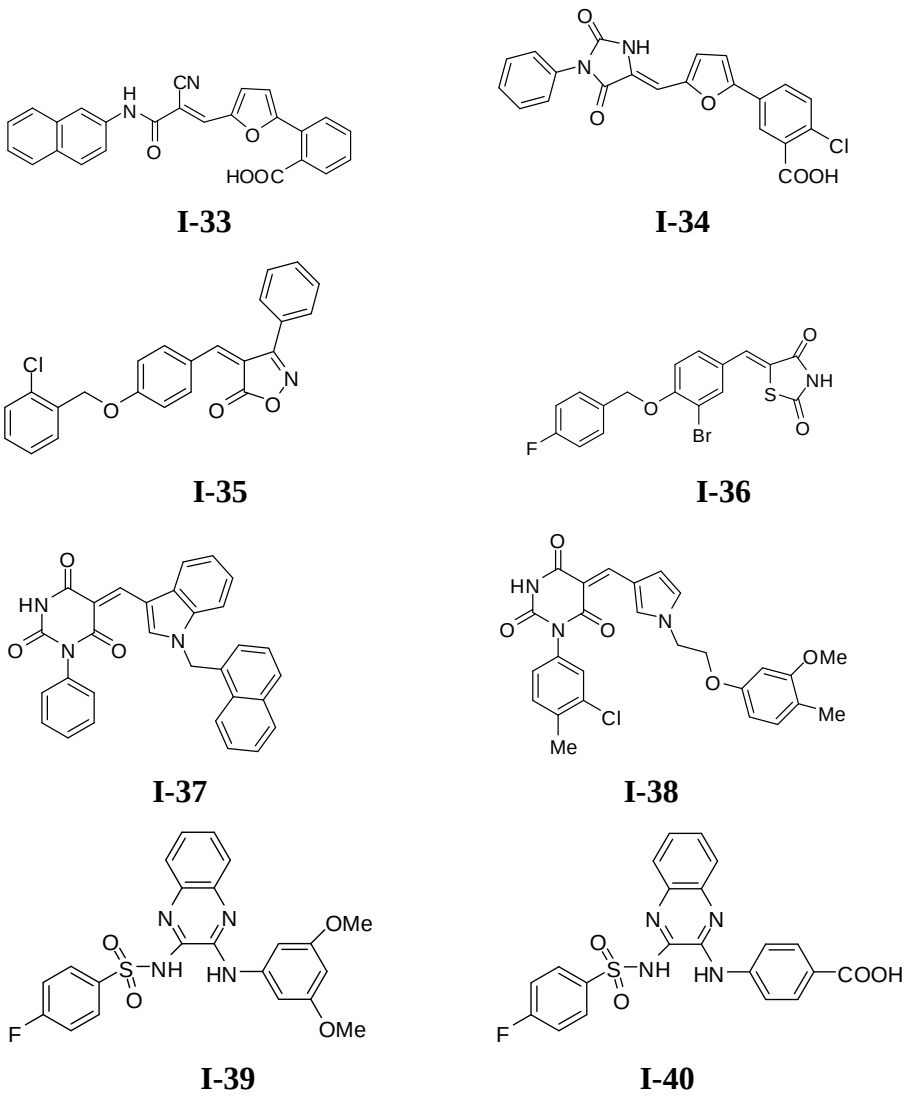

Figure I-12: Novel PTP1B Inhibitors Identified from Virtual Screening.

A series of compounds containing a thiazolidinedione moiety was synthesized and measured for their PTP1B inhibitory activity. Most of the thiazolidinedione series compounds exhibited IC_{50} values in below 10 μM against PTP1B. Compounds **I-41** and **I-42** exhibited the significant potency (1.3 μM and 5 μM respectively) for PTP1B inhibitors. Therefore, these two compounds were examined for antihyperglycemia and antiobesity effects *in*

vivo test. Feeding compounds **I-41** and **I-42** to the HFD-induced obese/diabetic mice suppressed HFD-induced body weight gain and improved glucose tolerance effect. Plasma levels of triglyceride, total cholesterol and free fatty acids were also lower compared to the HFD-fed control group.

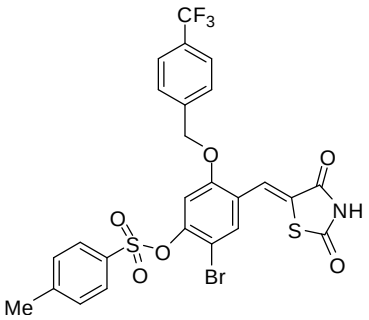

I-41

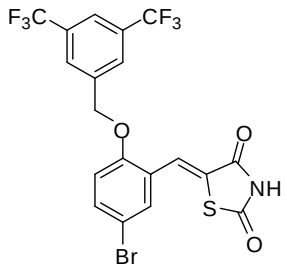

I-42

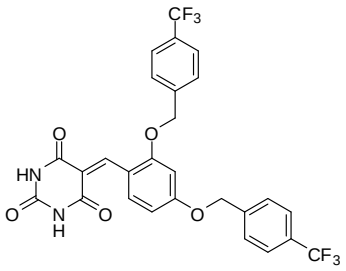

I-43

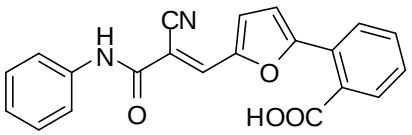

I-44

Figure I-13 A. PTP1B Inhibitors Reported from our Laboratory

LB plot analysis revealed that compound **I-36** behaves as a competitive inhibitor of PTP1B and compound **I-37** as a non-competitive inhibitor of PTP1B

A series of barbituric acid derivatives was also synthesized and examined for their potency and mode of inhibition steady-state kinetic experiments were performed for PTP1B and YPTP1 with compound **I-43**. The mode of inhibition was determined by the LB plot analysis. The

compound **I-43** showed a noncompetitive mode of inhibition for PTP1B and a mixed type noncompetitive inhibition for YPTP1. Noncompetitive inhibition of PTP1B might be explained by the possible binding of the barbituric acid moiety in the secondary aryl phosphate-binding site, present near the active site of PTP1B.

The mixed-type noncompetitive inhibition of YPTP1 by **I-38** could hardly be explained on the same basis, because no aryl phosphate–binding site distinct from the active site has been known on YPTP1. Nondiscriminative inhibition of the three structurally diverse PTPases by **I-44** also implicates the possible similarity of the inhibitor binding sites on this PTPases. Explanation of these apparently conflicting observations and considerations requires additional studies including X-ray crystallographic structure determination of the enzyme-inhibitor complex. Enzyme-inhibitor interaction yet to be explained at the molecular level, barbiturate moiety was proven to be a promising scaffold for the design of PTPase inhibitors.

By modifying the structure of compound **I-37**, several disubstituted barbituric acid compounds were synthesized to improve the inhibitory potency against PTP1B.

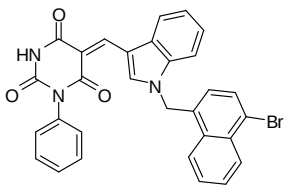

I-45

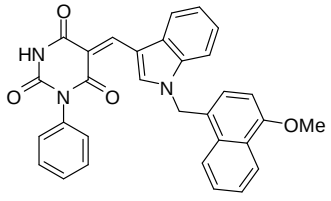

I-46

Figure I-13 B: PTP1B Inhibitors Reported from our Laboratory

LB plot analysis revealed that compound **I-45** inhibited PTP1B and YPTP1 in a noncompetitive fashion. On the other hand, compound **I-45**

exhibited a competitive inhibition pattern for VHR phosphatase, which indicates that the inhibitor competes with the substrate in binding on VHR phosphatase. The compound **I-44** was synthesized as an analogue of compound **I-33**. On the basis of inhibitory action and kinetic study, the compound **I-44** was proved as a promising competitive inhibitor of PTP1B. Further modification of compound **I-44** is in progress.

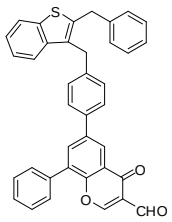

I-47

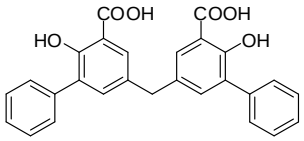

I-48

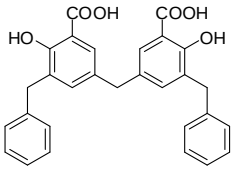

I-49

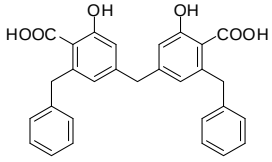

I-50

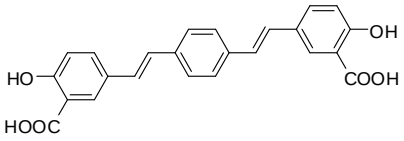

I-51

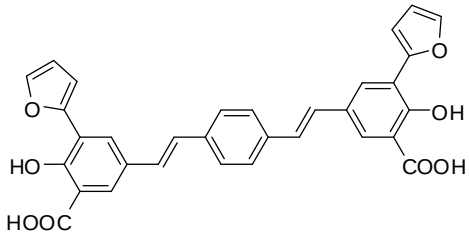

I-52

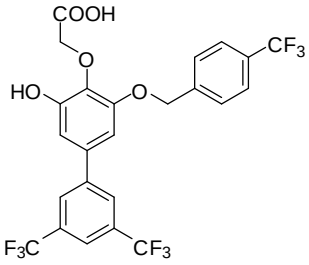

I-53

Figure I-13 C. PTP1B Inhibitors Reported from our Laboratory

PTP1B inhibitors reported from our laboratory also include formylchromone derivatives,[92] disalicylic acid derivatives,[93] and pyrogallol derivatives.[94] Compound **I-47** was the most potent from formylchromone

derivatives with IC_{50} in 1 μM. It showed good selectivity over several PTPases including TC-PTP and inhibited PTP1B irreversibly.

Disalicylic acid derivatives were also synthesized and examined for the inhibitory activity against diverse PTPases. The three potent compounds **I-48**, **I-49** and **I-50** from disalicylic acid derivatives demonstrated about 10-fold selectivity over TC-PTP and two of the compounds **I-48** and **I-50** were proved to be reversible PTP1B inhibitors. Feeding compounds **I-48** and **I-50** to DIO mice significantly reduced body weight gain compared with that of the untreated HFD control group without suppressing food intake.[93] Disalicylic acid derivatives with a longer chain, **I-51** (IC_{50} = 5 μM) and **I-52** (IC_{50} = 0.5 μM), also showed PTP1B inhibitory effect. Compound **I-51** exhibited *in vivo* effects by lowering glucose level and improving glucose tolerance in HFD- induced diabetic mice.[95]

Compound **I-53,** the most potent among pyrogallol derivatives, was 7-fold selective for PTP1B over TC-PTP. The compound **I-53** showed IC_{50} value up to 2 μM and Ki value of 1.1 μM against PTP1B. Oral administration of the compound **I-53** improved glucose tolerance in DIO mice without observable toxicity.[91]

Chapter II

2. 1-Phenyl Barbituric Acid Containing *N*-Substituted Indole Derivatives as a Non-Competitive Inhibitor against PTP1B Enzyme

2.1. Introduction

Barbiturates generally refer to derivatives of barbituric acid. Barbituric acid was first synthesized in 1864 by condensing urea and diethyl malonate, an ester derived from an acid obtained from apples. The principal mode of action of barbiturates is believed to be their binding to the $GABA_A$ receptor. GABA is the principal inhibitory neurotransmitter in the mammalian central nervous system (CNS). Barbiturates bind to the beta subunit of the $GABA_A$ receptor at a site distinct for GABA itself. Barbiturates intensify the effects of GABA binding at this receptor. In addition to this GABA-ergic effect, barbiturates also block the AMPA receptor, a subtype of glutamate receptor. Glutamate is the principal excitatory neurotransmitter in the mammalian CNS. Taken together, the findings that barbiturates potentiate inhibitory $GABA_A$ receptors and inhibit excitatory AMPA receptors can explain the CNS-depressant effects of barbiturates. At higher concentration, they inhibit the Ca^{2+}-dependent release of neurotransmitters. Barbiturates produce their pharmacological effects by increasing the duration of chloride ion channel opening at the $GABA_A$ receptor. Whereas benzodiazepines increase the frequency of the chloride ion channel opening at the $GABA_A$ receptor.

Commonly used barbiturates like phenobarbital and secobarbital have substituents at the 5 position on this basic skeleton. CNS functions of barbiturates have been used to treat medical conditions such as epileptic seizures and as anesthesia for surgical procedures.[95] Beside the effects as

CNS depressants, barbiturates have been shown to exhibit wide variety of other biological activities, including anti-tumor activities, immuno-modulating activities, herbicidal or insecticidal activities, PPARγ agonistic activities, and inhibitory activities against mucosal addressin cell adhesion molecule-1 interactions.[96-100] Notably, barbiturates, including phenobarbital and secobarbital, were also found to inhibit the phosphatase activity of calcineurin, a protein Ser/Thr phosphatase.[101] In view of this observation, the barbituric acid moiety was considered as a candidate scaffold for the design of PTPase inhibitors in this study.

2.2. Aim of the Research

The objective of this work is to seeking a potent and selective inhibitor of PTP1B. PTP1B is a negative regulator of insulin and leptin signaling. Inhibition of its activity is the strategy for the development of diabetes and obesity drug.

The specific objectives of the research were;

1. To synthesize a series of disubstituted barbituric acid derivatives
2. To evaluate their inhibitory potency against PTPases
3. To study the kinetics of inhibition

2.3. Results and Discussion

2.4. Experimental Section

2.4.1. Materials for Chemical Synthesis

Commercial reagents were purchased from Aldrich Chemical Co. (Milwaukee, WI), TCI (Tokyo, Japan) and Alfa Aesar (Johnson Matthey Company, Germany). All the chemicals and solvents were analytical grade and used without further purification. Chemical reactions were monitored by thin-layer chromatography (TLC) using precoated silica gel plates (Silica gel 60 F_{254}, Merck) and spots were visualized with UV light (254 nm). Column chromatography was done with silica gel 60 (mesh 0.063-0.200 mm, Merck).

Melting points were determined on a MEL-TEP Electro-thermal apparatus and the readings were uncorrected. ^{1}H NMR was recorded on a Varian Gemini 2000 (200 MHz) and Varian Inova 400 (400 MHz) spectrometers. Chemical shifts (δ) are expressed in part per million relative to internal tetramethylsilane, coupling constants (J) are in Hertz (Hz) and signals are designated as follows: s, singlet; d, doublet; t, triplet; q, quartet; m, multiplet; brs, broad singlet.

2.5. Synthesis of Compounds

The series of barbituric acid derivatives were synthesized as described in **Scheme II-1** and they are shown in **Table II-1**. Commercially available aniline derivatives, **II-1a-i,** was treated with sodium isocyanate to obtain urea derivatives, which are further converted to monosubstituted barbiturate derivatives, **II-3a-i**.

Knovenagel condensation of the latter compounds (**II-3a-i**) with N-substituted imidazole (**II-4j-p)** afforded disubstituted barbituric acid

derivatives **II-5a-o.**

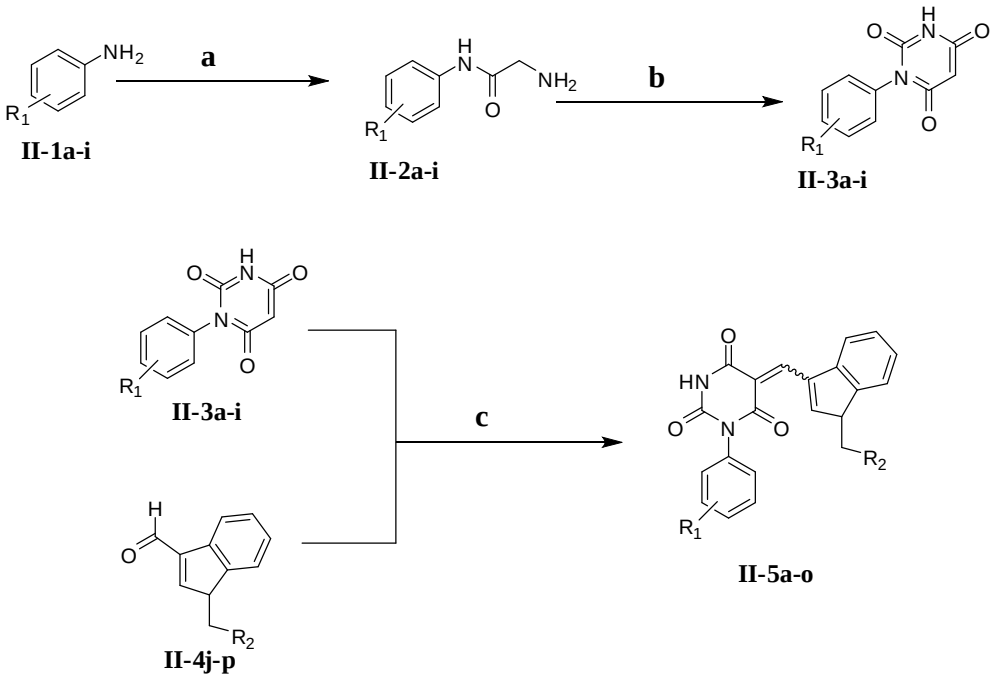

Where,

a = H	f = 4-F	k = 1-phenyl
b = 4-OCH_3	g = 3-OCH_3	l = 3-chlorophenyl
c = 3-NO_2	h = 4-(4-chlorophenoxy)	m = 1-(4-methoxy)napthyl
d = 3-Cl	i = 3,5-$(CF_3)_2$	n = 1-(4-bromo)napthyl
e = 3-CF_3	j = 1-napthyl	o = 2-napthyl
		p = 4-methoxyphenyl

Scheme II-1. Synthetic Strategy of the Synthesis of Barbituric Acids derivatives II-5a-o. Reagents and conditions: (a) NaOCN, AcOH/H_2O, 37 ˚C, 2-3 h; (b) Diethyl malonate, Na/EtOH, 70-80 ˚C, Overnight; (c) DMF, 60-70 ˚C, 6 h.

First set of compounds **II-5a-g** was prepared with R_1 fixed to H and varying R_2 as shown in the upper part of Table **II-1**. The final products were obtained as mixtures of (E) and (Z)-isomers. These compounds were

examined for their inhibitory activity against PTP1B. Among the various substituted phenyl and naphthyl derivatives, compound **II-5a** and **II-5e** with a 1-naphthyl and 1-(4-bromo)naphthyl moiety for R_2 gave the lowest IC_{50} values against PTP1B. Among the two, 1-(4-bromo)naphthyl moiety was selected for R_2 due to the smaller molecular weight compared to the corresponding naphthyl moiety. The second set of compounds **II-5h-o** was then prepared with R_2 fixed to 1-naphthyl moiety. Various derivatives of **II-3** were subjected to condensation reaction with **II-4** as the counterpart. Among the 1-naphthyl series of compounds, **II-5e** proved to be the most potent inhibitor of PTP1B.

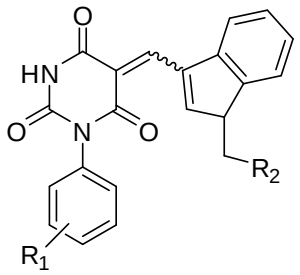

Compound II-5a-o

Table II-1. Barbituric Acid Derivatives Synthesized in This Study

Compounds	R_1	R_2
II-5a	H	1-naphthyl
II-5b	H	1-phenyl
II-5c	H	3-chlorophenyl
II-5d	H	1-(4-methoxy)naphthyl
II-5e	H	1-(4-bromo)naphthyl
II-5f	H	2-naphthyl
II-5g	H	4-methoxyphenyl
II-5h	4-methoxy	1-naphthyl

II-5i	3-NO_2	1-naphthyl
II-5j	3-Cl	1-naphthyl
II-5k	3-CF_3	1-naphthyl
II-5l	4-F	1-naphthyl
II-5m	3-methoxy	1-naphthyl
II-5n	4-(4-chlorophenoxy)	1-naphthyl
II-5o	3,5-$(CF_3)_2$	1-naphthyl

Synthesis of **II-4j-p** was accomplished by the S_N2 reaction between **II-4j-p**, and indole-3-carbaldehyde (Scheme **II-2**). **II-6** was obtained by the reduction of aldehyde using $NaBH_4$ as a reducing agent. Compound **II-7** was prepared by treatment of **II-6** with PBr_3. The mechanism involves initial activation of the alcohol oxygen by the electrophilic phosphorus, followed by an S_N2 substitution at the alcohol carbon.

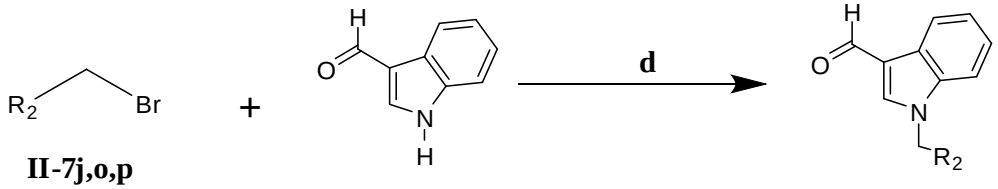

II-7j,o,p **II-4j,o,p**

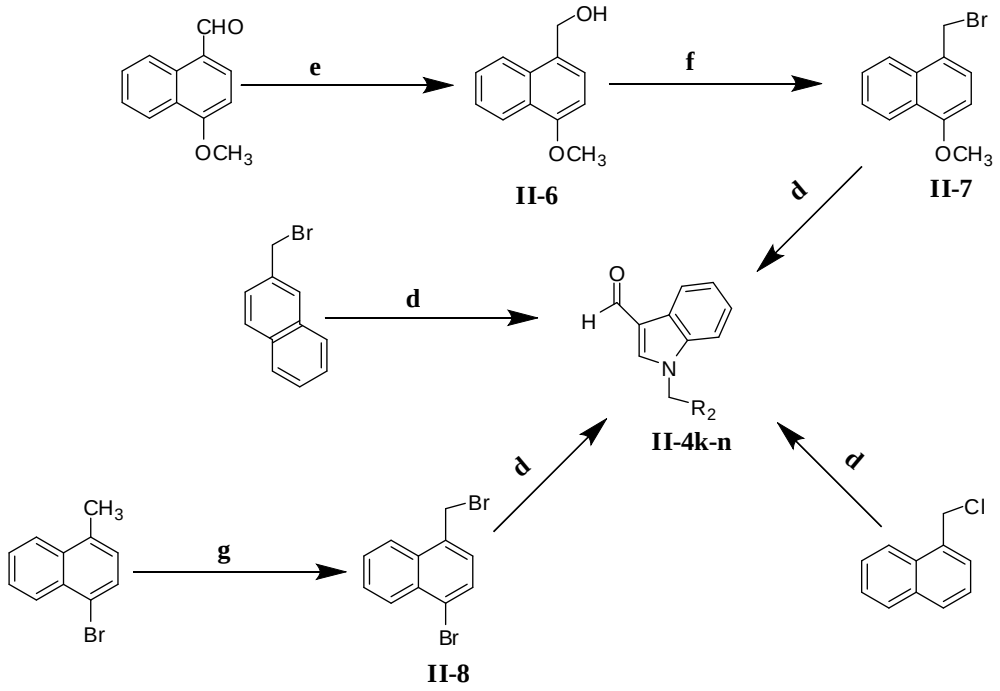

Scheme II-2. Synthetic Strategy for the Synthesis of Indole Derivatives (II-4k-n). Reagent and conditions: (d) Indole, KOH, DMSO, rt, 2 h; (e) $NaBH_4$, EtOH, rt, 10 min; (f) PBr_3, DCM, 0˚C, 2 min; (g) AIBN, NBS, Benzene, reflux, 3 h.

2.5.1. Chemical Synthesis of Compound II-2a-i

Urea Formation Reaction

Sodium cyanate (260 mg, 4 mmol) in water (8 mL) was added gradually to a stirred solution of aniline (4 mmol) in a mixture of acetic acid (8 mL) and water (16 mL) at 35 ˚C. After 2 h, the reaction mixture was cooled to the room temperature and dissolved in ethyl acetate (30 mL), washed with water (25 mL × 2) and brine (20 mL) successively, dried over anhydrous sodium sulfate, filtered, and concentrated under reduced pressure. The crude product was recrystallized in ethyl acetate to obtain yellow

crystals of phenylurea.

1-phenylurea (II-2a). White crystalline solid (407 mg, 74% yield): m.p. 150-151 ˚C; R_f = 0.6 (EtOAc w/ 1% Et_3N); ^1H NMR (DMSO-d_6, 400 MHz) δ 5.8 (s, 2H), 6.8 (m, 1H), 7.2 (m, 2H), 7.3 (m, 2H), 8.5 (s, 1H).

1-(4-methoxyphenyl)urea (II-2b). White solid (206 mg, 63% yield): m.p. 162-163 ˚C; R_f = 0.6 (EtOAc w/ 1% Et_3N); ^1H NMR (DMSO-d_6, 400 MHz) δ 3.6 (q, J = 15.6 Hz, 3H), 5.8 (s, 2H). 6.7 (d, J = 8.8 Hz, 2H), 7.2 (m, 2H), 8.6 (s, 1H).

1-(3-nitrophenyl)urea (II-2c). Yellow crystal (391 mg, 35% yield): m.p. 193-194 ˚C; R_f = 0.7 (EtOAc w/ 1% Et_3N); ^1H NMR (DMSO-d_6, 400 MHz) δ 6.0 (s, 2H), 7.5 (t, J = 8.4 Hz, 1H), 7.6 (m, 1H), 7.7 (m, 1H), 8.4 (t, J = 2 Hz, 1H), 9.0 (s, 1H).

1-(3-chlorophenyl)urea (II-2d). White needle shaped crystalline solid 586 mg, 57% yield): m.p. 151-152 ˚C; R_f = 0.5 (EtOAc w/ 1% Et_3N); ^1H NMR (DMSO-d_6, 400 MHz) δ 5.9 (s, 2H), 6.9 (m, 1H), 7.1 (m, 2H), 7.6 (t, J = 2 Hz, 1H), 8.7 (s, 1H).

1-(3-(trifluoromethyl)phenyl)urea (II-2e). White solid (580 mg, 71% yield): m.p. 100-101 ˚C; R_f = 0.45 (EtOAc w/ 1% Et_3N); ^1H NMR (DMSO-d_6, 400 MHz) δ 5.9 (s, 2H), 7.2 (br., 1H), 7.4 (m, 2H), 7.9 (s, 1H), 8.8 (s, 1H).

1-(4-fluorophenyl)urea (II-2f). White crystalline solid (470 mg, 51% yield): m.p. 189-190 ˚C; R_f = 0.4 (EtOAc w/ 1 % Et_3N); ^1H NMR (DMSO-d_6, 400 MHz) δ 5.8 (s, 2H), 7.0 (m, 2H), 7.3 (m, 2H), 8.5 (s, 1H).

1-(3-methoxyphenyl)urea (II-2g). White crystalline solid (736 mg, 73% yield): m.p. 129-130 ˚C; R_f = 0.44 (EtOAc w/ 1% Et_3N); 1H NMR

(DMSO-d_6, 400 MHz) δ 5.7 (s, 2H), 6.4 (s, 1H), 6.8 (s, 1H), 8.4 (s, 1H).

1-(4-(4-chlorophenoxy)phenyl)urea (II-2h). White solid (817 mg, 78% yield): m.p. 153-154 ˚C; R_f = 0.5 (EtOAc); ^{1}H NMR (DMSO-d_6, 400 MHz) δ 5.8 (s, 2H), 6.9 (m, 4H), 7.4 (m, 4H), 8.5 (s, 1H).

1-(3, 5-bis(trifluoromethyl)phenyl)urea (II-2i). White (550 mg, 33 % yield): mp 195-196 ˚C; R_f = 0.37 (EtOAc: Hexane, 9: 1); ^{1}H NMR (DMSO-d_6, 400 MHz) δ 6.2 (s, 2H), 7.5 (s, 1H), 8.0 (s, 2H), 9.2 (s, 1H).

2.5.2. Chemical Synthesis of Compound II-3a-i

Cyclization Reaction

Sodium (60 mg, 2.61 mmol) was added into a two-necked round bottom flask containing anhydrous ethanol (2 mL) fitted with a reflux condenser and a calcium chloride tube. When the sodium has disappeared, phenylurea (2.14 mmol) and diethyl malonate (2.2 mmol) in anhydrous ethanol (2 mL) was added sequentially. After 12 h at 70-80 ˚C, the reaction mixture was cooled to room temperature and concentrated to ~1-2 mL by rotary evaporator. The reaction mixture was dissolved in water (20 mL) and washed with ethyl acetate (15 × 3 mL). 1 M hydrochloric acid (5 mL) was added to the reaction mixture and was extracted with ethyl acetate (15 mL × 3**)**. The combined organics were washed with water (15 mL × 3) and brine (15 mL) successively, dried with anhydrous sodium sulfate, filtered, and concentrated under reduced pressure. A pure solid (by TLC) thus obtained was the desired product.

1-phenylpyrimidine-2,4,6-trione (II-3a). Yellowish white solid (130 mg, 29% yield): m.p. 234-235 ˚C; R_f = 0.3 (EtOAc: Acetone, 1: 1); ^{1}H NMR (DMSO-d_6, 400 MHz) δ 3.7 (s, 2H), 7.2-7.4 (br, 5H), 11.4 (s, 1H).

1-(4-methoxyphenyl)pyrimidine-2,4,6-trione (II-3b). White solid (347 mg, 43 % yield): m.p. 208-209 ˚C; R_f = 0.45 (EtOAc: Acetone, 1: 1); ^{1}H NMR (DMSO-d_6, 400 MHz) δ 3.6-3.7 (m, 5H), 7.0-7.1 (m, 4H), 11.3 (s, 1H).

1-(3-nitrophenyl)pyrimidine-2,4,6-trione (II-3c). Yellow solid (368 mg, 36% yield): m.p. 231-232 ˚C; R_f = 0.4 (EtOAc: Acetone, 1: 1); ^{1}H NMR (DMSO-d_6, 400 MHz) δ 3.7 (*d, J*=8 Hz, 2H), 7.75-7.67 (m, 2H), 8.15-8.2 (m, 2H), 11.58 (s, 1H).

1-(3-chlorophenyl)pyrimidine-2,4,6-trion (II-3d). Light yellow solid (356 mg, 75% yield): m.p. 179-180 ˚C; R_f = 0.3 (EtOAc); ^{1}H NMR (DMSO-d_6, 400 MHz) δ 3.6 (s, 2H), 7.3 (b, 4H), 11.5 (s, 1H).

1-(3-(trifluoromethyl)phenyl pyrimidine-2,4,6-trion (II-3e). White solid (196 mg, 72% yield): m.p. 86-87 ˚C; R_f = 0.45 (EtOAc); ^{1}H NMR (DMSO-d_6, 400 MHz) δ 3.6 (s, 2H), 7.5-7.7 (m, 4H), 11.5 (s, 1H).

1-(4-fluorophenyl) pyrimidine-2,4,6-trion (II-3f). White solid (174 mg, 78% yield): m.p. 223-224 ˚C; R_f = 0.24 (EtOAc w/ 1% Et_3N); ^{1}H NMR (DMSO-d_6, 400 MHz) δ 3.6 (s, 2H), 7.3 (m, 4H), 11.4 (s, 1H).

1-(3-methoxyphenyl)pyrimidine-2,4,6-trion (II-3g). Yellow solid (440 mg, 94% yield): m.p. 163-164 ˚C; R_f = 0.26 (EtOAc); ^{1}H NMR (DMSO-d_6, 400 MHz) δ 3.7 (t, *J* = Hz, 5H), 6.7 (d, *J* = 8.4 Hz, 2H), 6.9 (d, *J* = 6.8 Hz, 1H), 7.3 (t, *J* = 8 Hz, 1H), 11.4 (s, 1H).

1-(4-(4-chlorophenoxy)phenyl)pyrimidine-2,4,6-trion (II-3h). White solid (122 mg, 80% yield): m.p. 232-233 ˚C; R_f = 0.25 (EtOAc); ^{1}H NMR (DMSO-d_6, 400 MHz) δ 3.6 (s, 2H), 7.1 (q, *J* = 8.8 Hz, 4H), 7.2 (d, *J* = 8.4 Hz, 2H), 7.4 (t, *J* = 6.8 Hz, 2H), 11.4 (s, 1H).

1-(3, 5-bis(trifluoromethyl)phenyl)pyrimidine-2, 4, 6-trion (II-3i). Yellow solid (395 mg, 58% yield): m.p. 148-149 ˚C; R_f = 0.33 (EtOAc); ^{1}H NMR (DMSO-d_6, 400 MHz) δ 3.7 (s, 2H), 8.0 (s, 2H), 8.2 (s, 1H), 11.6 (s, 1H).

2.5.3. Chemical Synthesis of Compound II-5a-o

Knoevenagel Condensation

Compound **II-3a-i** (0.95 eq., 0.038 mmol) was added into an Eppendorf tube containing compound **II-4j-p** (0.04 mmol) in DMF (100 μL). The mixture was heated at 70-80 ˚C. After 6 h, the solid that formed in the reaction vessel was washed with *i*-PrOH (100 μL × 2). The yellow solid thus obtained was the target compound. The condensation products were obtained as mixtures of (E) and (Z)-isomers.

(Z)-5-((1-(naphthalen-1-ylmethyl)-1H-indol-3-yl)methylene)-1-phenylpyrimidine-2,4,6-trione (II-5a). Yellow solid (17 mg, 88% yield): mp >300 ˚C; R_f = 0.55 (EtOAc: Hexane, 1: 1); ^{1}H NMR (DMSO-d_6, 400 MHz) δ 6.19 (d, J = 10 Hz, 2H), 6.78 (d, J = 6.8 Hz, 1H), 7.21-7.58 (m, 11H), 7.79-8.13 (m, 4H), 8.33 and 8.71 (2s, rotamers, 1H), 9.49 and 9.55 (2s, rotamers, 1H), 11.31 and 11.47 (2s, rotamers, 1H).

(Z)-5-((1-benzyl-1H-indol-3-yl)methylene)-1-phenylpyrimidine-2,4,6-trione (II-5b). Yellow solid (15 mg, 86% yield): m.p. 298-299 ˚C; R_f = 0.38 (EtOAc: Hexane, 2: 1); ^{1}H NMR (DMSO-d_6, 400MHz) δ 5.68 (d, 2H, J = 11.2 Hz), 7.2-7.9 (m, 14H), 8.46 and 8.71 (2s, rotamers, 1H), 9.57 and 9.67 (2s, rotamers, 1H), 11.40 and 11.48 (2s, rotamers, 1H).

(Z)-5-((1-(3-chlorobenzyl)-1H-indol-3-yl)methylene)-1-

phenylpyrimidine-2,4,6-trione (II-5c). Yellow solid (12 mg, 64% yield): m.p. 279-280 ˚C; R_f = 0.5 (EtOAc: Hexane, 1: 1); ^{1}H NMR (DMSO-d_6, 400 MHz) δ 5.7 (d, J = 12.4 Hz, 2H), 7.94-7.13 (m, 13H), 8.72 and 8.81 (2s, rotamers, 1H), 9.58 and 9.62 (2s, rotamers, 1H), 11.42 and 11.49 (2s, rotamers, 1H).

(Z)-5-((1-((4-methoxynaphthalen-1-yl)methyl)-1H-indol-3-yl)methylene)-1-phenylpyrimidine-2,4,6-trione (II-5d). Yellow solid (16 mg, 78% yield): m.p. >300 °C; R_f = 0.6 (EtOAc: Hexane, 1: 1); ^{1}H NMR (DMSO-d_6, 400 MHz) δ 3.9 and 4.0 (2s, rotamers, 3H), 6.0 (d, J = 12.4 Hz, 2H), 6.8, 6.9 and 7.0 (3d, J = 8 Hz, J = 8 Hz, J = 8 Hz, rotamers, 2H), 7.2-7.6 (m, 10H), 7.8-7.9 (m, 2H), 8.0-8.2 (m, 1H), 8.64 and 8.80 (2s, rotamers, 1H), 9.4 and 9.5 (2s, rotamers, 1H), 11.3 and 11.4 (2s, rotamers, 1H).

(Z)-5-((1-((4-bromonaphthalen-1-yl)methyl)-1H-indol-3-yl)methylene)-1-phenylpyrimidine-2,4,6-trione (II-5e). Yellow solid (18 mg, 80% yield): m.p. > 300 ˚C; R_f = 0.6 (EtOAc: Hexane, 1: 1); ^{1}H NMR (DMSO-d_6, 400 MHz) δ 6.2 (d, J = 8.4 Hz, 2H), 6.9 (d, J = 7.2 Hz, 1H), 7.0 (d, J =7.6 Hz, 1H), 7.3-8.2 (m, 13H), 8.7 and 8.8 (2s, rotamers, 1H), 9.5 and 9.6 (2s, rotamers, 1H), 11.34 and 11.48 (2s, rotamers, 1H) .

(Z)-5-((1-(naphthalen-2-ylmethyl)-1H-indol-3-yl)methylene)-1-phenylpyrimidine-2,4,6-trione (II-5f). Yellow solid (17 mg, 83% yield): m.p. > 300 ˚C; R_f = 0.53 (EtOAc: Hexane, 1: 1); ^{1}H NMR (DMSO-d_6, 400 MHz) δ 5.85 (d, J =10.8 Hz, 2H), 7.3-7.9 (m, 16H), 8.7 and 8.8 (2s, rotamers, 1H), 9.6 and 9.7 (2s, rotamers, 1H), 11.4 and 11.5 (2s, rotamers, 1H).

(Z)-5-((1-(4-methoxybenzyl)-1H-indol-3-yl)methylene)-1-phenylpyrimidine-2,4,6-trione (II-5g). Yellow solid (16 mg, 78% yield):

m.p. >300 ˚C; R_f = 0.6 (EtOAc: Hexane, 1: 1); ^{1}H NMR (DMSO-d_6, 400 MHz) δ 3.8 (dd, J = 0.4 Hz, 3H), 5.6 (d, J = 10 Hz, 2H), 6.8 and 6.9 (2 doublets, J = 7.2 Hz and 7.2 Hz, 3H), 7.2-7.9 (m, 11H), 8.7 and 8.8 (2s, rotamers, 1H), 9.5 and 9.6 (2s, rotamers, 1H), 11.3 and 11.4 (2s, rotamers, 1H).

(Z)-1-(4-methoxyphenyl)-5-((1-(naphthalen-1-ylmethyl)-1H-indol-3-yl)methylene)pyrimidine-2,4,6-trione (II-5h). Yellow solid (16 mg, 78% yield): m.p. >300 ˚C; R_f = 0.6 (EtOAc: Hexane, 1: 1); ^{1}H NMR (DMSO-d_6, 400 MHz) δ 3.8 (dd, J = 0.4 Hz, 3H), 6.2 (d, J = 12 Hz, 2H), 6.8-8.0 (m, 15H), 8.7 and 8.8 (2s, rotamers, 1H), 9.5 and 9.6 (2s, rotamers, 1H), 11.3 and 11.4 (2s, rotamers, 1H).

(Z)-5-((1-(naphthalen-1-ylmethyl)-1H-indol-3-yl)methylene)-1-(3-nitrophenyl)pyrimidine-2,4,6-trione (II-5i). Yellow solid (19 mg, 90% yield): m.p. >300 ˚C; R_f = 0.54 (EtOAc : Hexane, 1: 1); ^{1}H NMR (DMSO-d_6, 400 MHz) δ 6.2 (d, J = 6 Hz, 2H), 6.8 (d, J = 6.4 Hz, 1H), 7.2-8.3 (m, 14H), 8.7 and 8.8 (2 doublets, J = 2.4 Hz, and 2.8 Hz, 1H), 9.5 and 9.5 (2s, rotamers, 1H), 11.4 and 11.6 (2s, rotamers, 1H).

(Z)-1-(3-chlorophenyl)-5-((1-(naphthalen-1-ylmethyl)-1H-indol-3-yl)methylene)pyrimidine-2,4,6-trione (II-5j). Yellow solid (17 mg, 82% yield): m.p. >300 ˚C; R_f = 0.53 (EtOAc: Hexane, 1: 1); ^{1}H NMR (DMSO-d_6, 400 MHz) δ 6. 2 (d, J = 14 Hz, 2H), 6.8 (d, J = 6.8 Hz, 1H), 7.2-8.1 (m, 14 Hz), 8.7 and 8.8 (2s, rotamers, 1H), 9.5 and 9.6 (2s, rotamers, 1H), 11.4 and 11.5 (2s, rotamers, 1H).

(Z)-5-((1-(naphthalen-1-ylmethyl)-1H-indol-3-yl)methylene)-1-(3-(trifluoromethyl)phenyl)pyrimidine-2,4,6-trione (II-5k). Yellow solid (17 mg, 77% yield): m.p. >300 ˚C; R_f = 0.58 (EtOAc: Hexane, 1: 1); ^{1}H NMR

(DMSO-d_6, 400 MHz) δ 6.19 (d, J = 10.4 Hz, 2H), 6.8 (d, J = 6.8 Hz, 1H), 7.2-8.1 (m, 14H), 8.7 and 8.8 (2s, rotamers, 1H), 9.5 and 9.6 (2s, rotamers, 1H), 11.4 and 11.5 (2s, rotamers, 1H).

(Z)-1-(4-fluorophenyl)-5-((1-(naphthalen-1-ylmethyl)-1H-indol-3-yl)methylene)pyrimidine-2,4,6-trione (II-5l). Yellow solid (14 mg, 70% yield): m.p. >300 ˚C; R_f = 0.4 (EtOAc: Hexane, 1: 1); ^{1}H NMR (DMSO-d_6, 400 MHz) δ 6.19 (d, J = 13.2 Hz, 2H), 6.8 (d, J = 7.2 Hz, 1H), 7.2-8.1 (m, 14H), 8.7 and 8.8 (2s, rotamers, 1H), 9.5 and 9.6 (2s, rotamers, 1H), 11.3 and 11.5 (2s, rotamers, 1H).

(Z)-1-(3-methoxyphenyl)-5-((1-(naphthalen-1-ylmethyl)-1H-indol-3-yl)methylene)pyrimidine-2,4,6-trione (II-5m). Yellow solid (14 mg, 68% yield): m.p. 297-298 ˚C; R_f = 0.37 (EtOAc: Hexane, 1: 1 × 2); ^{1}H NMR (DMSO-d_6, 400 MHz) δ 3.78 (dd, J = 0.4 Hz, 3H), 6.2 (d, J =13.6 Hz, 2H), 6.8-6.9 (m, 3H), 7.2-7.6 (m, 7H), 7.8-8.1 (m, 5H), 8.7 and 8.8 (2s, rotamers, 1H), 9.5 and 9.6 (2s, rotamers, 1H), 11.3 and 11.5 (2s, rotamers, 1H).

(Z)-1-(4-(4-chlorophenoxy)phenyl)-5-((1-(naphthalen-1 ylmethyl)-1H-indol-3-yl)methylene)pyrimidine-2,4,6-trione(II-5n). Yellow solid (17 mg, 70% yield): m.p. >300 ˚C; R_f = 0.35 (EtOAc: Hexane, 1: 1 × 2); ^{1}H NMR (DMSO-d_6, 400 MHz) δ 6.2 (d, J =18 Hz, 2H), 6.7 (d, J =7.2 Hz, 1H), 7.0-7.1 (m, 4H), 7.2-7.6 (m, 10H), 7.8-8.2 (m, 5H), 8.7 and 8.8 (2s, rotamers, 1H), 9.5 and 9.6 (2s, rotamers, 1H), 11.3 and 11.5 (2s, rotamers, 1H).

(Z)-1-(3,5-bis(trifluoromethyl)phenyl)-5-((1-(naphthalen-1-ylmethyl)-1H-indol-3-yl)methylene)pyrimidine-2,4,6-trione (II-5o). Brick red solid (23 mg, 92% yield): m.p. >300 ˚C; R_f = 0.56 (EtOAc: Hexane, 1: 1

× 2); ^{1}H NMR (DMSO-d_6, 400 MHz) δ 6.2 (d, J = 8.8 Hz, 2H), 6.8 (d, J = 6.8 Hz, 1H), 7.2-7.6 (m, 6H), 7.8-8.2 (m, 7H), 8.7 and 8.8 (2s, rotamers, 1H), 9.5 and 9.6 (2s, rotamers, 1H), 11.4 and 11.5 (2s, rotamers, 1H).

2.5.4. Chemical Synthesis of Compound II-4j-p

Benzyl bromide or Bromomethylnapthalene (0.44 mmol), freshly crushed KOH (4 eq., 1.76 mmol, 98 mg) and DMSO (1 mL) were taken in a round bottom flask and the mixture was stirred at room temperature. After 1 h, Indole (1.5 eq., 0.66 mmol, 166mg) in DMSO (500 µL) was added then the resulting mixture was stirred for an additional 1 h. After completing the reaction, the mixture was dissolved in ethyl acetate (15 mL), washed with water (15 mL × 3) and brine (15 mL) sequentially, dried with anhydrous sodium sulfate, filtered, and concentrated under reduced pressure. The crude product was purified by column chromatography on silica gel using Hexane: EtOAc mixture as a solvent system.

1-(naphthalen-1-ylmethyl)-1H-indole-3-carbaldehyde (II-4j). White brownish crystal (110 mg, 77% yield): m.p. 137-138 ˚C; R_f = 0.75 (EtOAc: Hexane, 1:1); ^{1}H NMR ($CDCl_3$, 200 MHz) δ 5.8 (s, 2H), 7.4 (m, 7.4-7.5, 8H), 7.8 -7.9 (m, 3H), 8.4 (m, 1H), 9.9 (s, 1H).

1-benzyl-1H-indole-3-carbaldehyde (II-4k). White solid (777 mg, 83% yield): m.p. 105-106 ˚C; R_f = 0.4 (EtOAc: Hexane, 1: 2); ^{1}H NMR ($CDCl_3$, 200 MHz) δ 5.4 (s, 2H), 7.2-7.4 (br, 8H), 7.7 (s, 1H), 8.5 (m, 1H), and 10 (s, 1H).

1-(3-chlorobenzyl)-1H-indole-3-carbaldehyde (II-4l). White solid (889 mg, 82% yield): m.p. 79-80 ˚C; R_f = 0.6 (EtOAc: Hexane, 1: 2); ^{1}H NMR ($CDCl_3$, 200 MHz) δ 5.3 (s, 1H), 7.1-7.4 (br, 7H), 7.7 (s, 1H), 8.4 (d, J = 6.2 Hz, 1H), 10 (s, 1H).

1-(4-methoxynaphthalen-1-yl)methyl)-1H-indole-3-carbaldehyde (II-4m). Brown solid (76 mg, 56% yield): m.p. 107-108 ˚C; R_f = 0.8 (EtOAc: Hexane, 1: 2); ^{1}H NMR ($CDCl_3$, 200 MHz) δ 4.1 (m, 3H), 5.7 (s, 2H), 6.8 (dd, J = 2.4 Hz, 1H), 7.45 (m, 7.2-7.7, 6H), 8.4 (m, 1H), and 9.9 (s, 1H).

1-((4-bromonaphthalen-1-yl)methyl)-1H-indole-3-carbaldehyde (II-4n) Brown solid (134 mg, 74% yield): m.p. 120-121 ˚C; R_f = 0.56 (EtOAc: Hexane, 1: 2); ^{1}H NMR ($CDCl_3$, 200 MHz) δ 5.8 (s, 2H), 7 (d, *J* = 7.8 Hz, 1H), 7.6 (m, 7.3-7.9, 9H), 8.4 (m, 2H), 9.9 (s, 1H).

1-(naphthalen-2-ylmethyl)-1H-indole-3-carbaldehyde (II-4o). Brown crystal (203 mg, 71% yield): m.p. 114-115 ˚C; R_f = 0.54 (EtOAc: Hexane, 1: 2); ^{1}H NMR ($CDCl_3$, 200 MHz) δ 5.5 (s, 2H), 7.3-7.9 (m, 11H), 8.4 (s, 1H), 10 (s, 1H).

1-(4-methoxybenzyl)-1H-indole-3-carbaldehyde (II-4p). White brownish crystal (219 mg, 82% yield): m.p. 125-126 ˚C; R_f = 0.57 (EtOAc: Hexane, 1: 1); ^{1}H NMR ($CDCl_3$, 200 MHz) δ 3.8 (s, 3H), 5.3 (s, 2H), 6.9-7.4 (m, 8H), 7.7 (s, 1H), 8.3 (s, 1H), 9.8 (s, 1H).

2.5.5. Chemical Synthesis of Compound II-6

(4-methoxynapthalen-1-yl)methanol

A round bottom flask (25 mL) was charged with 4-methoxy-1-napthaldehyde (1.07 mmol, 200 mg), EtOH (15 mL), and $NaBH_4$ (2 eq., 2.14 mmol, 82 mg) respectively. The mixture was stirred at room temperature. After 10 min, the reaction completion was monitored by TLC plate. The reaction mixture was completely dried under reduced pressure. Water (15 mL), and ethyl acetate (25 mL) and 1M HCl (0.5 mL) were added to the

reaction mixture. The combined organics were washed with H_2O (15 mL × 3**),** brine (15 mL) successively, dried with sodium sulfate, filtered, and concentrated under reduced pressure to afford (4-methoxynapthalen-1-yl)methanol as a pale yellow gelatinous liquid (180 mg, 90% yield); m.p. 67-68 ˚C; R_f = 0.5 (Hexane: EtOAc, 2: 1); ^{1}H NMR ($CDCl_3$, 200 MHz) δ 4.0 (s, 3H), 5.1 (s, 2H), 6.8 (d, *J* = 10Hz, 1H), 7.3-7.6 (m, 3H), 8.3 (dd, *J* = 7.6 Hz, 1H), 8.4 (dd, *J* = 7.6 Hz, 1H).

2.5.6. Chemical Synthesis of Compound II-7

1-(bromomethyl)-4-methoxynapthalene

Phosphorus tribromide (0.33 eq., 89 mg, 62 μL) was added drop wise to a stirred solution of (4-methoxynapthalen-1-yl)methanol in dichloromethane (5 mL) at room temperature. After 2 min, reaction was quenched by saturated sodium carbonate (~ 3 mL). The reaction mixture was dissolved in dichloromethane (15 mL), washed with water (15 mL × 3), and brine (15 mL) sequentially, dried with sodium sulfate, filtered and concentrated under reduced pressure. The crude product thus obtained was purified by column chromatography on silica gel using Hexane: EtOAc as a solvent system to obtain 1-(bromomethyl)-4-methoxynapthalene as a white solid (20 mg, 30% yield): m.p. 139-140 ˚C; R_f = 0.5 (Hexane: EtOAc, 9: 1). ^{1}H NMR ($CDCl_3$, 200 MHz) δ 4.0 (s, 3H), 5.0 (s, 2H), 6.8 (d, *J* = 7.6 Hz, 1H), 7.5-7.7 (m, 4H), 8.1-8.4 (m, 1H).

2.5.7. Chemical Synthesis of Compound II-8

1-bromo-4-(bromomethy)naphthalene

A two-necked round bottom flask equipped with a condenser, a magnetic stirring and a calcium chloride tube was charged with *N*-

bromosuccinamide (1.2 eq., 1.08 mmol, 192 mg), 2, 2'-azobisisobutyronitrile (0.07 eq., 0.06 mmol, 10 mg), anhydrous benzene (5 mL) and 1-bromo-4-methylnapthalene (0.9 mmol, 200 mg, 141 μL) sequentially. The reaction mixture was refluxed for 3 h. Then, the mixture was dissolved in ethyl acetate (25 mL), washed with water (15 mL × 3) and brine (15 mL) successively, dried with anhydrous sodium sulfate, filtered, and concentrated under reduced pressure to obtain 1-bromo-4-(bromomethy)naphthalene as a dirty white solid (245 mg, 91% yield): m.p. 86-87 ˚C; R_f = 0.6 (Hexane: EtOAc, 19: 1); ^{1}H NMR ($CDCl_3$, 200 MHz) δ 4.9 (s, 2H), 7.4 (d, J = 8 Hz, 1H), 7.6-7.7 (m, 3H), 8.1 (d, J = 8 Hz, 1H), 8.3 (m, 1H).

2.6. *In vitro* studies

2.6.1. Materials

*p*NPP, a substrate for the PTPase assay was purchased from Sigma (St. Louis, USA) in a di(Tris) salt form. The absorbance was measured using Novaspec-II spectrophotometer (Amersham Pharmacia) or DU650 spectrophotometer (Beckman Coulter). Catalytic domain of YPTP1, VHR and the native form of PTP1B were expressed in *E. coli* expression systems.

2.6.2. Determination of IC_{50}

General Procedure

The PTPase activities were measured in buffer A (50 mM Hepes, 5 mM EDTA, 2mM DTT, pH 7.0) at 37 ˚C with *p*NPP concentration of 2 mM. Enzymes were diluted with enzyme dilution buffer (25 mM Hepes, 5 mM EDTA, 1 mM DTT, 1 mg/mL bovine serum albumin, pH 7) and inhibitors were dissolved in DMSO. The concentration of inhibitor that decreases the rate of an enzyme-catalyzed reaction by 50% (IC_{50}) was determined by

measuring PTPase activity in a range of inhibitor concentrations. The final reaction mixture contained 5 μL of *p*NPP, 5 μL of diluted enzyme, 5 μL of inhibitor solution, 10 μL of 5 × buffer A and 25 μL H_2O. Enzyme and inhibitor were incubated at 37 ˚C for 10 min before the initiation of the reaction by addition of *p*NPP. After 3 min at 37 ˚C, the enzyme-catalyzed reaction was quenched by addition of 0.5 M NaOH (0.95 mL) and the absorbance at 405 nm was taken to measure the amount of *p*-nitrophenol produced. For correction of non-enzymatic hydrolysis of *p*NPP, control reaction rate was measured by adding NaOH prior to the addition of an enzyme. The concentrations of PTPases in the assay mixture were 40 nM for PTP1B, 15 nM for YPTP1 and 500 nM for VHR. The kinetic data were analyzed using GraFit 5.0 program (Erithacus Software).

2.6.3. IC_{50} of II-5a-o

The Barbituric acid derivatives were evaluated for their inhibitory activities against PTP1B and VHR with *p*NPP as the substrate. The enzymes and compounds were preincubated for 10 min before the initiation of enzyme reaction by addition of the substrate. The IC_{50} value for each of the compounds determined under this condition is presented in **Table II-2**.

Table II-2. Inhibition of PTPases by Barbiturate Derivatives II-5a-o

Compounds	IC_{50} (μM)	
	PTP1B	VHR
II-5a	12 ± 2	43 ± 1
II-5b	28 ± 4	66 ± 6
II-5c	23 ± 4	45 ± 10
II-5d	15 ± 1	19 ± 0

II-5e	11 ± 1	27 ± 2
II-5f	24 ± 2	46 ± 9
II-5g	25 ± 3	66 ± 11
II-5h	28 ± 1	45 ± 1
II-5i	14 ± 3	24 ± 1
II-5j	18 ± 1	36 ± 2
II-5k	18 ± 3	25 ± 3
II-5l	24 ± 2	25 ± 7
II-5m	25 ± 2	33 ± 1
II-5n	14 ± 2	31 ± 2
II-5o	16 ± 8	19 ± 1

2.6.4. Nature of Inhibition

General Procedure

To determine the nature of inhibition, PTP1B-catalyzed hydrolysis of *p*NPP in presence of **II-5e** was measured at 37 ˚C in buffer A by modification of the procedure used to determine IC_{50}. In this case, the reaction was initiated by addition of diluted enzyme (5 μL) to the reaction mixture (45 μL) containing various concentrations of *p*NPP (5 μL) and various fixed concentrations of **II-5e** (5 μL). The reaction was quenched 5 min later by addition of 0.5 M NaOH (0.95 mL). The absorbance at 405 nm was measured to quantitate the *p*-nitrophenol produced and the inhibition pattern was evaluated by LB-plot analysis using GraFit 5.0 program.

2.6.5. Inhibition by II-5e

The nature of inhibition by compound **II-5e** was investigated by steady-state kinetic experiment for two human PTPases, PTP1B (**Figure II-**

1) and VHR (**Figure II-2**), and a yeast PTPase, YPTP1 (**Figure II-3**). The mode of inhibition was determined by the LB plot analysis of the kinetic experiments. Noncompetitive inhibition of PTP1B might suggest a possible interaction of the compound with PTP1B on the second phosphate-binding site near the active site. However, noncompetitive inhibition of YPTP1 is not explained in the same way because the second phosphate-binding site is not present in YPTP1. On the other hand, compound **II-5e** exhibited a competitive inhibition pattern for VHR (**Figure II-3**) indicating that the inhibitor competes with the substrate in binding to the active site of VHR.

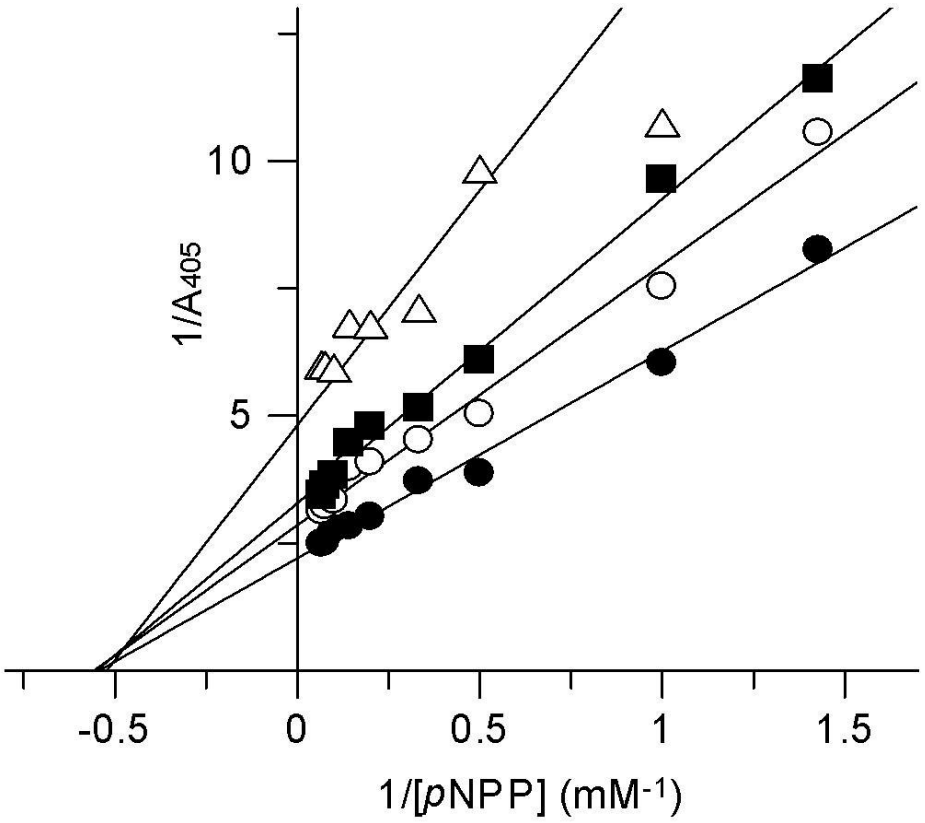

Figure II-1. Lineweaver-Burk Analysis for PTP1B Catalyzed Reaction in the Presence of II-5e. Phosphatase activity was measured against *p*NPP in the presence of **II-5e**; none (○), 25 μM (●), 50 μM (□), and 100 μM (Δ).

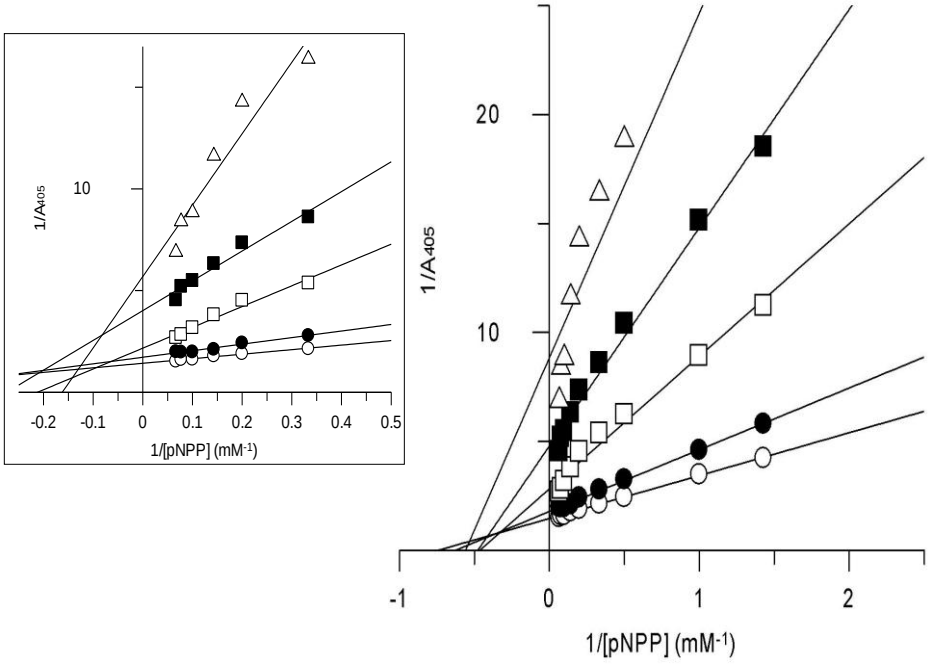

Figure II-2. Lineweaver-Burk Analysis for YPTP1Catalyzed Reaction in the Presence of II-5e. Phosphatase activity was measured against *p*NPP in the presence **II-5e**; none (○), 25 μM (●), 50 μM (□), 75 μM (■) and 100 μM (Δ). In the inset, the graph shows the plot of the data points at high *p*NPP concentrations.

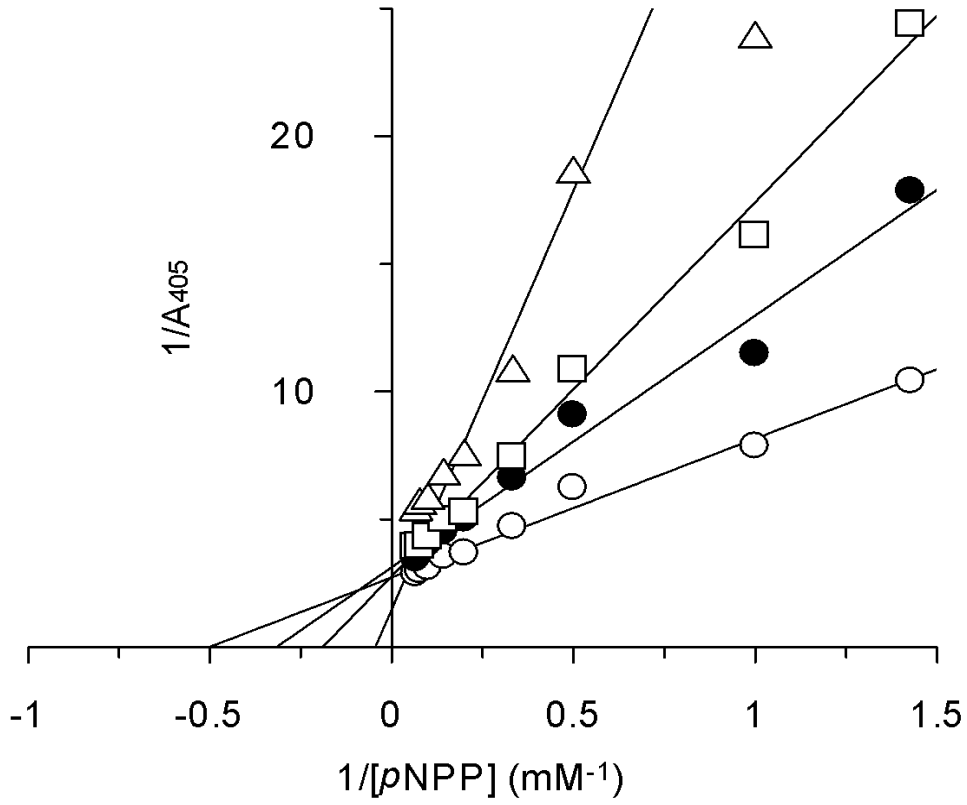

Figure II-3. Lineweaver-Burk Analysis for VHR Catalyzed Reaction in the Presence of II-5e. Phosphatase activity was measured against *p*NPP in the presence **II-5e;** none (○), 25 μM (●), 50 μM (□), and 100 μM (Δ).

2.7. Summary and Conclusion

We synthesized several derivatives of barbituric acid and their inhibitory activity against PTP1B and VHR was determined. The compounds showed high potency to the PTP1B in the comparison with VHR.

Among them, compound **II-5e** was the most potent and the nature of inhibition was examined toward various phosphatases. Compound **II-5e** was demonstrated as a competitive inhibitor against VHR and a non-competitive inhibitor against PTP1B and YPTP1.

Chapter III

3. Vaccinia Virus H1 Related Phosphatase

3.1. Introduction

Vaccinia virus H1 related phosphatase (VHR) was isolated from human fibroblasts by Ishibashi *et al.*[102] as the first identified dual specific phosphatase (DUSPase). Being a DUSPase, it dephosphorylates pTyr as well as pSer/pThr but preferably pSer/pThr. A positively charged crevice near the active site may explain the enzyme's preference for the substrates with two vicinally phosphorylated residues. DUSPases are known to regulate mitogenic signal transduction and cell cycle.

3.2. Biological Function of VHR

Several studies have indicated that the human VHR phosphatase would be involved in the regulation of cell-cycle progression.[103] VHR was suggested as a promising therapeutic target for cancer because the cells lacking VHR are arrested at the G1-S and G2-M transitions of the cell cycle with a decreased telomerase activity. The VHR activity has also been known to be related with the immune response of activated T cells.[104]

3.2.1. VHR Downregulates JNK Pathway in T Cell

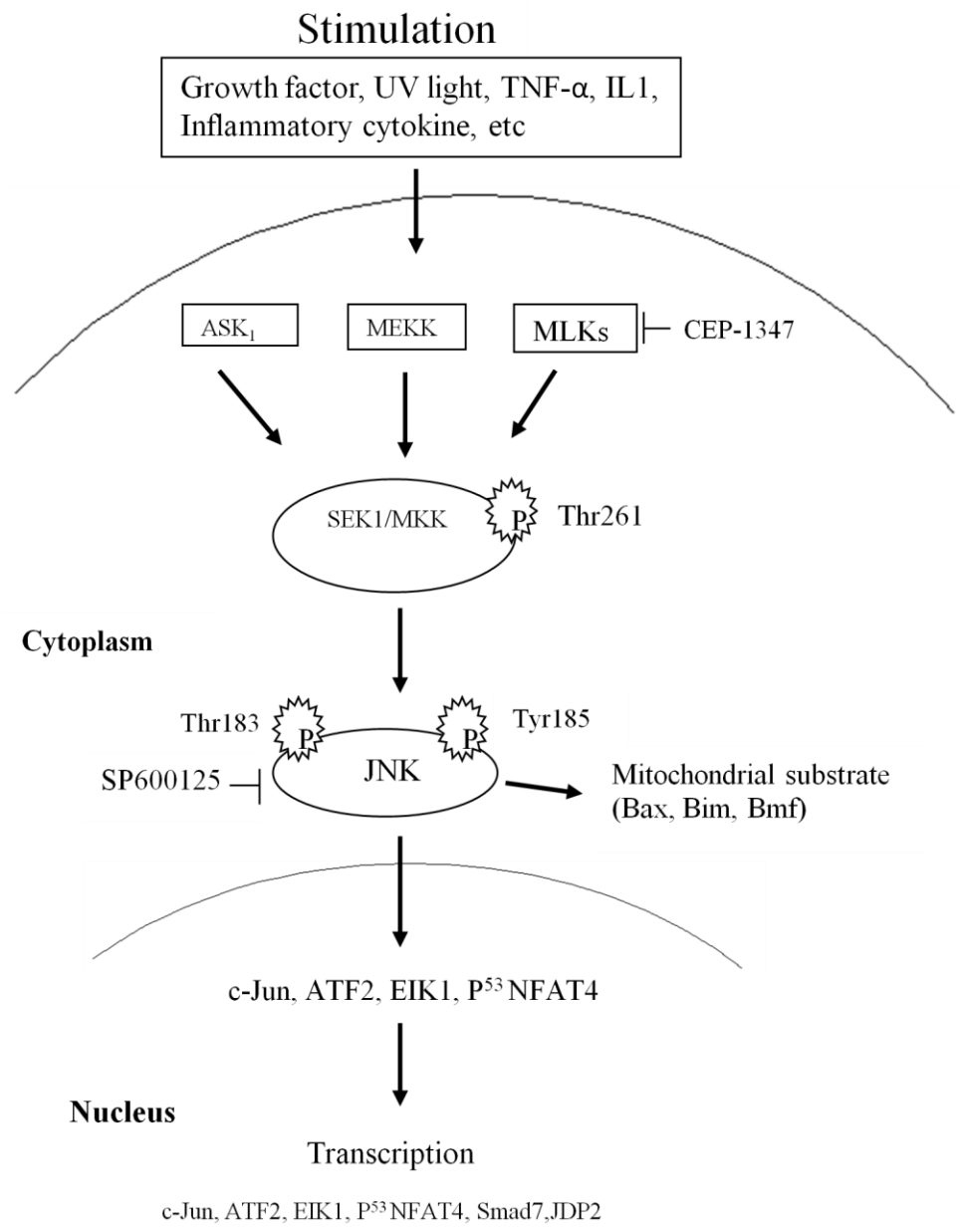

Figure III-1. JNK Signaling Pathway

VHR down-regulates the JNK signaling pathway at the level of JNK dephosphorylation. The c-Jun NH_2-terminal kinase (JNK) pathway is one of the downstream pathways of the mitogen-activated protein (MAP) kinase and plays an important role in various inflammatory diseases, including inflammatory bowel disease (IBD). The intestinal inflammatory disorder can be treated by blocking the JNK pathway. Current data suggest that specific JNK inhibitors hold promise as novel therapies for IBD.

Initially mammalian JNK were called stress activated protein kinase (SAPK) because they are activated by a variety of environmental stresses.[105] Later, the JNK pathway was also found to respond to cytokines, such as TNF-α and IL-1, and growth factors. JNK is a multi-functional kinase involved in several physiological and pathological processes. Specific stimuli trigger the activation of MAP3Ks, which then phosphorylate and activate the MAP2K isoforms MKK4 and MKK7, which in turn phosphorylate and activate JNK.[106] JNK phosphorylates c-Jun at the NH_2-terminal Ser-63 and 73 residues, and thus termed JNK. However, recent studies have shown that JNK can phosphorylate a variety of substrates, including additional transcription factors, including JunB, JunD, c-fos, ATF2 and ATF3, and some non-nuclear proteins.[105] The above mentioned transcription factors and c-Jun form various heterodimeric transcription factors, called activator protein-1 (AP-1), which regulates the expression of a variety of genes.

3.2.2. VHR is Associated with Cervix Cancer

Cervical cancer is one of the most prevalent cancers in women worldwide and is a leading cause of cancer death for women in developing countries. Recent studies[107] established the connection between VHR and cervical cancer. VHR protein levels were upregulated in several cervix

cancer cell lines as well as in cervix cancer biopsies, including squamous intraepithelial lesions and squamous cell carcinomas of the uterine cervix.[107] Loss of VHR phosphatase causes cell cycle arrest in HeLa carcinoma cells, suggesting that VHR inhibition may be a useful approach to halt the growth of cancer cells. VHR expression is not induced in response to activation of MAP kinases.[108] Several reports showed that HeLa cervix carcinoma cells lacking VHR were arrested at the G1-S and G2-M transitions of the cell cycle with initial signs of senescence. Loss of VHR increased the expression of the cyclin-dependent kinase inhibitor p21Cip-waf1 but downregulated genes for cell cycle regulators, DNA replication, transcription, and mRNA processing.[109,110]

3.3. Catalytic Mechanism of VHR

DUSPases have the common active-site sequence motif HCXXGXXRS(T). The cysteine residue is catalytically crucial for the catalysis forming a covalent thiol-phosphate intermediate.[111] Activity of VHR toward both pTyr and pSer/pThr residues is abolished when this catalytic cysteine is replaced with serine, indicating that both pTyr and pSer/pThr hydrolysis proceeds via a common active site.[111] The conserved acidic residue Asp92 in VHR serves as an apparent general acid in the catalytic mechanism.[112] The interaction between Ser131 and the thiolate anion (Cys124) in the Michaelis complex [ES] is not significant. However, Ser131 of VHR could hydrogen bond with Cys124 in the phosphoenzyme intermediate and this interaction is critical for the hydrolysis of the intermediate. Stabilization of the negative charge developing in the transition state of the intermediate hydrolysis would make the thiolate a better leaving group.

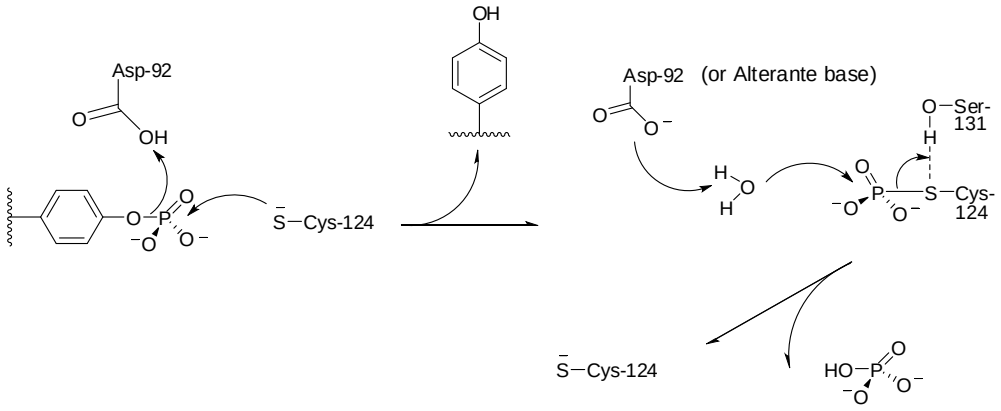

Figure III-2. Catalytic Mechanism of VHR

3.4. Potent VHR Inhibitors Reported in Literature.

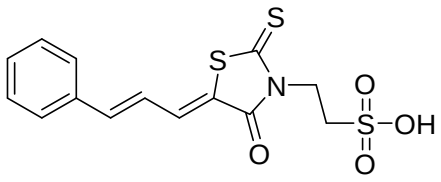

Ki = 0.809 µM

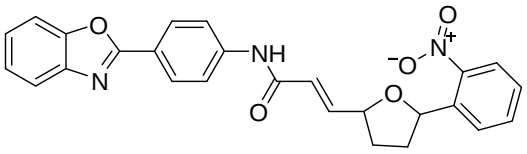

Ki = 1.76 µM

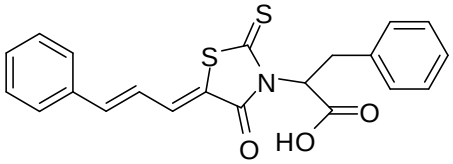

Ki = 2.01 µM

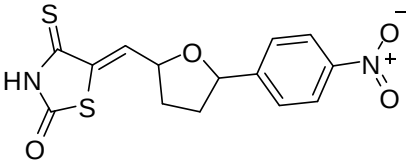

Ki = 1.86 µM

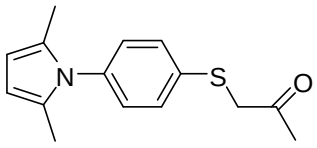

Ki = 2.09 µM

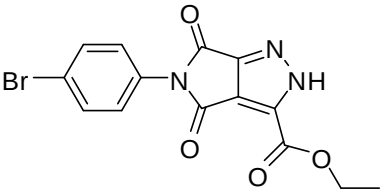

Ki = 2.64 µM

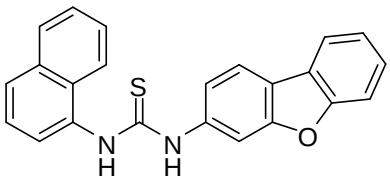

Ki = 2.94 µM

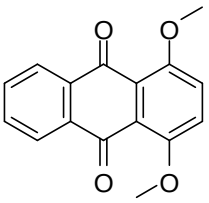

Ki = 3.07 µM

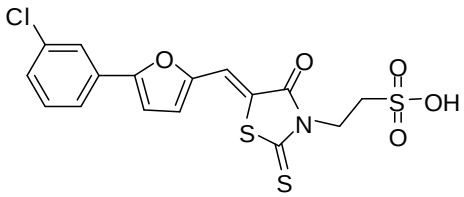

Ki = 3.13 µM

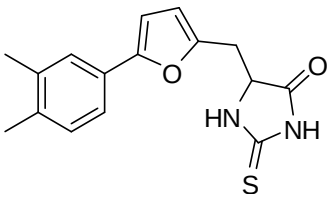

Ki = 3.19 µM

Figure III-3. Potent VHR Inhibitors Reported in Literature.

3.5. Experimental Section

3.5.1. Overexpression of VHR Enzyme in our Laboratory

Materials to be Autoclaved

- Falcon tube 250 mL × 4

- Falcon tube 50 mL × 5

- Sticks

- Micropipette tips (200 µL and 1 mL each one box)

- Hard glass test tube × 5

- Hard glass test tube cover × 5

- LB medium 200 mL × 2

These above mentioned materials were wrapped with aluminium foil

and autoclaved at 120 °C for 90 minutes.

Ingredients for LB Medium 200 mL

Particulars	**Quantity**
Trypton	2 gm
Yeast extraction	1 gm
NaCl	2 gm
Deionized H_20	200 mL

6 mL Medium Culture

A glycerol stock of the *E. coli* strain carrying a VHR expression vector (pET-21A-VHR) was scrapped with a sterilized stick and dipped into a glass test tube containing 6 mL of LB medium containing Amphicillin (30 µL, 10mg/mL). Resulting culture was incubated at 37 °C (Shaking incubator, 250 rpm) overnight.

Inoculation

The overnight culture was added into a LB medium (200 mL) containing 400 µL of Amphicillin (50mg/mL) and the resulting mixture was incubated at 37 °C (Shaking incubator, 250 rpm). When the optical density of the culture at 590 nm reached 0.7, 200 µL of Isopropyl β-D-1-thiogalactopyranoside (IPTG, 950 mg/mL) was added to the culture, which was then incubated at 37 °C (Shaking incubator, 250 rpm) for about 6 hours.

Before the harvest of the cultured cells, the culture was cooled on ice for 15 minutes. The cold culture was centrifugated at 4 °C (3000 rpm, 10 min). The supernatant was discarded and the precipitated cells were

transferred into a Falcon tube (500 mL). Buffer A (2.4 mL) and lysozyme (95 mg/mL, 130 µL) were added to the Falcon tube and mixed well. Freezing in liquid nitrogen and thawing in warm water were repeated three times. Thirteen µL of 1 M $MgCl_2$ and 7 µL of 16 mg/mL DNase I were added into the tube and the whole mixture was incubated in a shaking incubator (30 °C, 250 rpm, 30 minutes). The DNase reaction was then quenched by addition of 67 µL of EDTA (0.4 M, pH 8) and 160 µL of 10% Triton × 100. After centrifugation (4 °C, 10000 rpm, 30 minutes), the supernatant was collected in an eppendorf tube (500 µL in each tube), frozen in liq. nitrogen and stored at -50 °C. The crude lysate was analyzed for its specific activity and protein concentration before purification.

3.5.1.1. Bradford Assay

A mixture of Bradford solution (1 mL) in an eppendorf tube and 5 µL of 10-fold diluted crude lysate (diluted in buffer A) was kept at room temperature for 10 minutes. The absorbance was measured at 595 nm to determine the protein concentration.

3.5.1.2. *p*NPP Assay

A mixture containing H_2O (30 µL), 10 µL of 5 × acetate buffer (Sodium acetate 50 mM, Tris HCl 25 mM, Bis-tris propane 25 mM, pH 6), 1/10 diluted crude lysate (5 µL) and 200mM of *p*NPP (5 µL) was incubated at 30 °C. The mixture was quenched by addition of 0.5 M NaOH (950 µL) at 1 or 2 minute time points. The absorbance was measured at 405 nm.

3.5.1.3. Purification of Crude Lysate

For the purification of the crude lysate, a column was loaded by resin (1 × 8 cm, SP Sephadex C-50, Pharmacia LKB, Biotechnology AB, Uppsala,

Sweden) in MES buffer (MES 20 mM, EDTA 1 mM, β-ME 1mM, pH 6). The crude lysate was diluted 10 fold in MES buffer (pH 6). The diluted crude lysate (1 mL) was loaded to the column and eluted with increasing NaCl concentrations. The fractions were collected in separate tubes. Protein concentration and specific activity of each tube were measured and the fractions with significant *p*NPP hydrolase activity were selected.

To concentrate the purified enzyme solution, a membrane concentrator (10,000 kD MWCO, Millipore Corporation, Bedford, MA) was utilized. It was centrifugated at 4 °C, 4000 rpm to a concentration of about 1 mg/mL

3.5.2. Stability of VHR

3.5.2.1. Stability at 4 °C

It was noted that VHR enzyme could be stored at 4 °C for more than a week without significant loss of the enzyme activity.[113] To determine the stability of the enzyme at 4 °C, VHR was stored at 4 °C and the protein concentration and the specific activity of the enzyme were measured once a day for a 10 days period. The storage experiment demonstrated that the protein concentration and specific activity were maintained without significant loss of the enzyme activity **(Figure III-4)**.

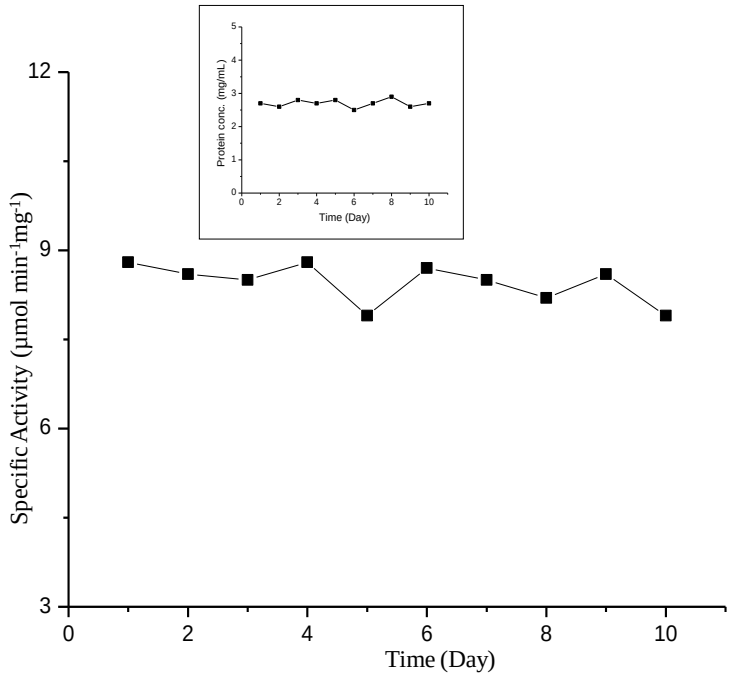

Figure III-4. Stability of VHR at 4 ˚C. Specific activity and protein concentration were calculated from *p*NPP and Bradford assay. For *p*NPP assay, a mixture of H_2O (30 μL), 10 mL of 5 × acetate buffer (CH_3COONa 50 mM, Tris HCl 25 mM, bis-tris propane 25 mM), 10 mM *p*NPP (5 μL), 1/10 fold diluted VHR (2.3 mg/mL) in MES buffer (MES 20 mM, EDTA 1 mM, β-ME 1mM) was incubated at 30 ˚C for 2 min. The reaction was quenched with 0.5 M NaOH (950 μL) and the absorbance was measured at 405 nm. For Bradford assay, Bradford solution (1 mL) was added to an eppendorf tube containing 5 μL of 10-fold diluted crude lysate (diluted in buffer A). Resulting solution was kept at room temperature for 10 minutes and the absorbance was measured at 595 nm to determine the protein concentration. (**Inset**: Protein concentration vs. time)

3.5.2.2. Enzyme Activity of VHR in Various Enzyme Dilution Buffers and Reaction Buffers

3.5.2.2.1. MES Buffer (w/ DTT) as an Enzyme Dilution Buffer and MES buffer (w/ DTT, w/ β-ME, or w/o thiol) as a Reaction Buffer

To examine the effects of thiol reagents in enzyme reaction buffer on the activity of VHR, the rate of VHR-catalyzed hydrolysis of *p*NPP was measured with or without thiol reagents in the reaction buffer. In all cases, VHR was dissolved in a buffer containing DTT. A MES buffer (MES 20 mM, EDTA 1 mM, DTT 1 mM, pH 6) was used as an enzyme dilution buffer and MES buffers with or without thiol were used as reaction buffers (MES 20 mM, EDTA 1 mM, pH 6, containing DTT 1 mM or β-ME 1mM or in the absence of any thiol). A bulk solution was prepared by mixing 525 μL of H_2O, 210 μL of reaction buffer, 105 μL of 1/10 diluted VHR enzyme (diluted in MES buffer, VHR concentration 0.23 mg/mL). Forty five μL aliquots of the bulk solution were incubated at 30 °C for the given time periods before starting the enzyme reaction by addition of 5 μL of 20 mM *p*NPP. The enzyme reaction mixture was then incubated at 30 °C for an additional 3 min. The reaction was quenched by addition of 0.5 M NaOH (950 μL) and the absorbance at 405 nm was measured.

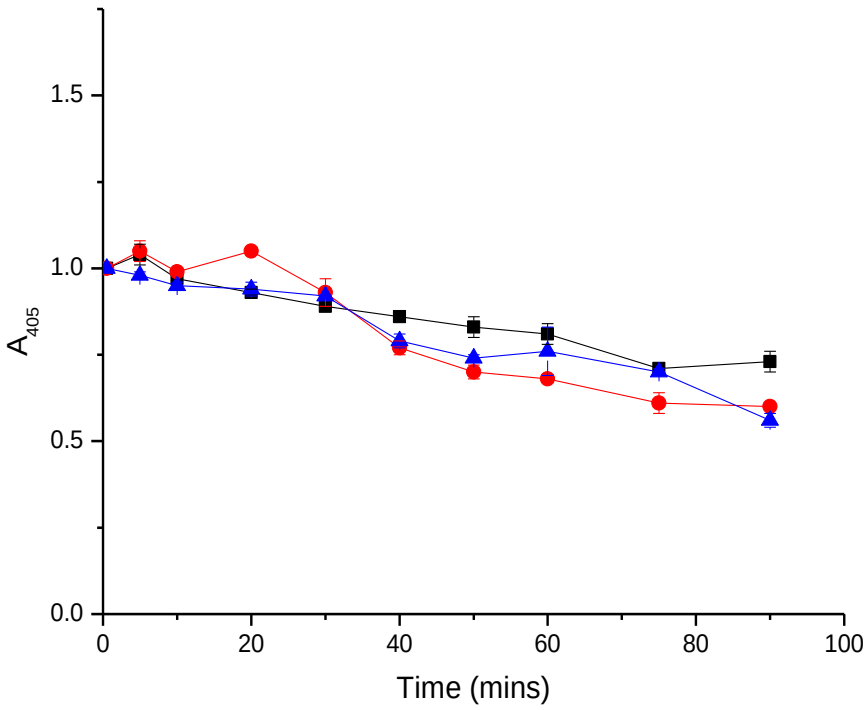

Figure III-5. Enzyme Activity of VHR with DTT in Enzyme Dilution Buffer and with or without Thiol in Reaction Buffer. Enzyme dilution buffer contained DTT in all cases but reaction buffer contained DTT**,** (■) or β-mercaptoethanol (●), or did not contain DTT or β-mercaptoethanol (▲).

3.5.2.2.2. MES Buffer (w/ DTT) as an Enzyme Dilution Buffer and 3 Component Buffer (Sodium acetate, Tris HCl, Bis-tris propane) with or without DTT as a Reaction Buffer

The effects of thiol reagents in enzyme reaction buffer on the activity of VHR was examined in a way similar to **3.5.2.2.1.** but in a different reaction buffer. In all cases, VHR was dissolved in a buffer containing DTT. For this experiment, a MES buffer containing DTT (MES 20 mM, EDTA 1 mM, DTT 1 mM, pH 6) was used as an enzyme dilution buffer and 3

component buffers with or without thiol were used as reaction buffers (Sodium acetate 50 mM, Tris HCl 25 mM, Bis-tris propane 25 mM, pH 6, containing DTT 1 mM or β-ME 1mM or in the absence of any thiol). The experimental procedure was described in **3.5.2.2.1**.

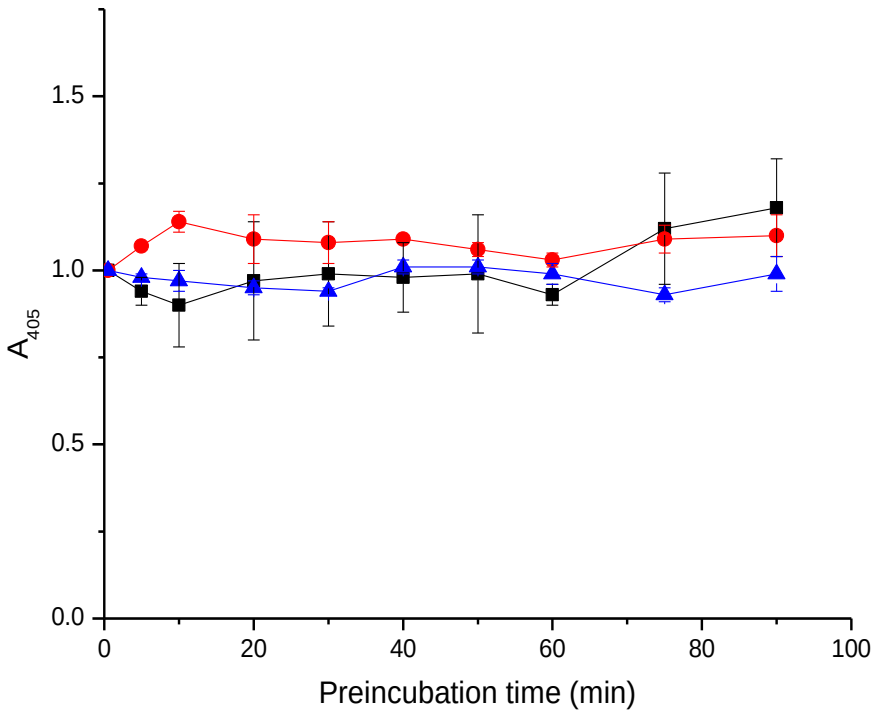

Figure III-6. Enzyme activity of VHR with DTT in Enzyme Dilution Buffer and with or without Thiol in 3 Component Reaction Buffer. Enzyme dilution buffer contained DTT in all cases, but reaction buffer contained DTT, (■) or β-mercaptoethanol (●), or did not contain DTT or β-mercaptoethanol (▲).

3.6. Summary and Conclusion

VHR was successfully overexpressed in an *E. coli* expression system. VHR was also proved to be stable at 4 °C for at least 10 days. When the enzyme was diluted in a buffer containing DTT, the enzyme activity of VHR was essentially identical in different reaction buffers regardless of the presence of an additional thiol reagent.

References;

1. Cozzone, A. J. *Annu. Rev. Microbiol.* **1988**, *42*, 97–125.

2. Ciesla, J.; Fraczyk, T.; Rode, W. *Acta Biochim. Pol.* **2011**, *58*, 137-147.

3. Stock, J. B.; Ninfa, A. J.; Stock, A. M. *Microbiol. Rev.* **1989**, *53*, 450–490.

4. Deutscher, J.; Saier, M. H. *J. Mol. Microbiol. Biotechnol.* **2005**, *9*, 125-131.

5. Walton, K. M.; Dixon, J. E. *Annu. Rev. Biochem.* **1993,** *62*, 101-120.

6. Hornberg, J. J.; Bruggerman, F. J.; Binder, B.; Geest, C. R.; de Vaate A. J.; Lankelma, J.; Heinrich, R.; Westerhoff, H. V. *FEBS J.* **2005**, *272*, 244-258.

7. Fischer, E. H.; Charbonneau, H.; Tonks, N. K. *Science* **1991**, *253*, 401-406.

8. Alonso, A.; Sasin, J.; Bottini, N.; Friedberg, I.; Osterman, A.; Godzik, A.; Hunter, T.; Dixon, J.; Mustelin, T. *Cell* **2004**, *117*, 699-711.

9. van Hooft, H. R. *Gene* **1998**, *225*, 1-8.

10. Andersen, J. N.; Mortensen, O. H.; Peters, G. H.; Drake, P. G.; Iversen, L. F.; Olsen, O. H.; Jansen, P. G.; Andersen, H. S.; Tonks, N.

K.; Moller, N. P. H. *Mol. Cell Biol.* **2001**, *21*, 7117-7136.

11. Tonks, N. K.; Neel, B. G. *Curr. Opin. Cell Biol.* **2001**, *13*, 182-195.

12. Pathak, M. K.; Yi, T. *J. Imunol.* **2001**, *67*, 3391-3397.

13. Higashi, H.; Tsutumi, R.; Muto, S.; Sugiyama, T.; Azuma, T.; Asaka, M.; Hatakeyma, M. *Science* **2002**, *295*, 683-686.

14. Byth, K. F.; Conroy, L. A.; Howlett, S.; Smith, A. J. H.; May, J.; Alexander, D. R.; Holmes, N. *J. Exp. Med.* **1996**, *183*, 1707–1718.

15. Saha, S.; Bardelli, A.; Buckhaults, P.; Velculescu, V. E.; Rago, C.; St. Croix, B.; Romans, K. E.; Choti, M. A.; Lengauer, C.; Kinzler, K. W.; Vogelstein, B. *Science* **2001**, *294*, 1343–1346.

16. Galaktionov, K.; Lee, K.; Eckstein, J.; Draetta, G.; Meckler, J.; Loda, M.; Beach, D. *Science* **1995**, *269*, 1575–1577.

17. Fachinger, G.; Deutsch, U.; Risau, W. *Oncogene* **1999**, *18*, 5948–5953.

18. McLean, J.; Batt, J.; Doering, L. C.; Rotin, D.; Bain, J. R. *J. Neurosci.* **2002**, *22*, 5481–5491.

19. Buckley, D. A.; Cheng, A.; Kiely, P. A.; Tremblay, M. L.; O'Connor, R. *Mol. Cell. Biol.* **2002**, *22*, 1998–2010.

20. Suhr, S. M.; Pamula, S.; Baylink, D. J.; Lau, K.-H. *J. Bone Miner. Res.* **2001**, *16*, 1795–1803.

21. Schmidt, A.; Rutledge, S. J.; Endo, N.; Opas, E. E.; Tanaka, H.; Wesolowski, G.; Leu, C. T.; Huang, Z.; Ramachandran, C.; Rodan, S. B.; Rodan, G. A. *Proc. Natl. Acad. Sci. U.S.A.* **1996**, *93,* 3068–3073.

22. Jia, Z.; Barford, D.; Flintk, A. J.; Tonks, N. K. *Science* **1995**, *268,* 1754-1758.

23. Bhooshan Kafle, *A Dissertation for a Doctor of Philosophy;* **2011**, Department of Chemistry, Graduate School, Inha University, South Korea.

24. Tonks, N. K.; Diltz, C. D.; Fischer, E. H. *J. Biol. Chem*. **1988**, *263,* 6722-6730.

25. Barford, D.; Flint, A. J.; Tonks, N. K. *Science* **1994**, *263*, 1397-1404.

26. Kamerlin, S. C. L.; Rucker, R.; Boresch, S. *Biochem. Biophys. Res. Commun.* **2007**, *356,* 1011–1016.

27. Dunn, D.; Chen, L.; Lawrence, D. S.; Zhang, Z. Y. *J. Biol. Chem*. **1996**, *271*, 168–173.

28. Yuvaniyama, J.; Denu, J. M.; Dixon, J. E.; Saper, M. A., *Science* **1996**, *272*, 1328–1331.

29. Stewart, A. E.; Dowd, S.; Keyse, S. M.; McDonald, N. Q. *Nat. Struct. Biol*. **1999**, *6*, 174–181.

30. Puius, Y. A.; Zhao, Y.; Sullivan, M.; Lawrence, D. S.; Zhang, Z. Y. *Proc.*

Natl. Acad. Sci. U.S.A. **1997**, *94*, 13420–13425.

31. Hadjuk, P. J.; Meadows, R. P.; Fesik, S. W. *Science* **1997**, *278*, 497–499.

32. Groves, M. R.; Yao, Z. J.; Roller, P. P.; Burke, T. R.; Barford, D. *Biochemistry* **1998**, *37*, 17773–17783.

33. Ward, C. W.; Lawrence, M. C. *Bioessays* **2009**, *31*, 422–434.

34. White, M. F.; Kahn C. R. *J. Biol. Chem.* **1994**, *269*, 1–4.

35. Gustafson, T. A.; Moodie, S. A.; Lavan, B. E. *Rev. Physiol. Biochem. Pharmacol.* **1999**, *137*, 71–190.

36. Taha, C.; Klip, A. *J. Membr. Biol.* **1999**, *169*, 1–12.

37. Seely, B. L.; Staubs, P. A.; Reichart, D. R.; Berhanu, P.; Milarski, K. L.; Saltiel, A. R., Kusari, J.; Olefsky, J. M. *Diabetes* **1996**, *45*, 1379–1385.

38. Ahmad, F.; Li, P. M.; Meyerovitch, J.; Goldstein, B. J. *J. Biol. Chem.* **1995**, *270*, 20503–20508.

39. Suzuki, T.; Hiroki, A.; Watanabe, T.; Yamashita, T.; Takei, I.; Umezawa, K. *J. Biol. Chem.* **2001**, *276*, 27511–27518.

40. Kruszynska, Y. T.; Olefsky, J. M. *J. Investig. Med.* **1996**, *44*, 413–428.

41. Xie, L.; Lee, S. Y.; Andersen, J. N.; Waters, S.; Shen, K.; Guo, X. L;

Moller, N. P.; Olefsky, J. M.; Lawrence, D. S.; Zhang, Z. Y. *Biochemistry* **2003**, *42*, 12792–12804.

42. Goldstein, B. J.; Ahmad, F.; Ding, W.; Li, P. M.; Zhang, W. R. *Mol. Cell. Biochem.* **1998**, *182*, 91–99.

43. Elchebly, M.; Payette, P.; Michaliszyn, E.; Cromlish, W.; Collins, S.; Loy, A. L.; Normandin, D.; Cheng, A.; Himms-Hagen, J.; Chan, C-C.; Ramachandran, C.; Gresser, M. J.; Tremblay, M. L.; Kennedy, B. P. *Science* **1999**, *283*, 1544–1548.

44. Klaman, L. D.; Boss, O.; Peroni, O. D.; Kim, J. K.; Martino, J. L.; Zabolotny, J. M.; Moghalj, N.; Lubkin, M.; Kim, Y, B.; Sharpe, A. H.; Krongrad, A. S.; Shulman, G. I.; Neel, B. G.; Kahn, B. B. *Mol. Cell. Biol.* **2000**, *20*, 5479–5489.

45. Fei, H.; Okano, H. J.; Li, C.; Lee, G. H.; Zhao, C.; Darnell, R.; Friedman, J. M. *Proc. Natl. Acad. Sci. U.S.A.* **1997**, *94*, 7001–7005.

46. Ahima, R. S.; Flier, J. S. *Annu. Rev. Physiol.* **2000**, *62*, 413–437.

47. Cook, W. S.; Unger, R. H. *Dev. Cell* **2002**, *2*, 385–387.

48. Cheng, A.; Uetani, N.; Simoncic, P. D.; Chaubey, V. P.; Lee-Loy, A. McGlade, C. J.; Kennedy, B. P.; Tremblay, M. L. *Dev. Cell* **2002**, *2*, 497–503.

49. Kopelman, P. G. *Nature* **2000**, *404*, 635–643.

50. Gan, D., ed. *International Diabetes Federation Diabetes Atlas* **2003**, ISBN 2–930229–27–6, pp 360.

51. Skyler, J. S. *J. Med. Chem.* **2004**, *47*, 4113–4117.

52. Zimmet, P.; Alberti, K. G.; Shaw, J. *Nature* **200**, *414*, 782–787.

53. Simpson, R. W.; Shaw, J. E.; Zimmet, P. Z. *Diabetes Res. Clin. Pract.* **2003**, *59*, 165–180.

54. Hall, J. E. *Hypertension* **2003**, *41*, 625–633.

55. Poirier, P.; Despres, J. P. *Med. Sci. (Paris)* **2003**, *19*, 943–949.

56. Bianchini, F.; Kaaks, R.; Vainio, H. *Obes. Rev.* **2002**, *3*, 5–8.

57. Conway, B.; Rene, A. *Obes. Rev.* **2004**, *5*, 145–151.

58. Young, T.; Peppard, P. E.; Gottlieb, D. J. *Am. J. Respir. Crit. Care Med.* **2002**, *165*, 1217–1239.

59. Clouston, A. D.; Powell, E. E. *Intern. Med. J.* **2004**, *34*, 187–191.

60. Dixon, J. B.; Dixon, M. E.; O'Brien, P. E. *Arch. Intern. Med.* **2003**, *163*, 2058–2065.

61. Saltiel, A. R.; Kahn, C. R. *Nature* **2001**, *414*, 799–806.

62. Mertins, P.; Eberl, C. H.; Renkawitz, J.; Olsen, V. J.; Tremblay, L. M.; Ullrich, A.; Daub, H. *Mol. Cell. Proteomics* **2008**, *7*, 1763–1777.

63. Zhao, H.; Liu, G.; Xin, Z.; Serby, M. D.; Pei, Z.; Szczepankiewicz, B. G.; Hajduk, P. J.; Abad–Zapatero, C.; Hutchins, C. W.; Lubben, T. H.; Ballaron, S. J.; Haasch, D. L.; Kaszubska, W.; Rondinone, C. M.; Trevillyan, J. M.; Jirousek, M. R. *Bioorg. Med. Chem. Lett.* **2004**, *14*, 5543–5546.

64. Thompson, K. H.; McNeill, J. H.; Orvig, C. *Chem. Rev.* **1999**, *99*, 2561–2572.

65. Poucheret, P.; Verma, S.; Grynpas, M. D.; McNeill, J. H. *Mol. Cell. Biochem.* **1998**, *188*, 73–80.

66. Huyer, G.; Liu, S.; Kelly, J.; Moffat, J.; Payette, P.; Kennedy, B.; Tsaprailis, G.; Gresser, M. J.; Ramachandran, C. *J. Biol. Chem.* **1997**, *272*, 843–851.

67. Taylor, S. D. *Curr. Top. Med. Chem.* **2003**, 3, 759–782.

68. Cebula, R. E.; Blanchard, J. L.; Boisclair, M. D.; Pal, K.; Bockovich, N. J. *Bioorg. Med. Chem. Lett.* **1997**, *7*, 2015–2020.

69. Han, Y.; Belley, M.; Bayly, C. I.; Colucci, J.; Dufresne, C.; Giroux, A.; Lau, C. K.; Leblanc, Y.; McKay, D.; Therien, M.; Wilson, M. C.; Skorey, K.; Chan, C. C.; Scapin, G.; Kennedy, B. P. *Bioorg. Med. Chem. Lett.* **2008**, *18*, 3200–3205.

70. Lau, C. K.; Bayly, C. I.; Gauthier, J. Y.; Li, C. S.; Therien, M.; Asante–Appiah, E.; Cromlish, W.; Boie, Y.; Forghani, F.; Desmarais, S.; Wang, Q.; Skorey, K.; Waddleton, D.; Payette, P.; Ramachandran, C.; Kennedy, B. P.; Scapin, G. *Bioorg. Med. Chem. Lett*. **2004**, *14*, 1043–1048.

71. Dufresne, C.; Roy, P.; Wang, Z.; Asante–Appiah, E.; Cromlish, W.; Boie, Y.; Forghani, F.; Desmarais, S.; Wang, Q.; Skorey, K.; Waddleton, D.; Ramachandran, C.; Kennedy, B. P.; Xu, L.; Gordon, R.; Chan, C. C.; Leblanc, Y. *Bioorg. Med. Chem. Lett.* **2004**, *14*, 1039–1042.

72. Holmes, C. P.; Li, X.; Pan, Y.; Xu, C.; Bhandari, A.; Moody, C. M.; Miguel, J. A.; Ferla, S. W.; De Francisco, M. N.; Frederick, B. T.; Zhou, S.; Macher, N.; Jang, L.; Irvine, J. D.; Grove, J. R. *Bioorg. Med. Chem. Lett.* **2005**, *15*, 4336–4341.

73. Klopfenstein, S. R.; Evdokimov, A. G.; Colson, A. O.; Fairweather, N. T.; Neuman, J. J.; Maier, M. B.; Gray, J. L.; Gerwe, G. S.; Stake, G. E.; Howard, B. W.; Farmer, J. A.; Pokross, M. E.; Downs, T. R.; Kasibhatla, B.; Peters, K. G. *Bioorg. Med. Chem. Lett.* **2006**, *16*, 1574–1578.

74. Gray, J. L; *PCT Int. Appl.* WO2008002570, **2008**, 166 pp, (The Procter & Gamble Company).

75. Liu, G.; Xin, Z.; Pei, Z.; Hajduk, P. J.; Abad–Zapatero, C.; Hutchins, C. W.; Zhao, H.; Lubben, T. H.; Ballaron, S. J.; Haasch, D. L.; Kaszubska, W.; Rondinone, C. M.; Trevillyan, J. M.; Jirousek, M. R.

J. Med. Chem. **2003**, *46*, 4232–4235.

76. Xin, Z.; Liu, G.; Abad–Zapatero, C.; Pei, Z.; Szczepankiewicz, B. G.; Li, X.; Zhang, T.; Hutchins, C. W.; Hajduk, P. J.; Ballaron, S. J.; Stashko, M. A.; Lubben, T. H.; Trevillyan, J. M.; Jirousek, M. R. *Bioorg. Med. Chem. Lett.* **2003**, *13*, 3947–3950.

77. Andersen, H. S.; Olsen, O. H.; Iverson, L. F.; Sorensen, A. L. P.; Mortensen, S. B.; Christensen, M. S.; Branner, S.; Hansen, T. K.; Lau, J. F.; Jeppesen, L.; Moran, E. J.; Su, J.; Bakir, F.; Judge, L.; Shahbaz, M.; Collins, T.; Vo, T.; Newman, M. J.; Ripka, W. C.; Moller, N. P. H. *J. Med. Chem.* **2002**, *45*, 4443–4459.

78. Adams, D. R.; Abraham, A.; Asano, J.; Breslin, C.; Dick, C. A. J.; Ixkes, U.; Johnston, B. F.; Johnston, D.; Kewnay, J.; Mackay, S. P.; MacKenzie, S. J.; McFarlane, M.; Mitchell, L.; Spinks, D.; Takano, Y. *Bioorg. Med. Chem. Lett.* **2007**, *17*, 6579–6583.

79. Van Zandt, M. C. *PCT Int. Appl.* WO2008033455, **2008**, 221 (The Institute for Pharmaceutical Discovery, LLC).

80. Wilson, D. P.; Wan, Z. K.; Xu, W. X.; Kirincich, S. J.; Follows, B. C.; Joseph–McCarthy, D.; Foreman, K.; Moretto, A.; Wu, J.; Zhu, M.; Binnun, E.; Zhang, Y. L.; Tam, M.; Erbe, D. V.; Tobin, J.; Xu, X.; Leung, L.; Shilling, A.; Tam, S. Y.; Mansour, T. S.; Lee. J. *J. Med. Chem.* **2007**, *50*, 4681–4698.

81. Black, E.; Breed, J.; Breeze, A. L.; Embrey, K.; Garcia, R.; Gero, T. W.; Godfrey, L.; Kenny, P. W.; Morley, A. D.; Minshull, C. A.; Pannifer,

A. D.; Read, J.; Rees, A.; Russell, D. J.; Toader, D.; Tucker, J. *Bioorg. Med. Chem. Lett.* **2005**, *15*, 2503–2507.

82. Traurig, M.; Hanson, R. L.; Kobes, S.; Bogardus, C.; Baier, L. J. *Diabetologia* **2007**, *50,* 985-989.

83. Combs, A. P.; Yue, E. W.; Bower, M.; Ala, P. J.; Wayland, B.; Douty, B.; Takvorian, A.; Polam, P.; Wasserman, Z.; Zhu, W.; Crawley, M. L.; Pruitt, J.; Sparks, R.; Glass, B.; Modi, D.; McLaughlin, E.; Bostrom, L.; Li, M.; Galya, L.; Blom, K.; Hillman, M.; Gonneville, L.; Reid, B. G.; Wei, M.; Becker–Pasha, M.; Klabe, R.; Huber, R.; Li, Y.; Hollis, G.; Burn, T. C.; Wynn, R.; Liu, P.; Metcalf, B. *J. Med. Chem.* **2005**, *48,* 6544–6548.

84. Combs, A. P.; Zhu, W.; Crawley, M. L.; Glass, B.; Polam, P.; Sparks, R. B.; Modi, D.; Takvorian, A.; McLaughlin, E.; Yue, E. W.; Wasserman, Z.; Bower, M.; Wei, M.; Rupar, M.; Ala, P. J.; Reid, B. M.; Ellis, D.; Gonneville, L.; Emm, T.; Taylor, N.; Yeleswaram, S.; Li, Y.; Wynn, R.; Burn, T. C.; Hollis, G.; Liu, P. C.; Metcalf, B. *J. Med. Chem.* **2006**, *49*, 3774–3789.

85. Sparks, R. B.; Polam, P.; Zhu, W.; Crawley, M. L.; Takvorian, A.; McLaughlin, E.; Wei, M.; Ala, P. J.; Gonneville, L.; Taylor, N.; Li, Y.; Wynn, R.; Burn, T. C.; Liu, P. C.; Combs, A. P. *Bioorg. Med. Chem. Lett.* **2007**, *17*, 736–740.

86. Douty, B.; Wayland, B.; Ala, P. J.; Bower, M. J.; Pruitt, J.; Bostrom, L.; Wei, M.; Klabe, R.; Gonneville, L.; Wynn, R.; Burn, T. C.; Liu, P. C. C.; Combs, A. P.; Yue, E. W. *Bioorg. Med. Chem. Lett.* **2008**, *18*,

66–71.

87. Wan, Z. K.; Follows, B.; Kirincich, S.; Wilson, D.; Binnun, E.; Xu, W.; Joseph–McCarthy, D.; Wu, J.; Smith, M.; Zhang, Y. L.; Tam, M.; Erbe, D.; Tam, S.; Saiah, E.; Lee, J. *Bioorg. Med. Chem. Lett.* **2007**, *17*, 2913–2920.

88. Barnes, D.; Coppola, G. M.; Stams, T.; Topiol, S. W. *PCT Int. Appl.* WO2007067612, **2007**, 29 (Novartis A.–G., Switzerland, Novartis pharma G.M.B.H.).

89. Barnes, D.; Bebernitz, G. R.; Coppola, G. M.; Stams, T.; Topiol, S. W.; Vedananda, T. R.; Wareing, J. R. *PCT Int. Appl.* WO2007067613, **2007**, 108 (Novartis A.–G., Switzerland, Novartis pharma G.M.B.H.).

90. Park, H.; Bhattarai, B. R.; Ham, S. W.; Cho H. *Eur. J. Med. Chem.* **2009**, *44*, 3280–3284.

91. Bharat Raj Bhattarai, *A Dissertation for a Doctor of Philosophy;* **2009**, Department of Chemistry, Graduate School, Inha University, South Korea.

92. Shim, Y. S.; Kim, K. C.; Lee, K. A.; Shrestha, S.; Lee, K. H.; Kim, C. K.; Cho, H. *Bioorg. Med. Chem.* **2005**, *13*, 1325–1332.

93. Suja Shrestha, *A Dissertation for a Doctor of Philosophy;* **2007**, Department of Chemistry, Graduate School, Inha University, South Korea.

94. Bhattarai, B. R.; Shrestha, S.; Ham, S. W.; Kim, K. R.; Cheon, H. G.; Lee, K. H.; Cho, H. *Bioorg. Med. Chem. Lett.* **2007**, *17*, 5357–5360.

95. Shrestha, S.; Bhatatrai, B. R.; Kafle, B.; Lee, K. H. and Cho, H. *Bioorg. Med. Chem.* **2008**, *16*, 8643–8652.

96. Jursic, B. S.; Neumann, D. M.; Bowdy, K. L.; Stevens, E. D. *J. Heterocyclic Chem*. **2004**, *41*, 233–246.

97. Driscoll, J. S.; Melnick, N. R.; Quinn, F. R.; Lomax, N.; Davignon, J. P.; Ing, R.; Abbott, B. J.; Congleton, G.; Dudeck, L. *Cancer Treat. Rep.* **1978**, *62*, 45–74.

98. Brewer, A. D.; Minatelli, J. A.; Plowman, J.; Paull, K. D.; Narayaman, V. L. *Biochem. Pharmacol.* **1985**, *34*, 2047–2050.

99. Sundriyal, S.; Viswanad, B.; Ramarao, P.; Chakraborti, A. K.; Bharatam, P. V. *Bioorg. Med. Chem. Lett.* **2008**, *18*, 4959–4962.

100. Harriman, G. C.; Brewer, M.; Bennett, R.; Kuhn, C.; Bazin, M.; Larosa, G.; Skerker, P.; Cochran, N.; Gallant, D.; Baxter, D.; Picarella, D.; Jaffee, B.; Luly, J. R.; Briskin, M. J. *Bioorg. Med. Chem. Lett.* **2008**, *18*, 2509–2512.

101. Humar, M.; Pischke, S. E.; Loop, T.; Hoetzel, A.; Schmidt, R.; Klaas, C.; Pahl, H. L.; Geiger, K. K.; Pannen, B. H. J. *Mol. Pharmacol.* **2004**, *65*, 350–361.

102. Ishibashi, T.; Bottaro, D. P.; Chan, A.; Miki, T.; Aaronson, S. A.

Proc. Natl. Acad. Sci. U.S.A. **1992**, *89*, 12170–12174.

103. Rahmouni, S.; Cerignoli, F.; Alonso, A.; Tsutji, T.; Henkens, R.; Zhu, C.; Louis–dit–Sully, C.; Moutschen, M.; Jiang, W.; Mustelin, T. *Nat. Cell Biol.* **2006**, *8*, 524–531.

104. Alonso, A.; Rahmouni, S.; Williams, S.; van Stipdonk, M.; Jaroszewski, L.; Godzik, A.; Abraham, R. T.; Schoenberger, S. P.; Mustelin, T. *Nat. Immunol.* **2003**, *4*, 44–48.

105. Cui, J.; Zhang, M.; Zhang, Y. Q.; Xu, Z. H. *Acta Pharmacol. Sin.* **2007**, *28*, 601–608.

106. Weston, C. R.; Davis, R. J. *Cell Biol.* **2007**, *19*, 142–149.

107. Henkens, R.; Delvenne, P.; Arafa, M.; Moutschen, M.; Zeddou, M.; Tautz, L.; Boniver, J.; Mustelin, T.; Rahmouni, S. *BMC Cancer* **2008**, *8*, 147–155.

108. Alonso, A.; Saxena, M.; Williams, S.; Mustelin, T. *J. Biol. Chem.* **2001**, *276*, 4766–4771.

109. Canagarajah, B. J.; Khokhlatchev, A.; Cobb, M. H.; Goldsmith, E. J. *Cell* **1997**, *90*, 859–869.

110. Sewing, A.; Wiseman, B.; Lloyd, A. C.; Land, H. *Cell Biol.* **1997**, *17*, 5588–5597.

111. Zhou, G.; Denu, J. M.; Wu, L.; Dixon, J. E. *J. Biol. Chem*. 1994, *269*,

28084–28090.

112. Denu, J. M.; Zhou, G.; Guo, Y.; Dixon, J. E. *Biochemistry* **1995**, *34*, 3396–3403.

113. John, M. D.; Gaochao, Z.; Li, W.; Rong, Z.; Jirundon, Y.; Mark, A. S.; Jack, E. D. *J. Biol. Chem.* **1995**, *8*, 3796–3803.

APPENDICES

APPENDIX A: ^{1}H NMR Spectra of Phenyl urea Derivatives (DMSO-d_6, 400 MHz)

1-phenylurea **(II-2a)**

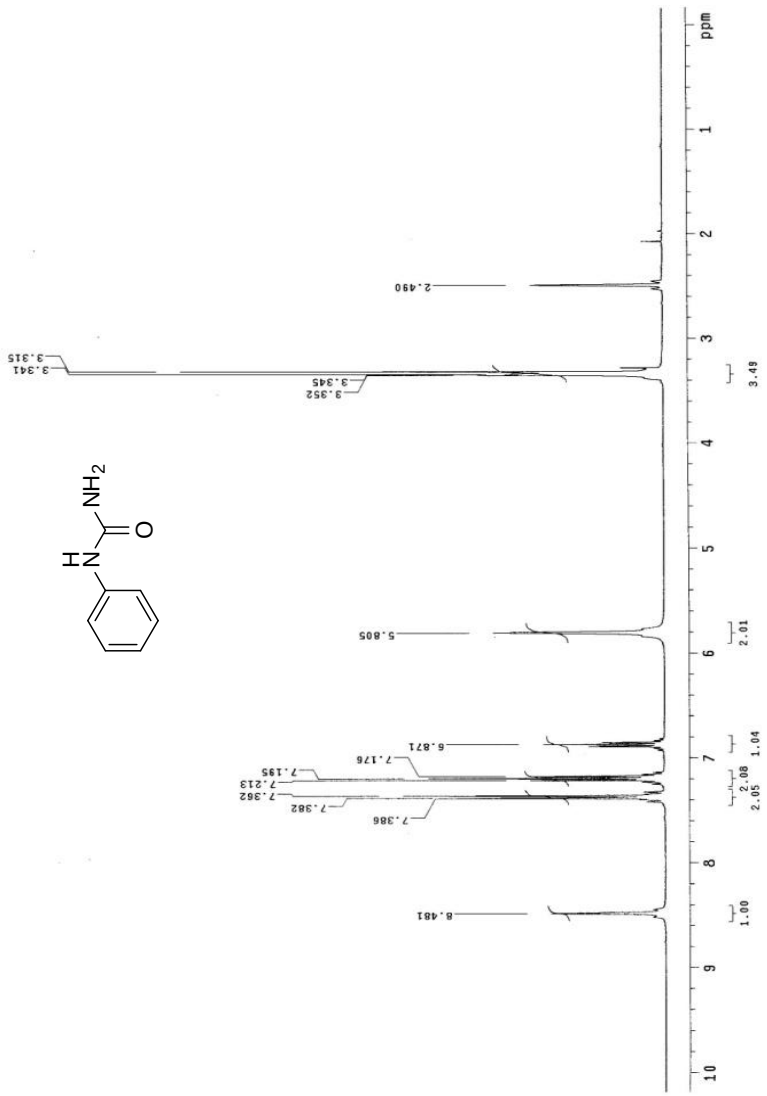

1-(4-methoxyphenyl)urea **(II-2b)**

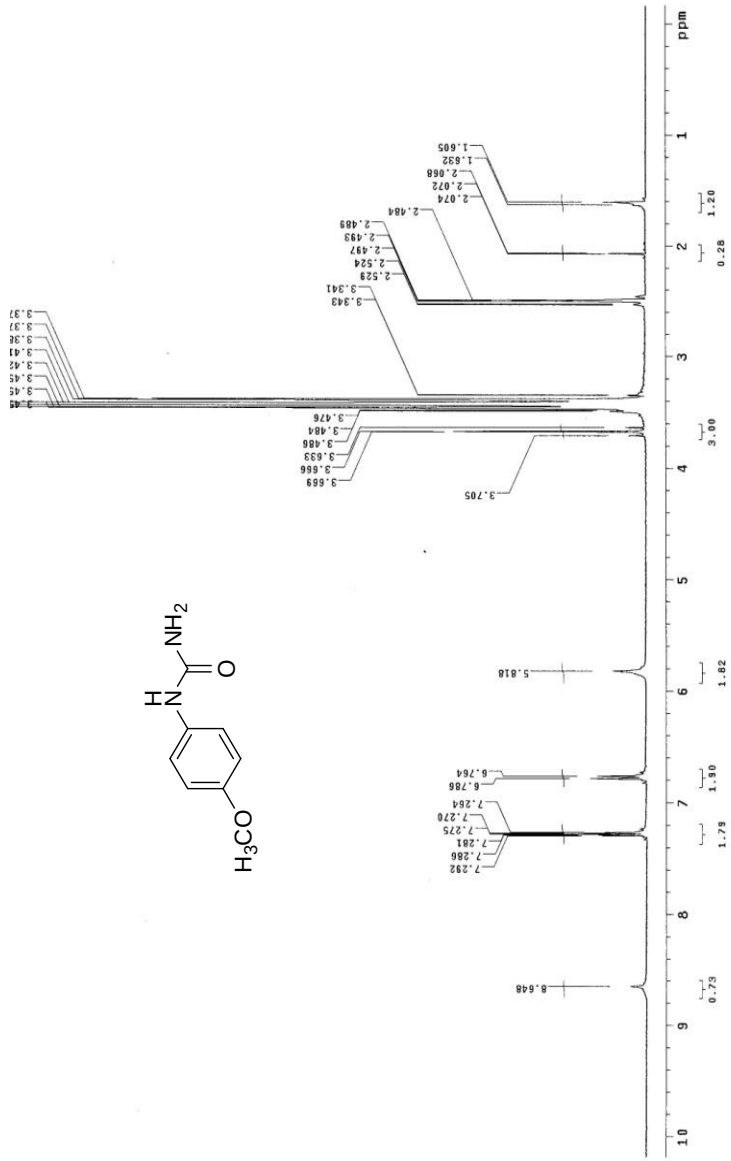

1-(4-nitrophenyl)urea **(II-2c)**

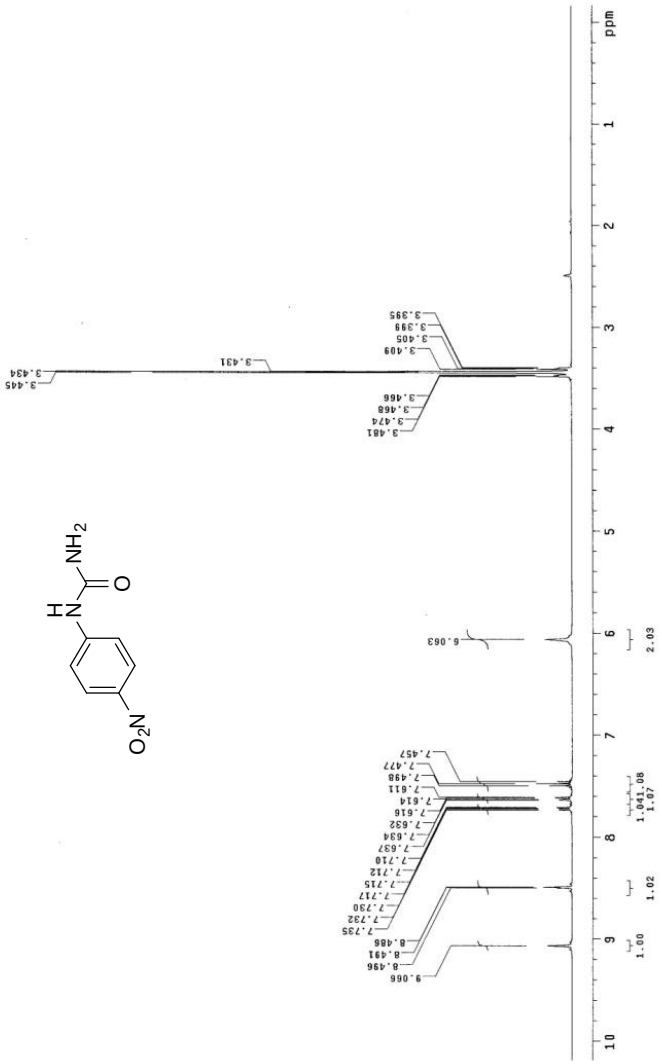

1-(3-chlorophenyl)urea **(II-2d)**

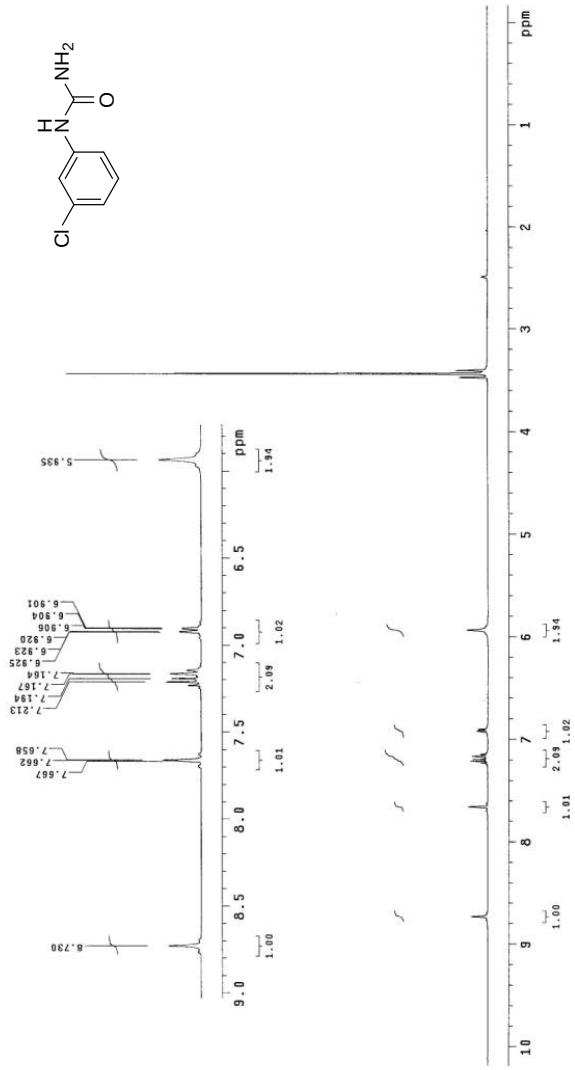

1-(3-(trifluoromethyl)phenyl)urea **(II-2e)**

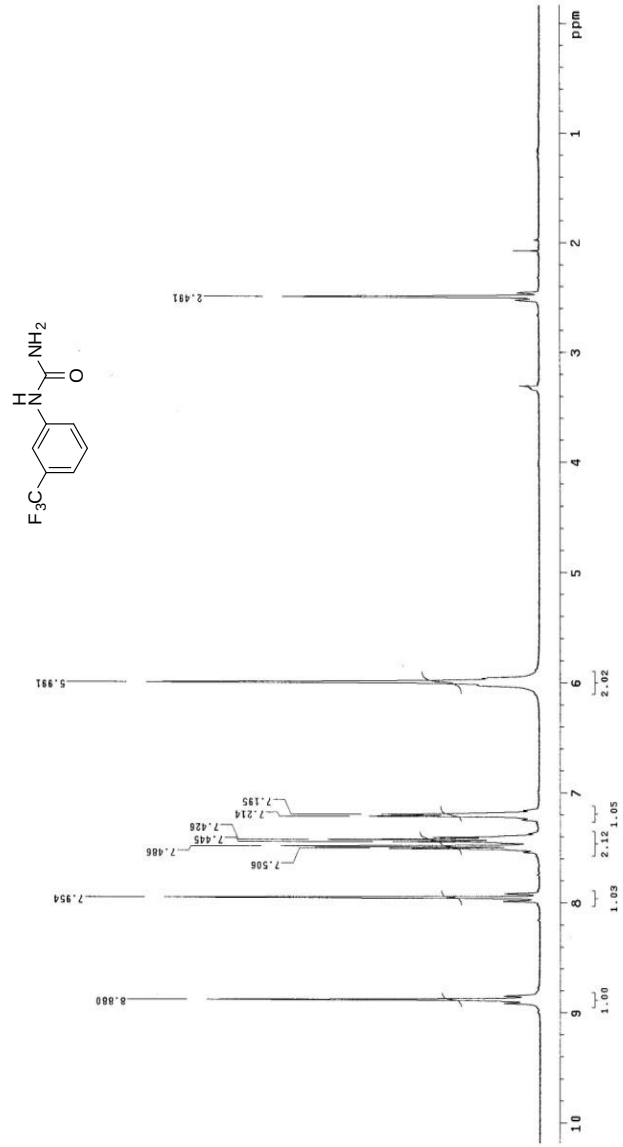

1-(4-fluorophenyl)urea **(II-2f)**

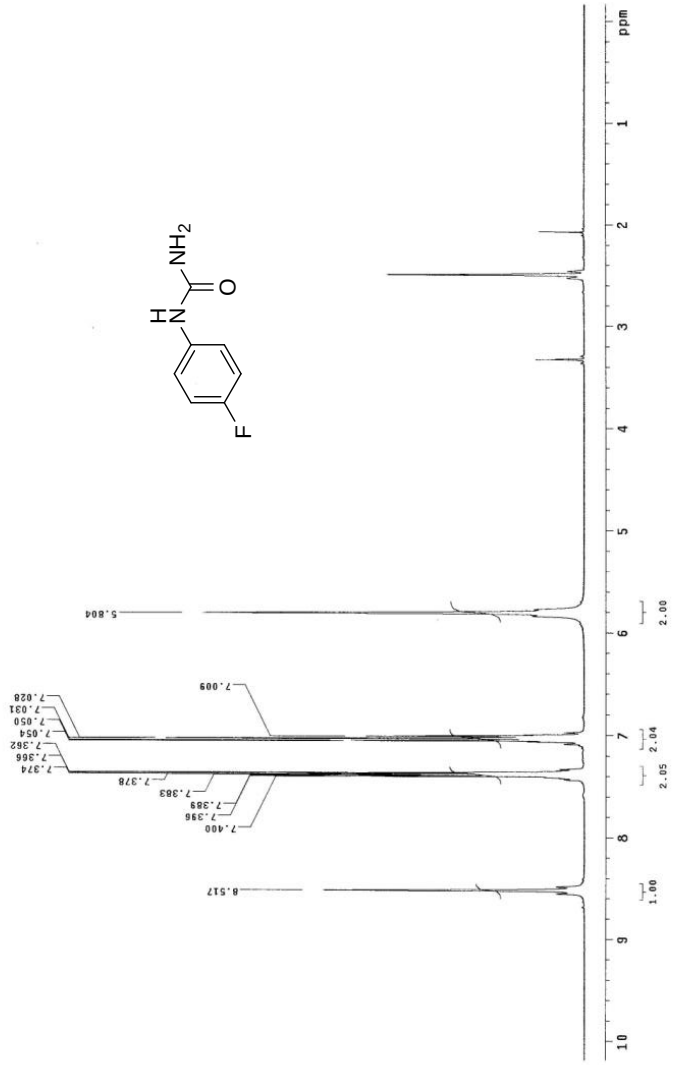

1-(3-methoxyphenyl)urea **(II-2g)**

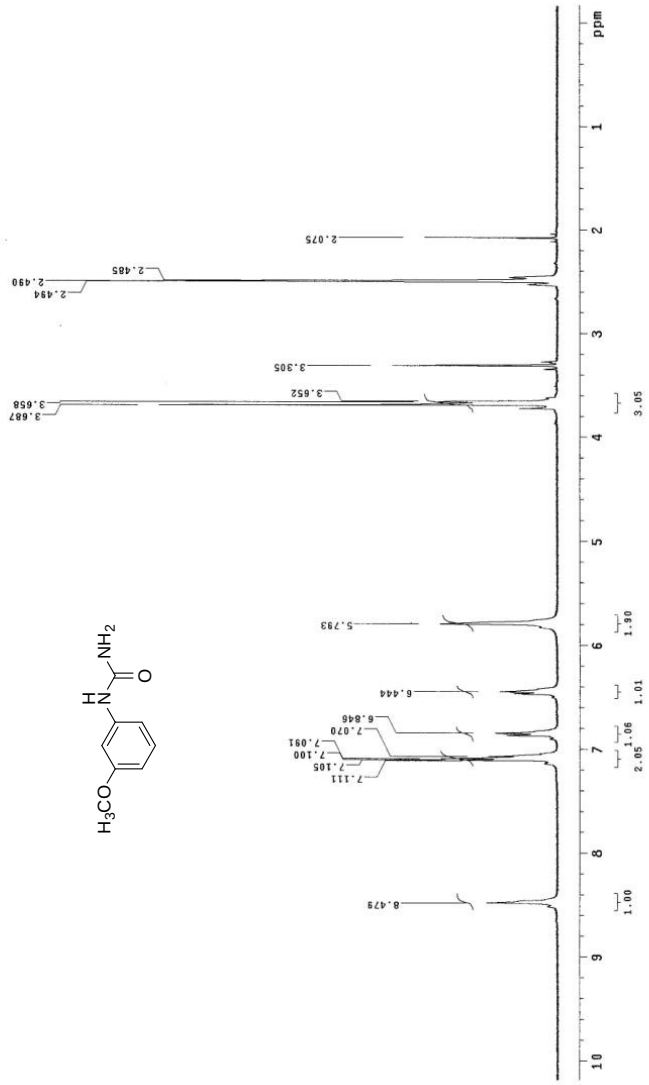

1-(4-(4-chlorophenoxy)phenyl)urea **(II-2h)**

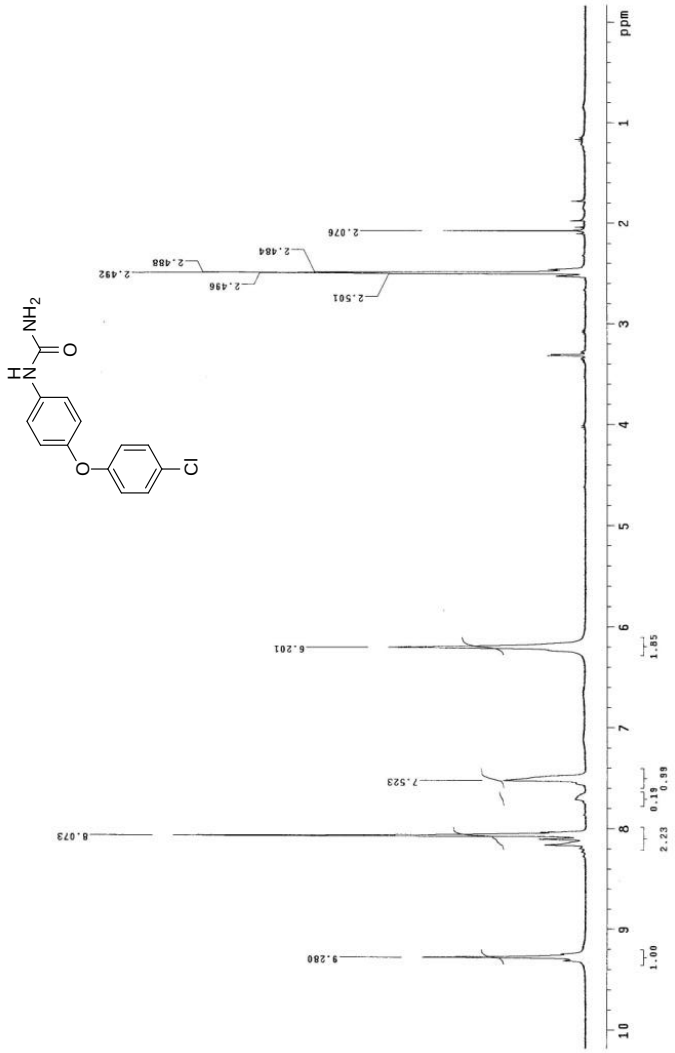

1-(3,5-bis(trifluoromethyl)phenyl)urea **(II-2i)**

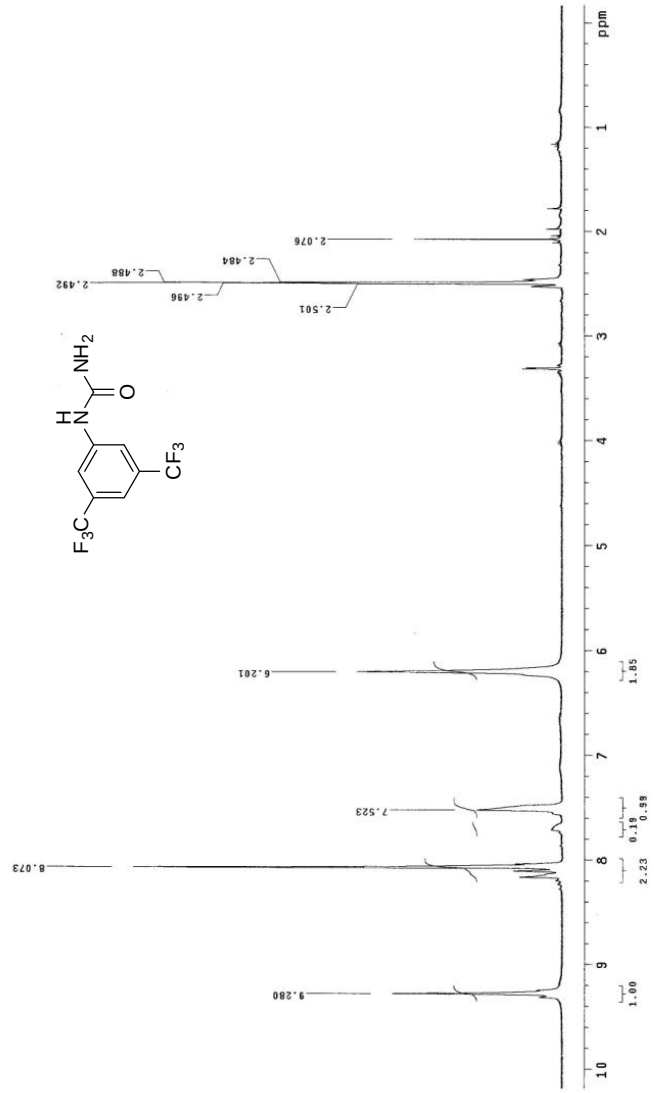

APPENDIX B. ^{1}H NMR Spectra of Monosubstituted Barbituric Acid Derivatives (DMSO-d_6, 400 MHz)

1-phenylpyrimidine-2,4,6(1H,3H,5H)-trione **(II-3a)**

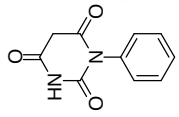

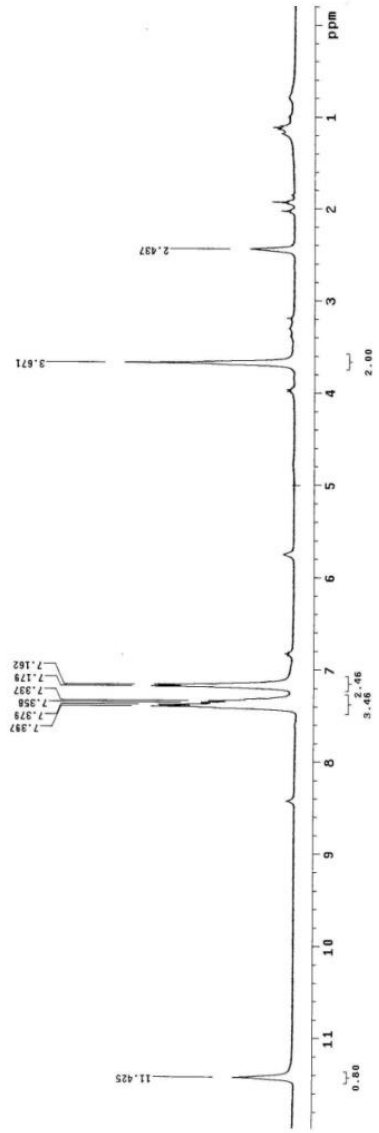

1-(4-methoxyphenyl)pyrimidine-2,4,6(1H,3H,5H)-trione **(II-3b)**

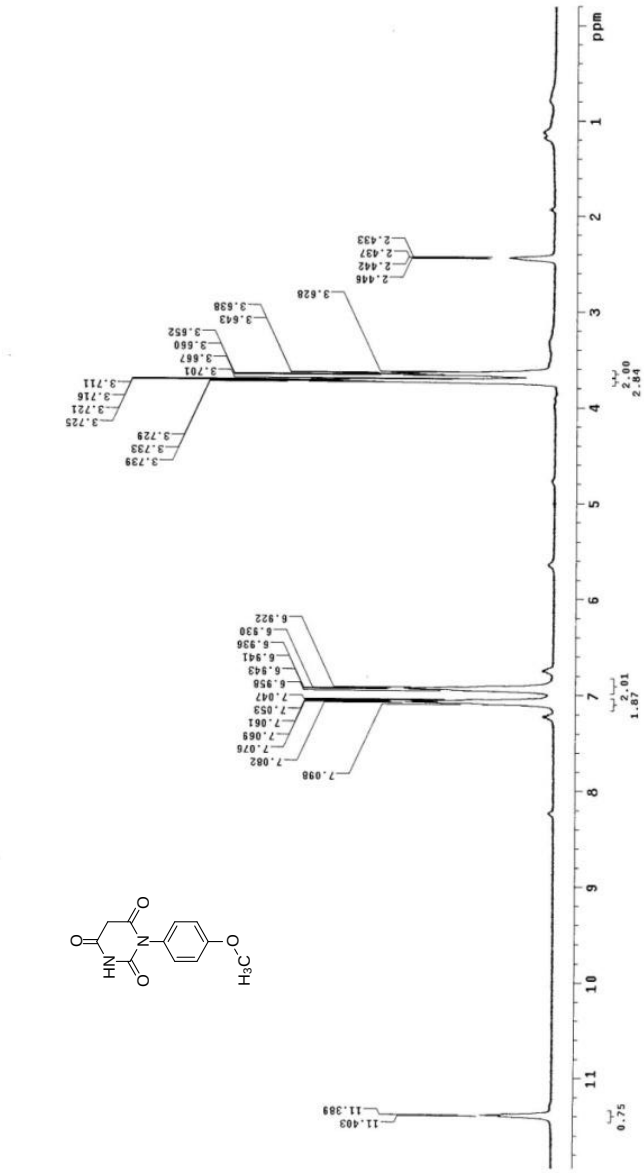

1-(3-nitrophenyl)pyrimidine-2,4,6(1H,3H,5H)-trione **(II-3c)**

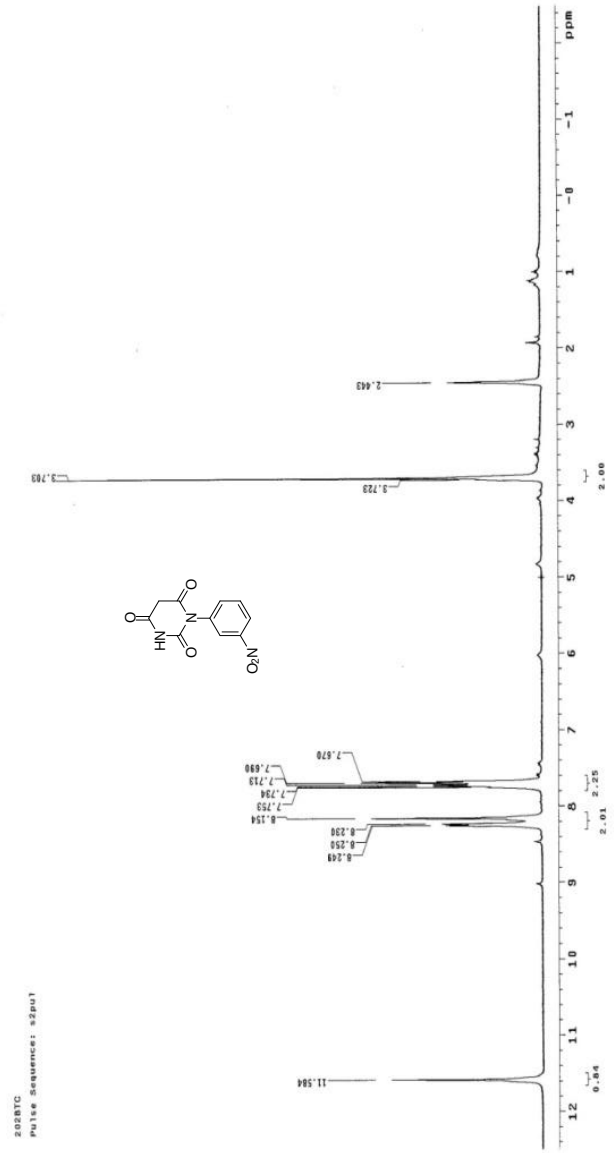

1-(3-chlorophenyl)pyrimidine-2,4,6(1H,3H,5H)-trione **(II-3d)**

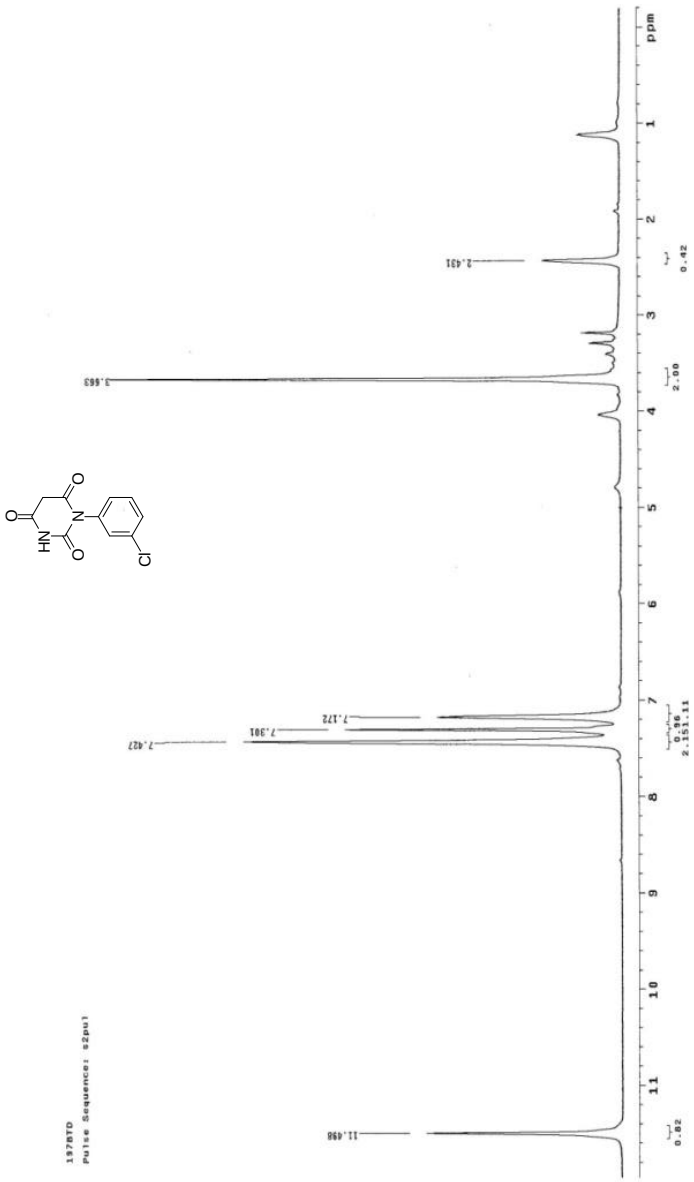

1-(3-(trifluoromethyl)phenyl)pyrimidine-2,4,6(1H,3H,5H)-trione **(II-3e)**

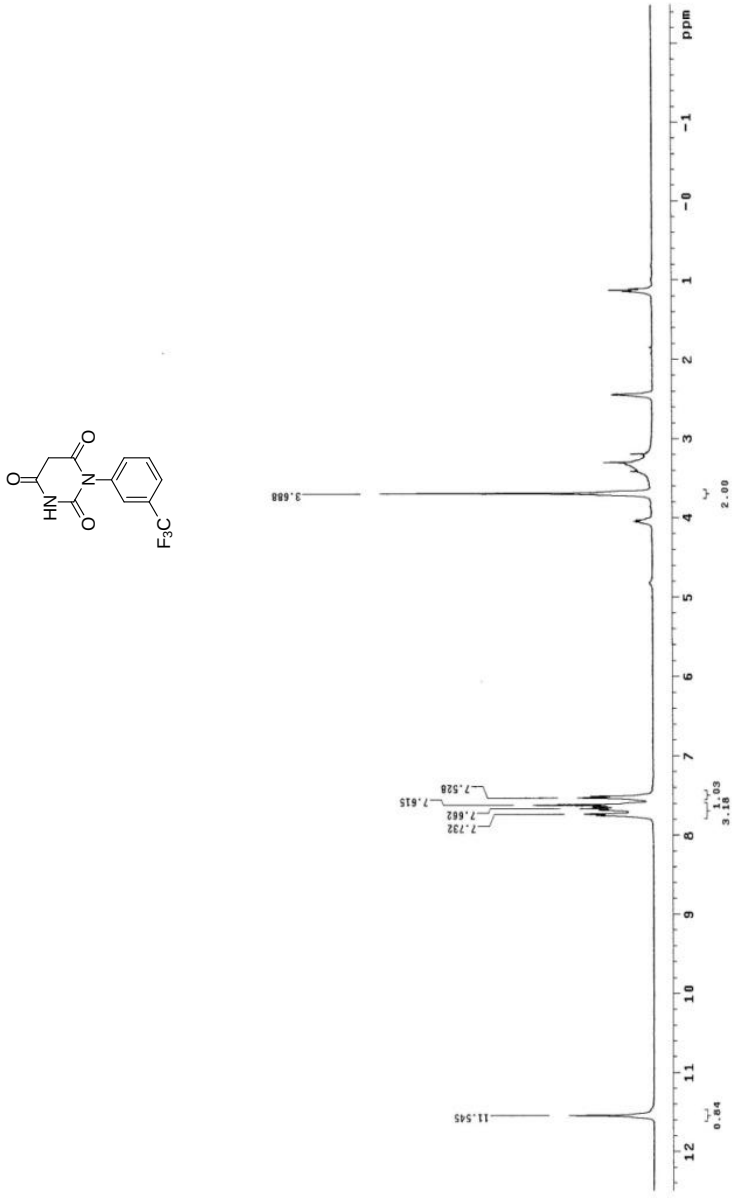

1-(3-fluorophenyl)pyrimidine-2,4,6(1H,3H,5H)-trione **(II-3f)**

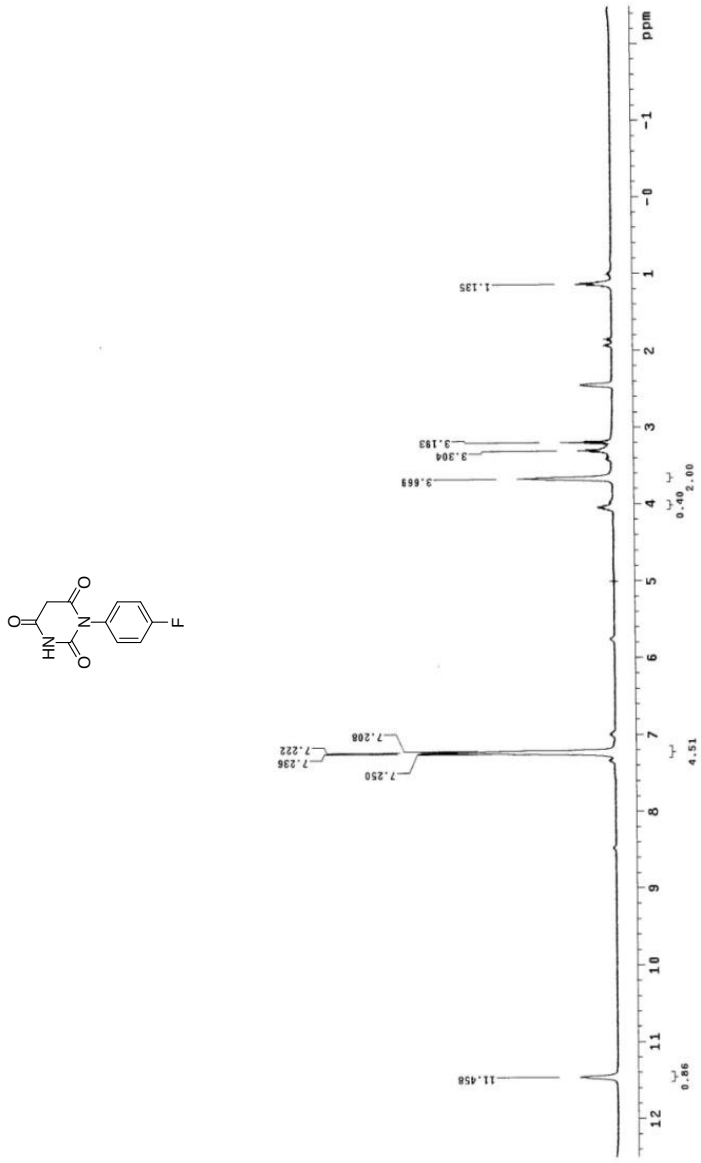

1-(3-methoxyphenyl)pyrimidine-2,4,6(1H,3H,5H)-trione **(II-3g)**

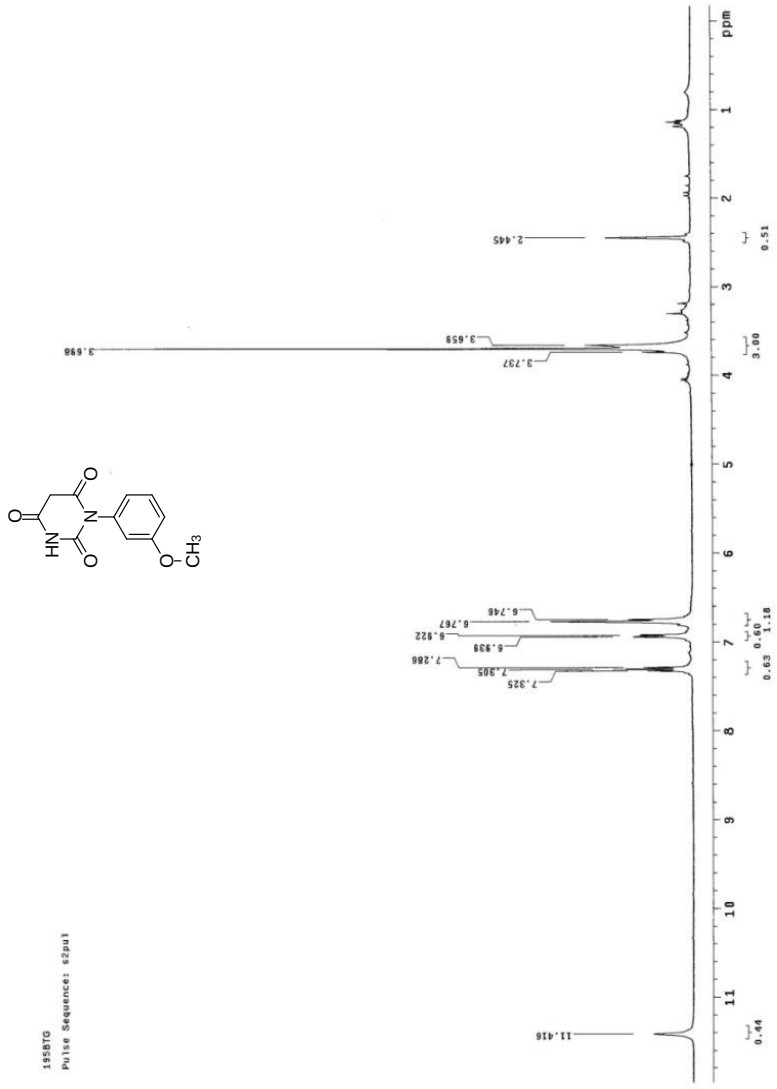

1-(4-(4-chlorophenoxy)phenyl)pyrimidine-2,4,6(1H,3H,5H)-trione **(II-3h)**

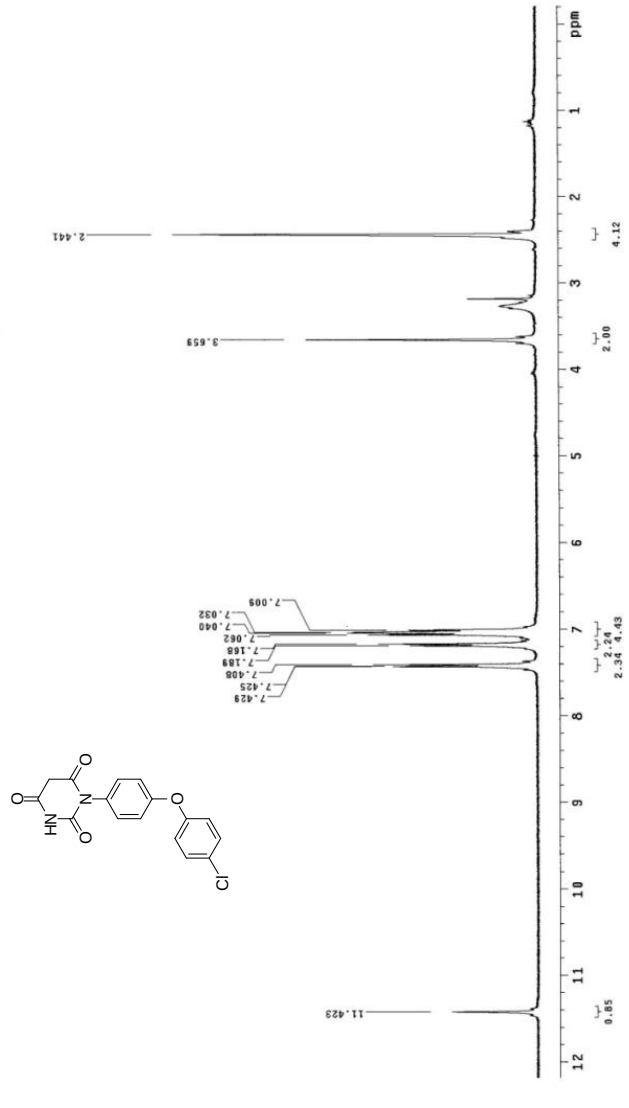

1-(3,5-bis(trifluoromethyl)phenyl)pyrimidine-2,4,6(1H,3H,5H)-trione **(II-3i)**

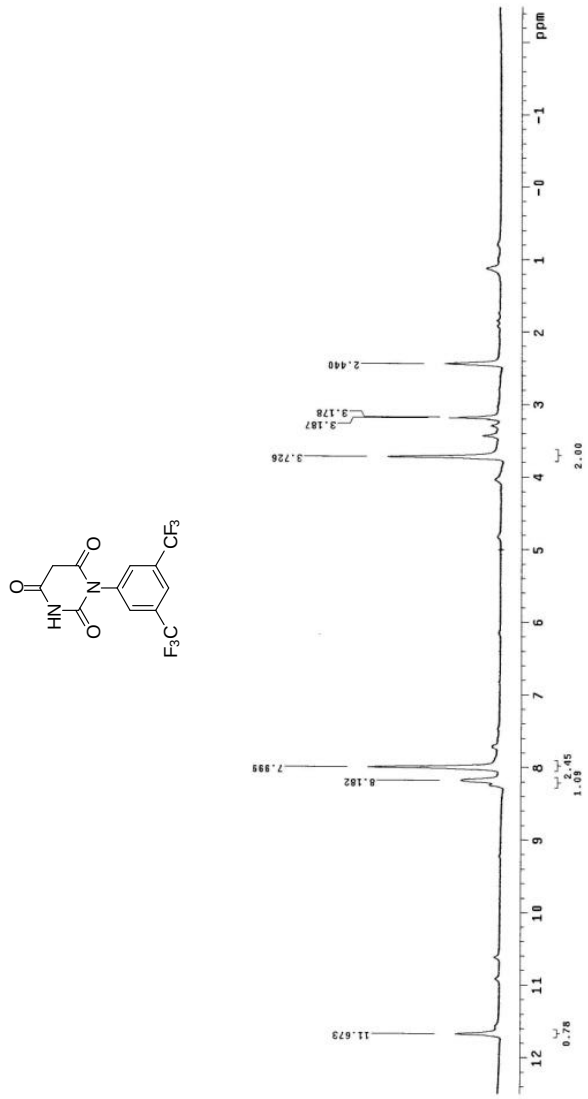

APPENDIX C. ^{1}H NMR of 3-Formyl Indole Derivatives ($CDCl_3$, 400 MHz)

1-benzyl-1H-indole-3-carbaldehyde (**II-4k)**

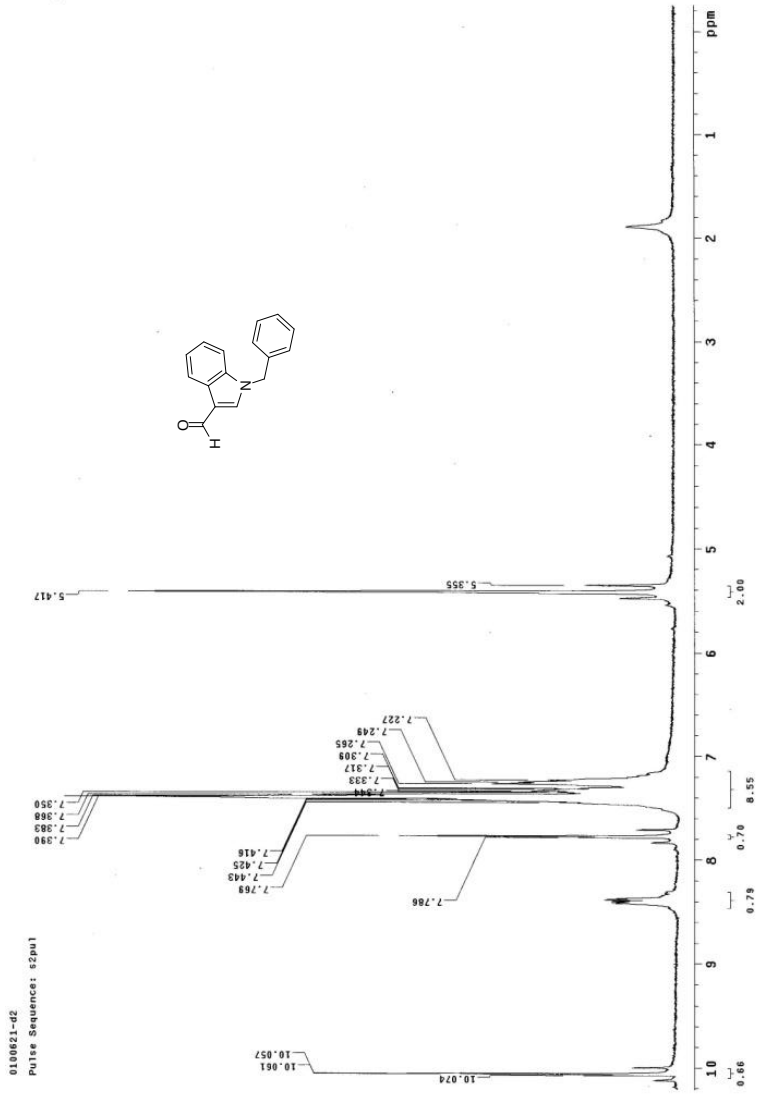

1-(3-chlorobenzyl)-1H-indole-3-carbaldehyde **(II-4l)**

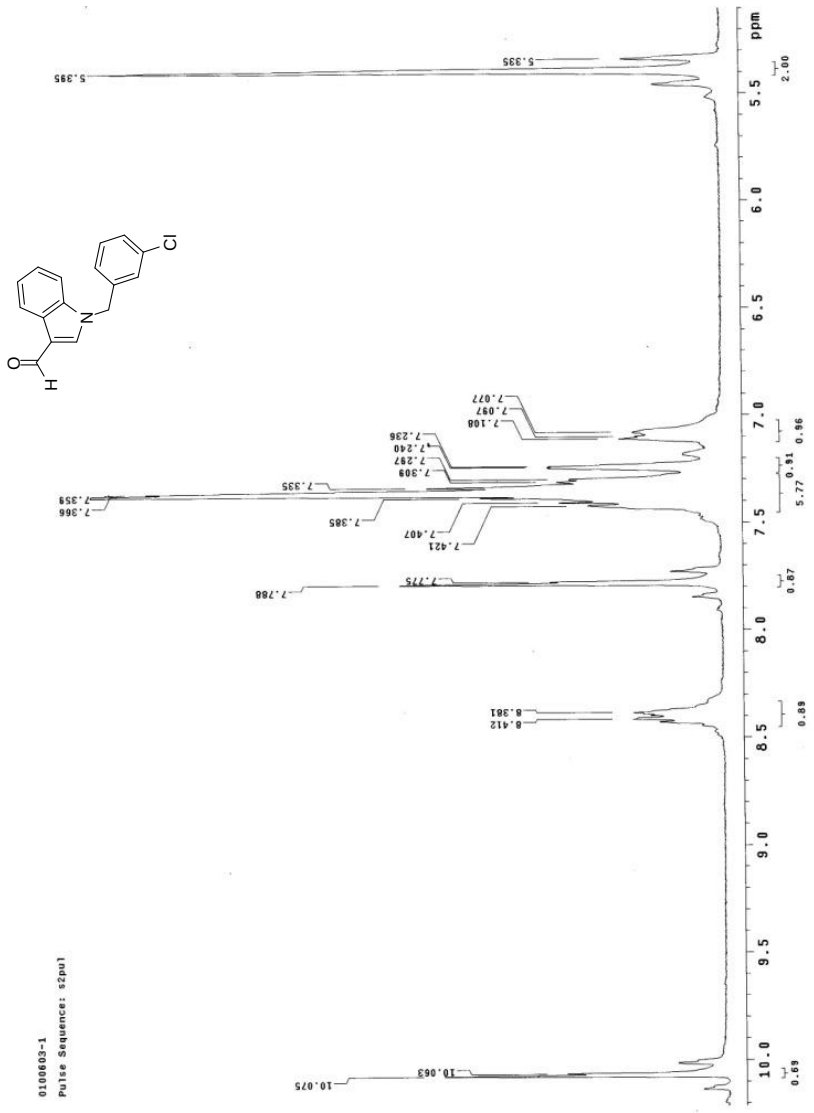

1-((4-methoxynaphthalen-1-yl)methyl)-1H-indole-3-carbaldehyde **(II-4m)**

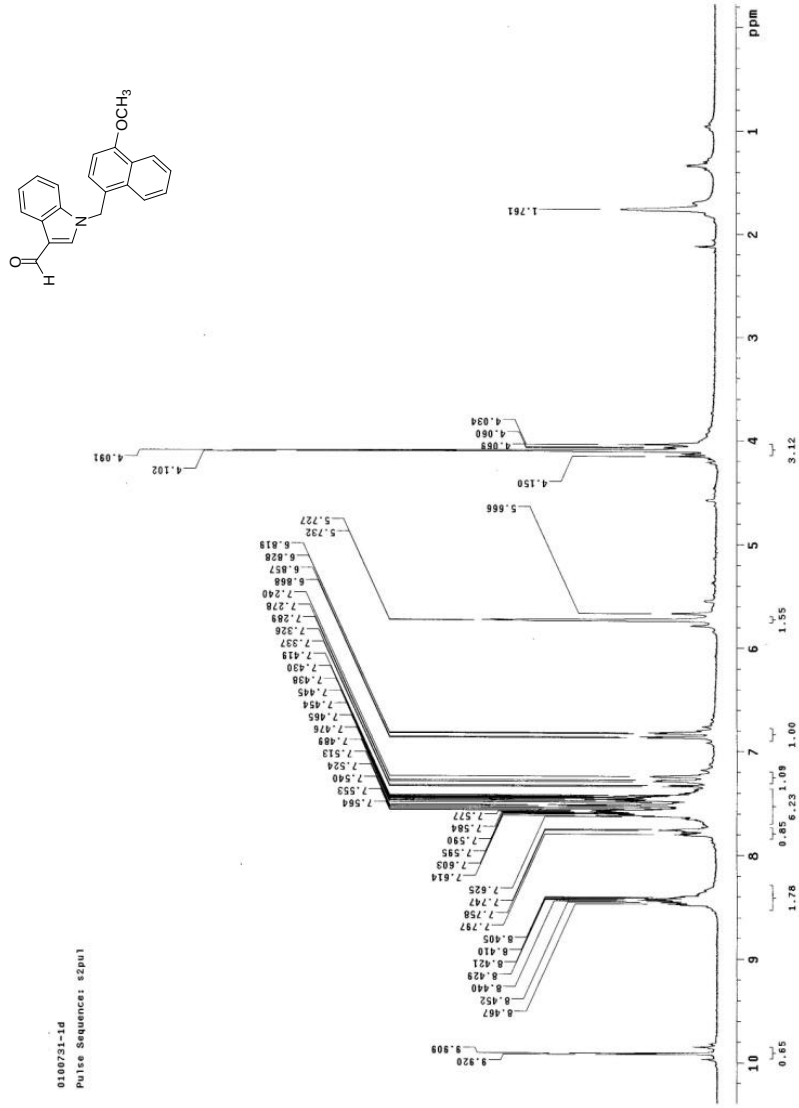

1-((4-bromonaphthalen-1-yl)methyl)-1H-indole-3-carbaldehyde **(II-4n)**

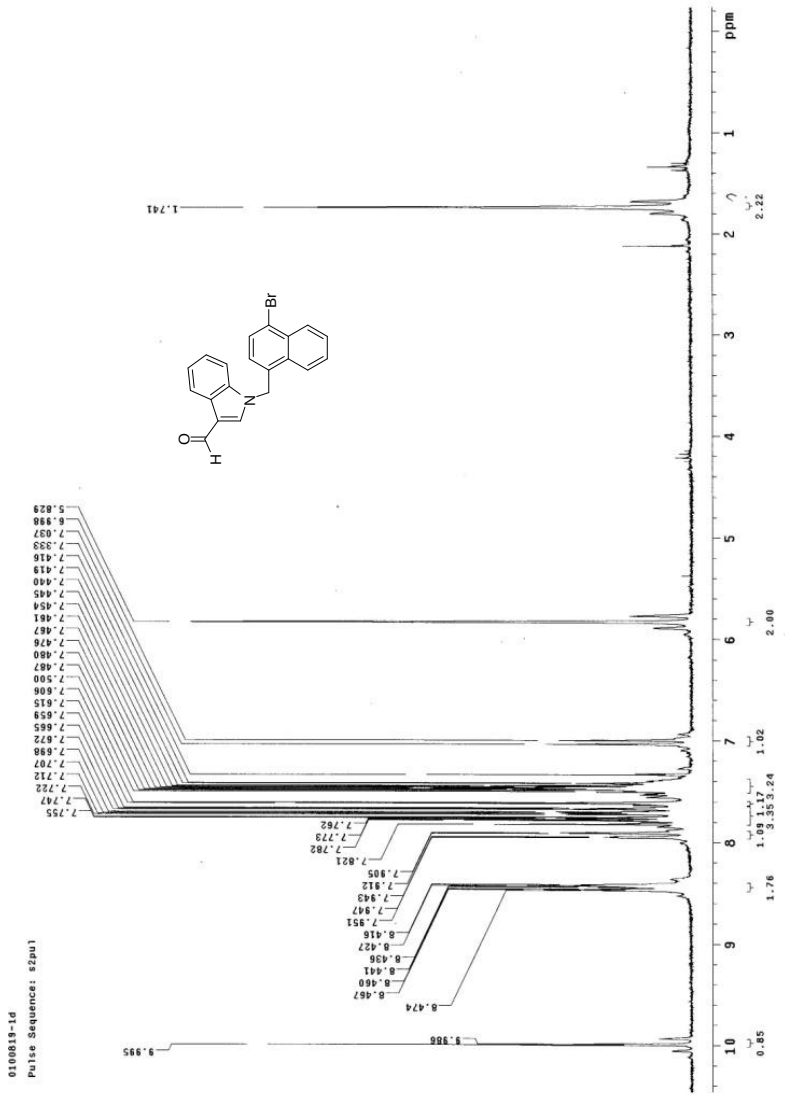

1-(naphthalen-2-ylmethyl)-1H-indole-3-carbaldehyde **(II-4o)**

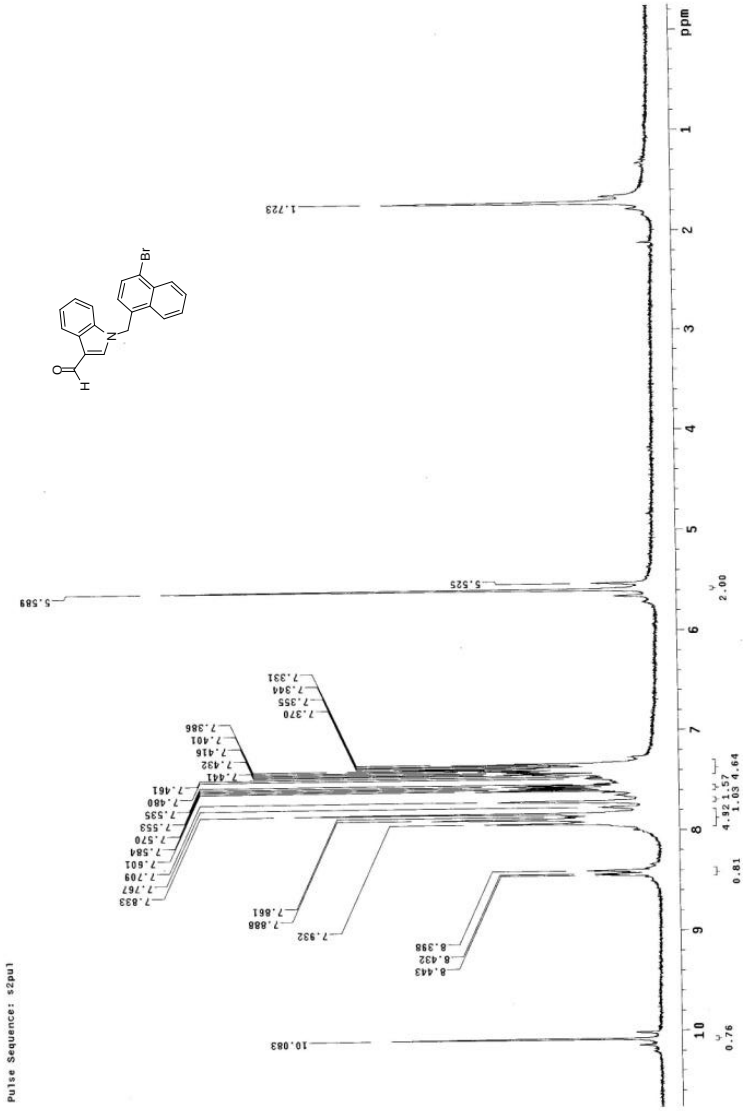

1-(4-methoxybenzyl)-1H-indole-3-carbaldehyde **(II-4p)**

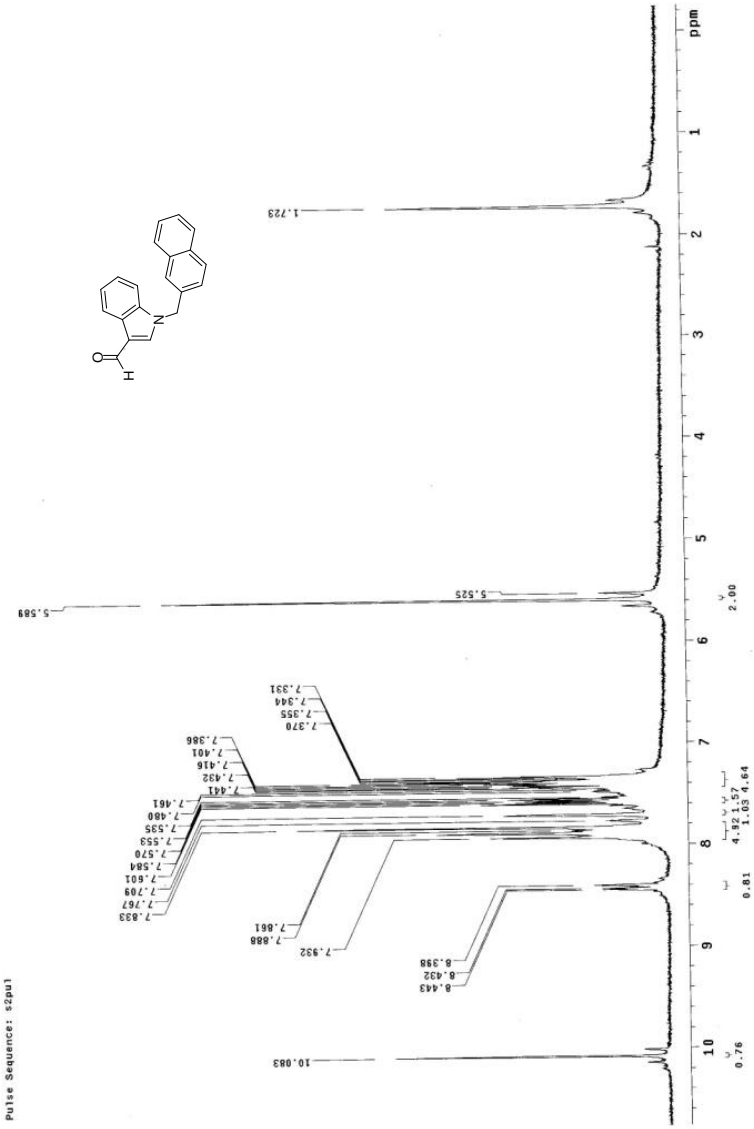

APPENDIX D. ^{1}H NMR of Disubstituted Barbituratic acid Derivatives

(DMSO-d6, 400 MHz)

(Z)-5-((1-(naphthalen-1-ylmethyl)-1H-indol-3-yl)methylene)-1 phenylpyrimidine-2,4,6(1H,3H,5H)-trione **(II-5a)**

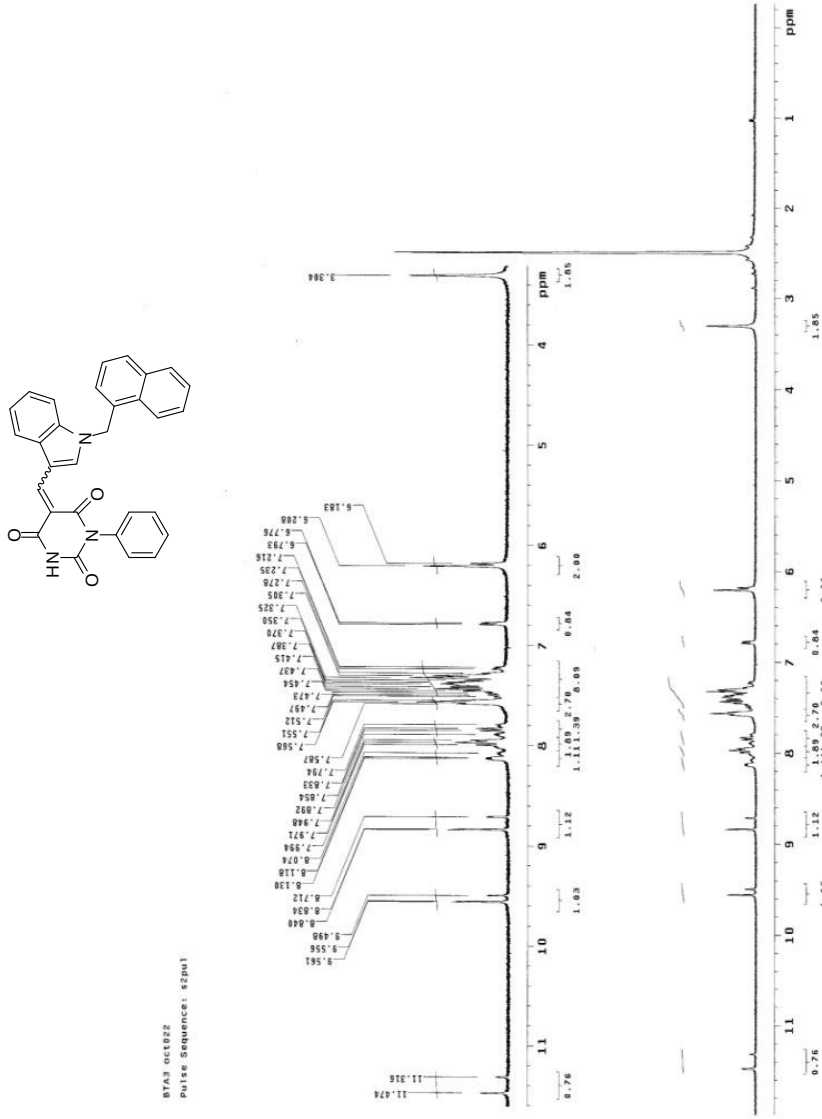

(Z)-5-((1-benzyl-1H-indol-3-yl)methylene)-1-phenylpyrimidine-2,4,6(1H,3H,5H)-trione **(II-5b)**

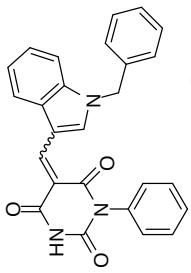

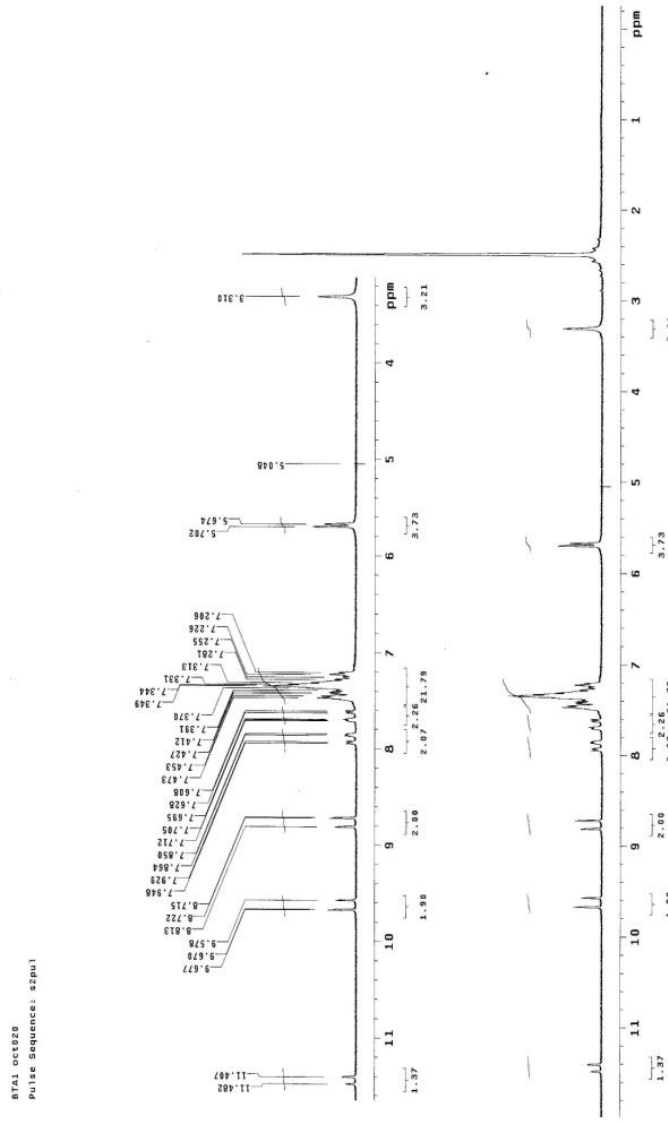

(Z)-5-((1-(4-chlorobenzyl)-1H-indol-3-yl)methylene)-1-phenylpyrimidine-2,4,6(1H,3H,5H)-trione **(II-5c)**

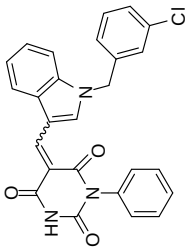

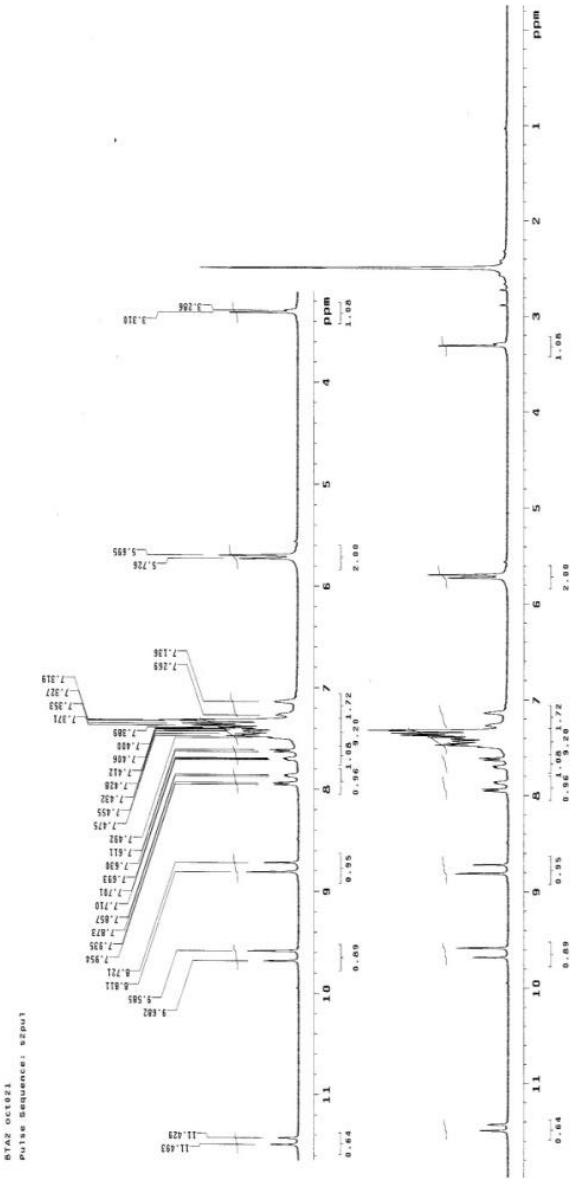

(Z)-5-((1-((4-methoxynaphthalen-1-yl)methyl)-1H-inden-3-yl)methylene)-1-phenylpyrimidine-2,4,6(1H,3H,5H)-trione **(II-5d)**

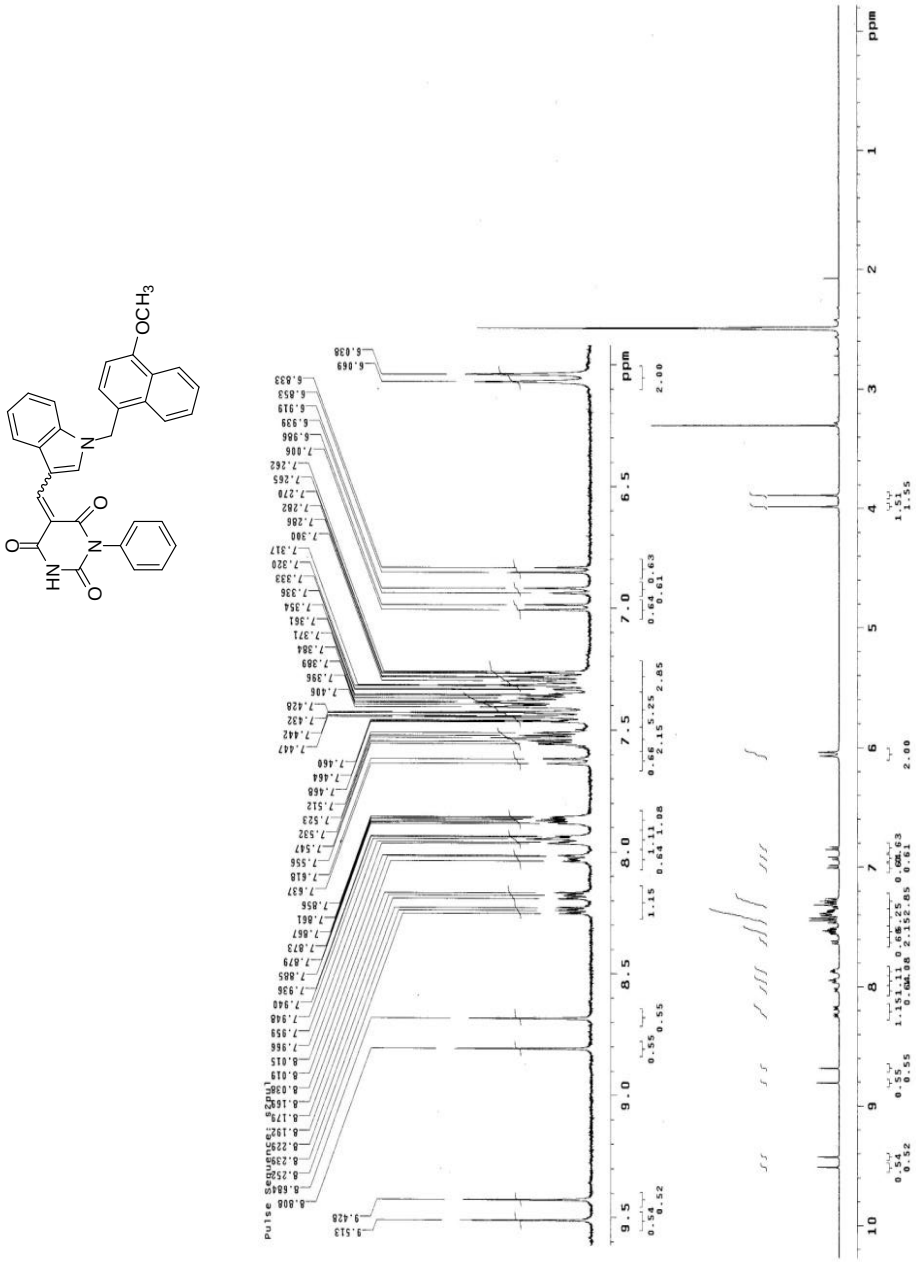

(Z)-5-((1-((4-bromonaphthalen-1-yl)methyl)-1H-inden-3-yl)methylene)-1-phenylpyrimidine-2,4,6(1H,3H,5H)-trione **(II-5e)**

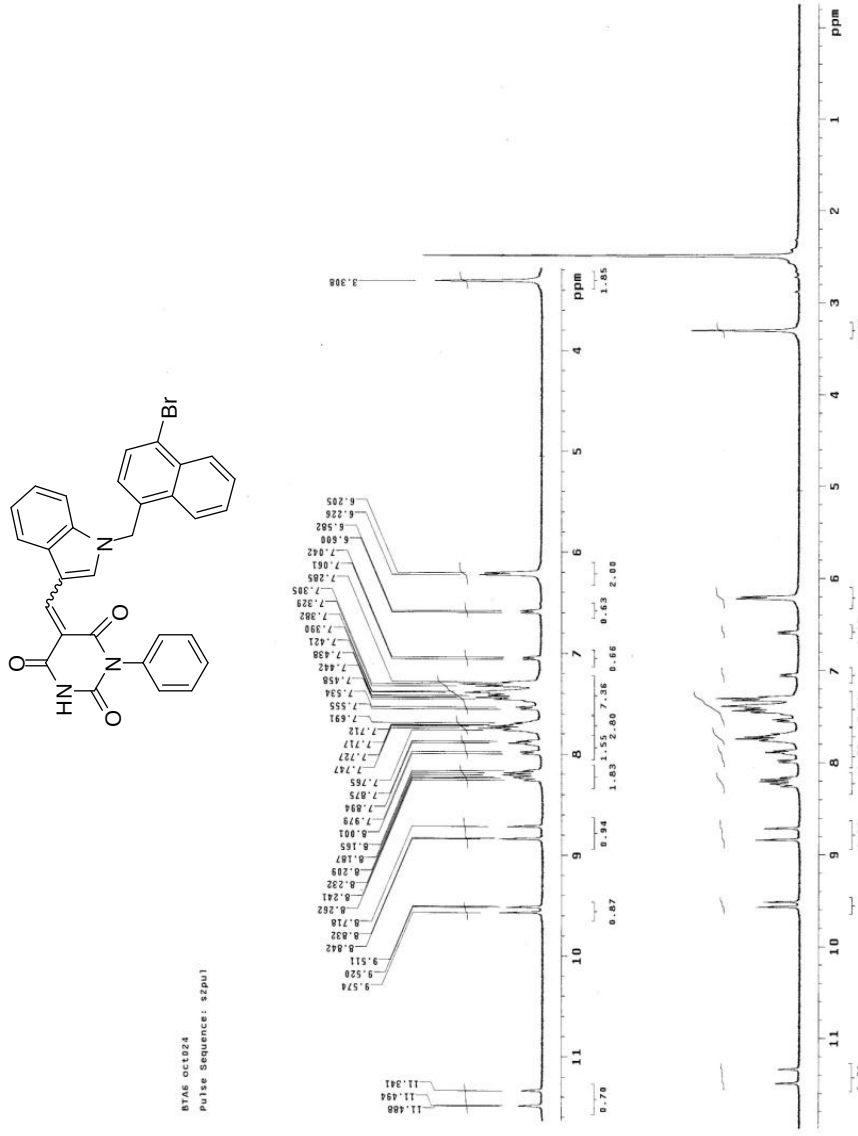

(Z)-5-((1-(naphthalen-2-ylmethyl)-1H-indol-3-yl)methylene)-1-phenylpyrimidine-2,4,6(1H,3H,5H)-trione **(II-5f)**

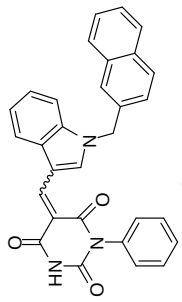

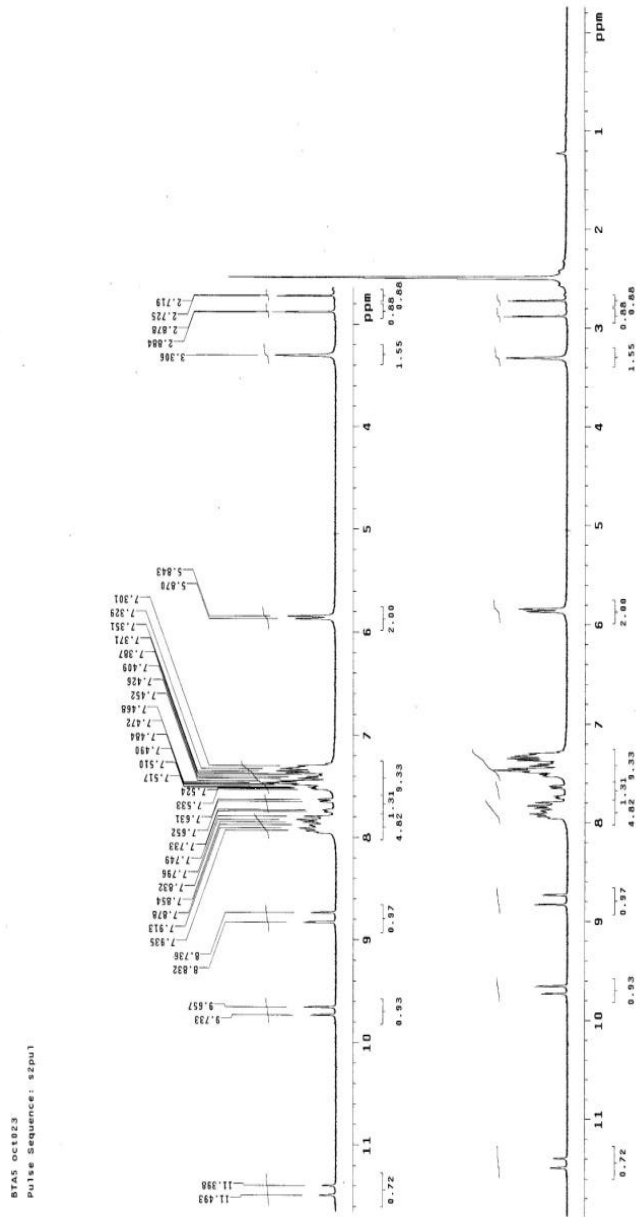

(Z)-5-((1-(4-methoxybenzyl)-1H-indol-3-yl)methylene)-1-phenylpyrimidine-2,4,6(1H,3H,5H)-trione **(II-5g)**

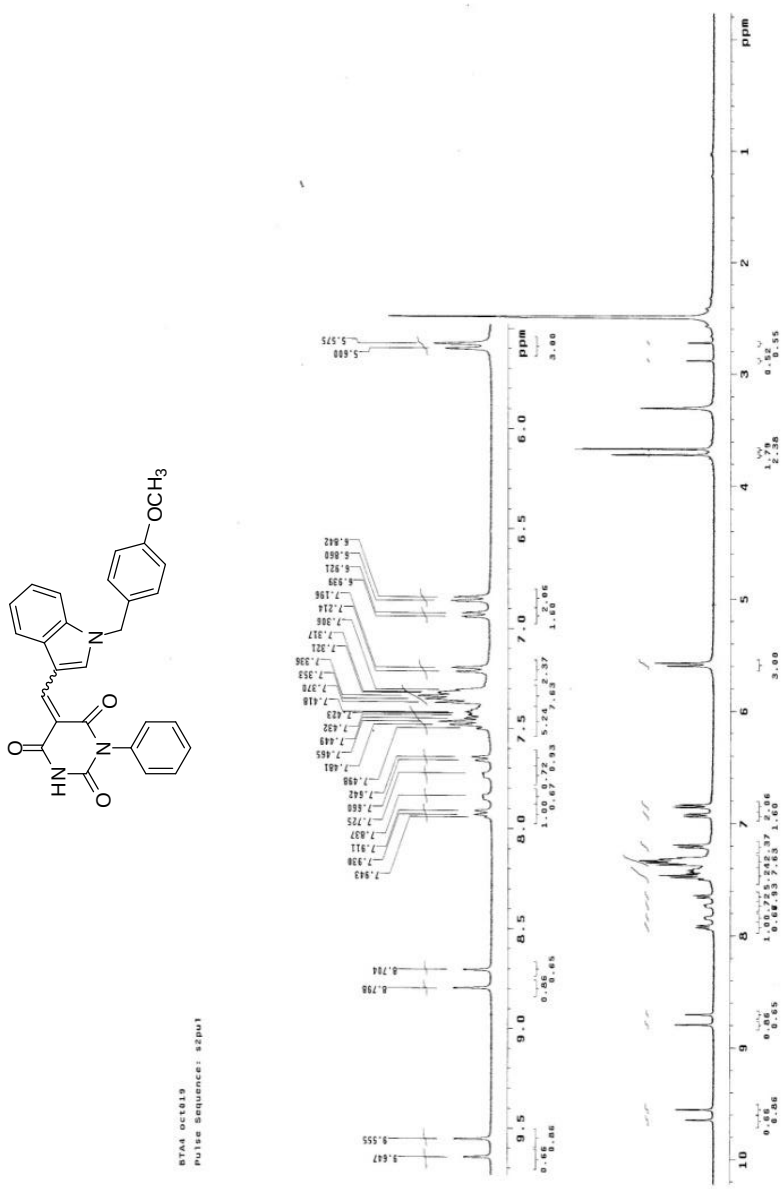

(Z)-1-(4-methoxyphenyl)-5-((1-(naphthalen-1-ylmethyl)-1H-indol-3-yl)methylene)pyrimidine-2,4,6(1H,3H,5H)-trione **(II-5h)**

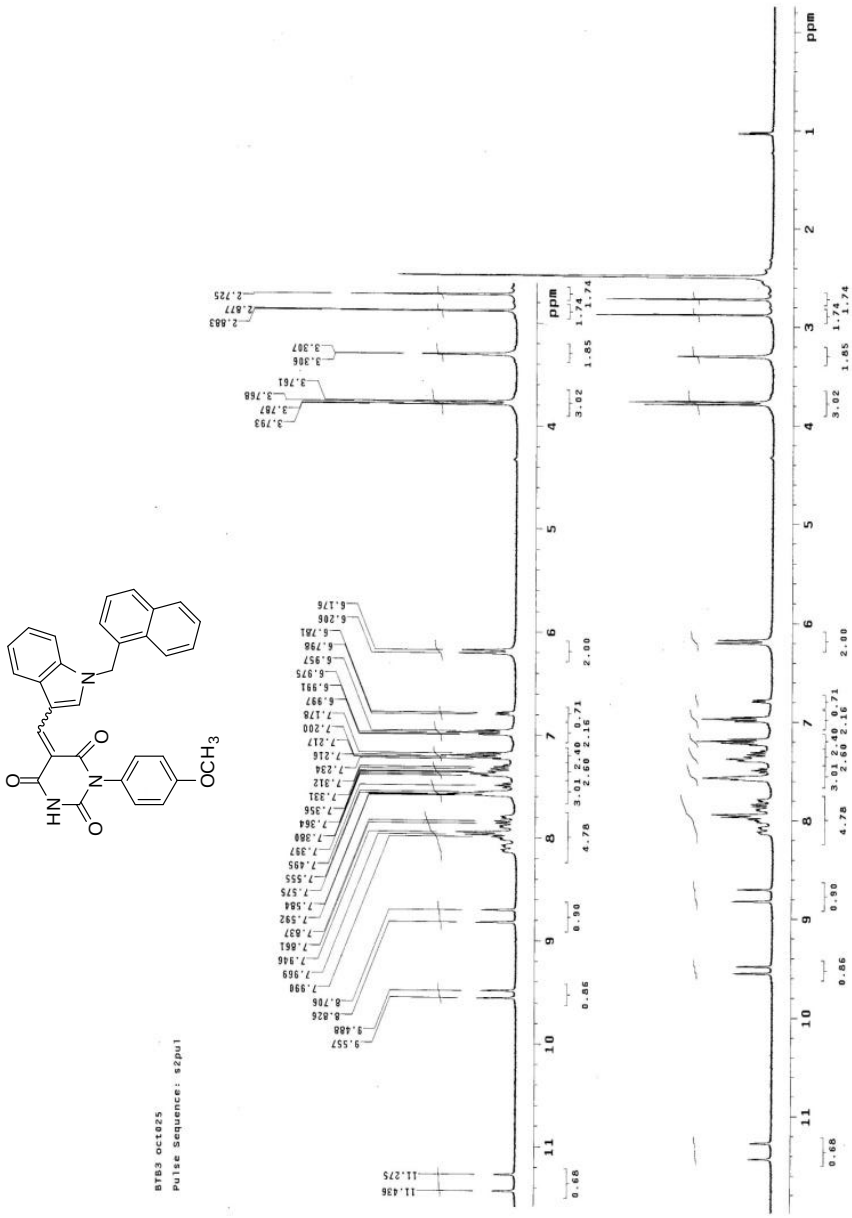

(Z)-5-((1-(naphthalen-1-ylmethyl)-1H-indol-3-yl)methylene)-1-(3-nitrophenyl)pyrimidine-2,4,6(1H,3H,5H)-trione **(II-5i)**

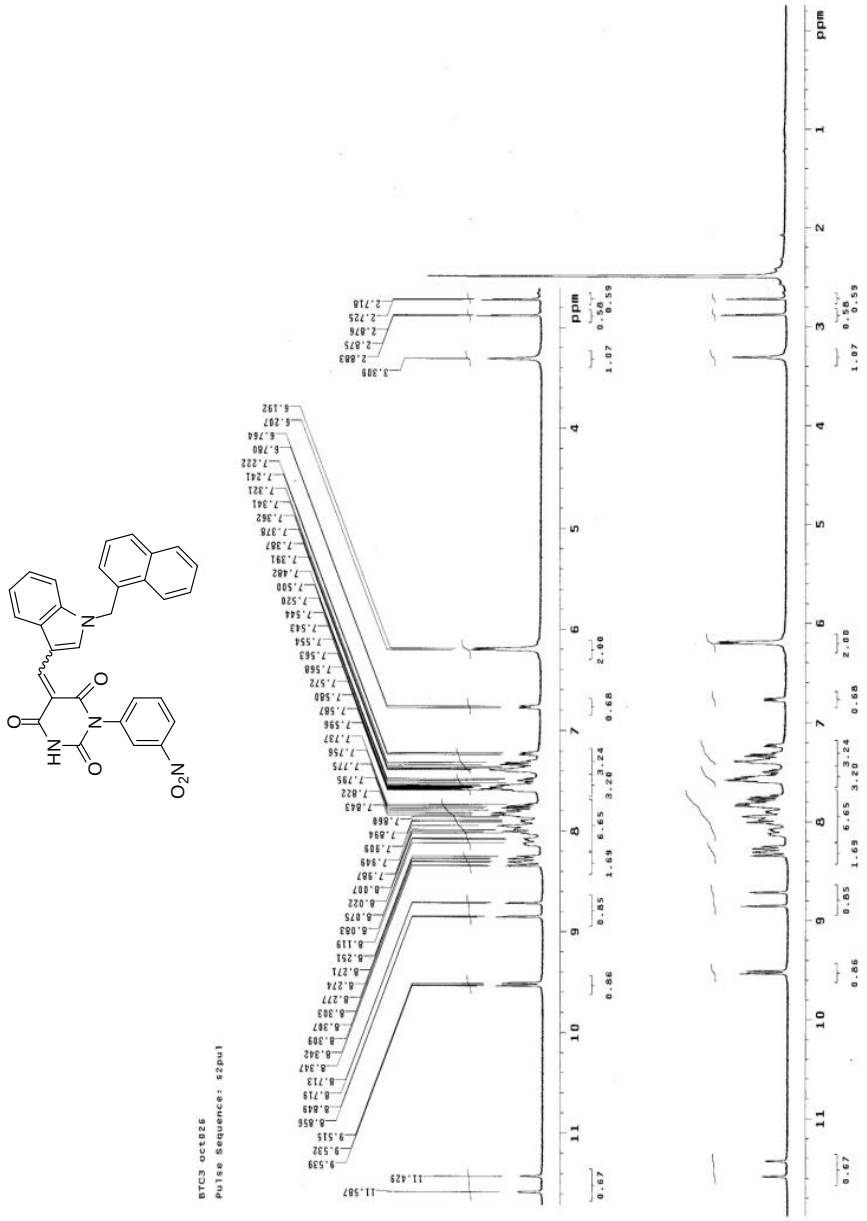

(Z)-1-(3-chlorophenyl)-5-((1-(naphthalen-1-ylmethyl)-1H-indol-3-yl)methylene)pyrimidine-2,4,6(1H,3H,5H)-trione **(II-5j)**

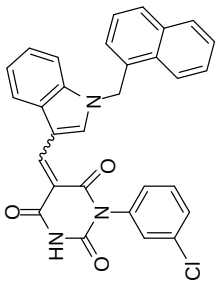

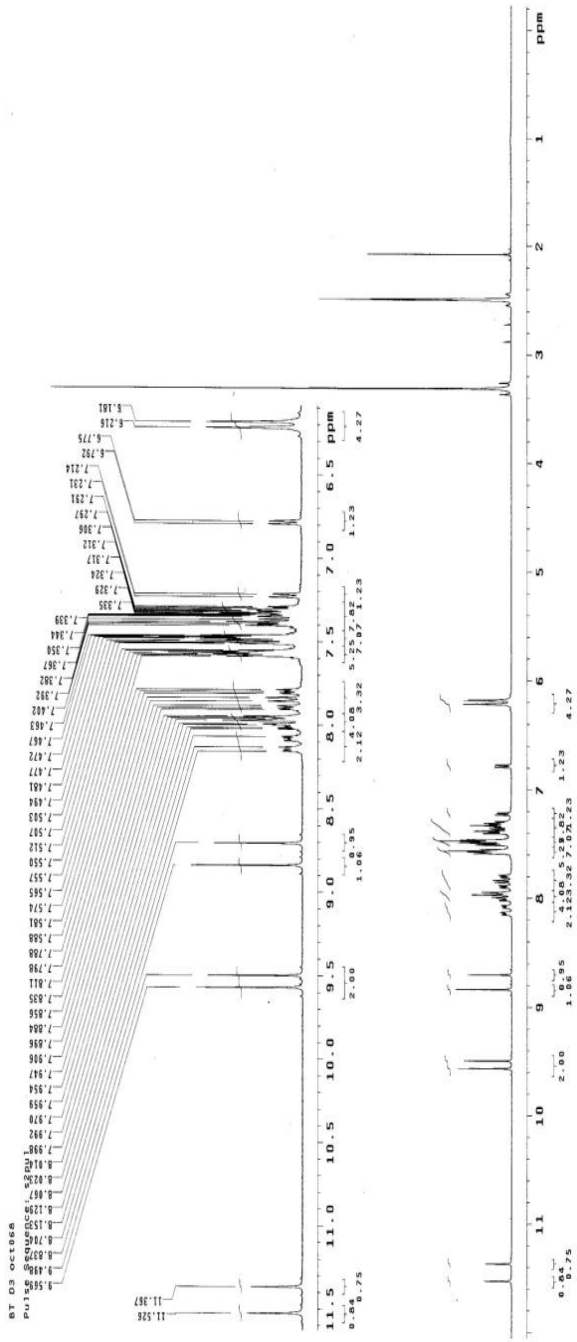

(Z)-5-((1-(naphthalen-1-ylmethyl)-1H-indol-3-yl)methylene)-1-(3-(trifluoromethyl)phenyl)pyrimidine-2,4,6(1H,3H,5H)-trione **(II-5k)**

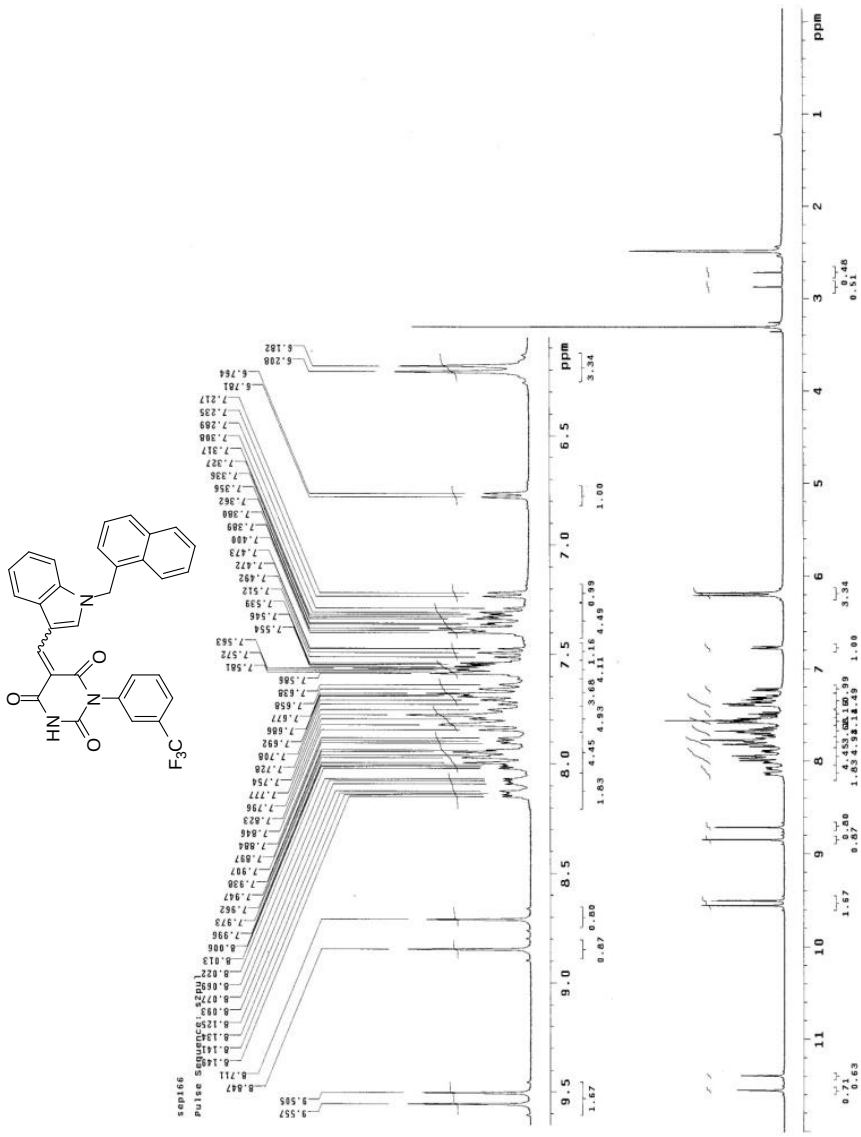

(Z)-1-(4-fluorophenyl)-5-((1-(naphthalen-1-ylmethyl)-1H-indol-3-yl)methylene)pyrimidine-2,4,6(1H,3H,5H)-trione **(II-5l)**

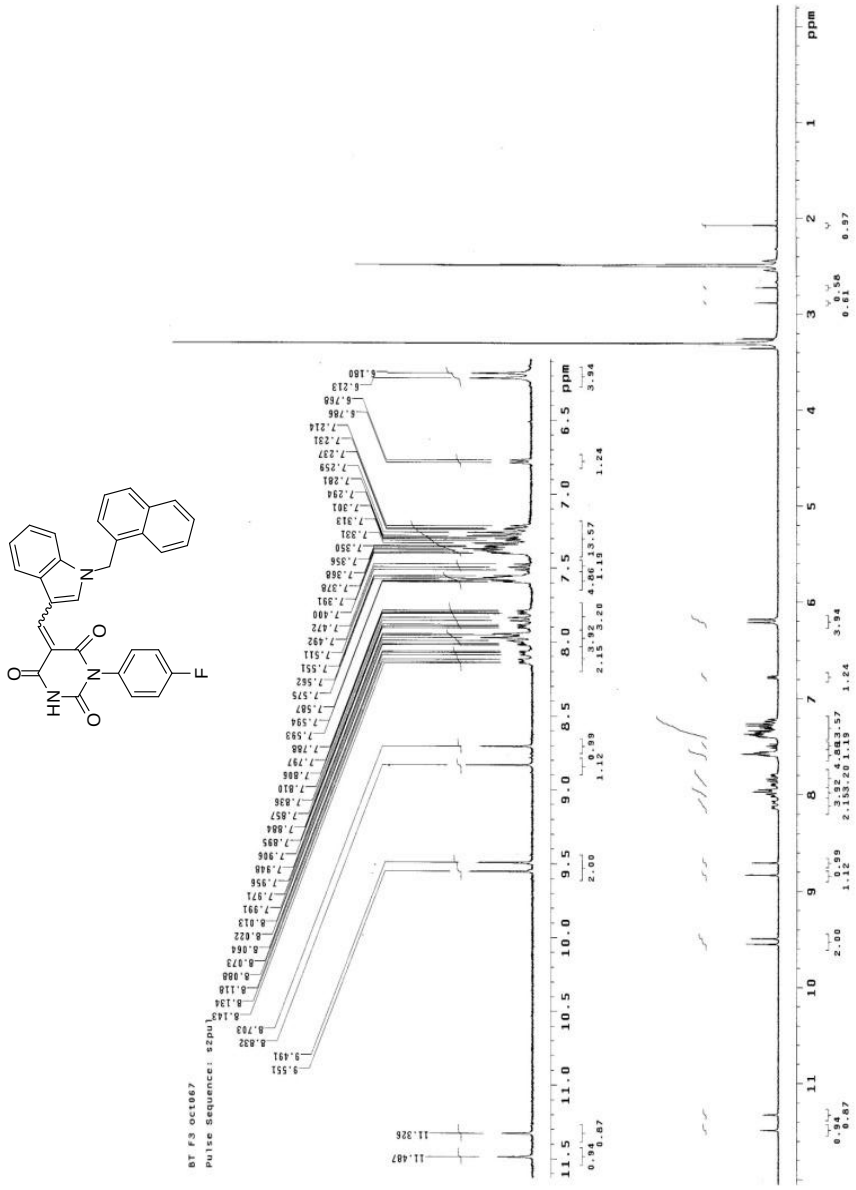

(Z)-1-(3-methoxyphenyl)-5-((1-(naphthalen-1-ylmethyl)-1H-indol-3-yl)methylene)pyrimidine-2,4,6(1H,3H,5H)-trione **(II-5m)**

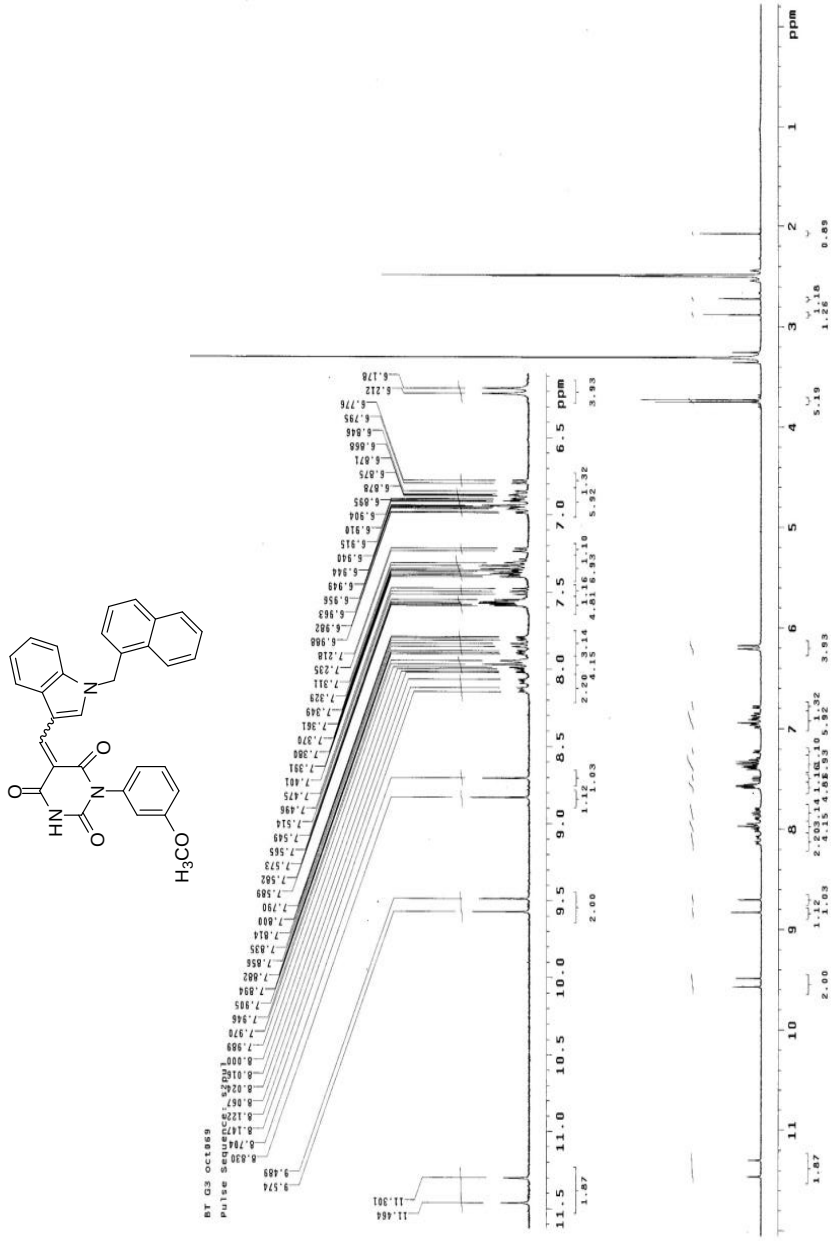

(Z)-1-(4-(4-chlorophenoxy)phenyl)-5-((1-(naphthalen-1-ylmethyl)-1H-indol-3-yl)methylene)pyrimidine-2,4,6(1H,3H,5H)-trione **(II-5n)**

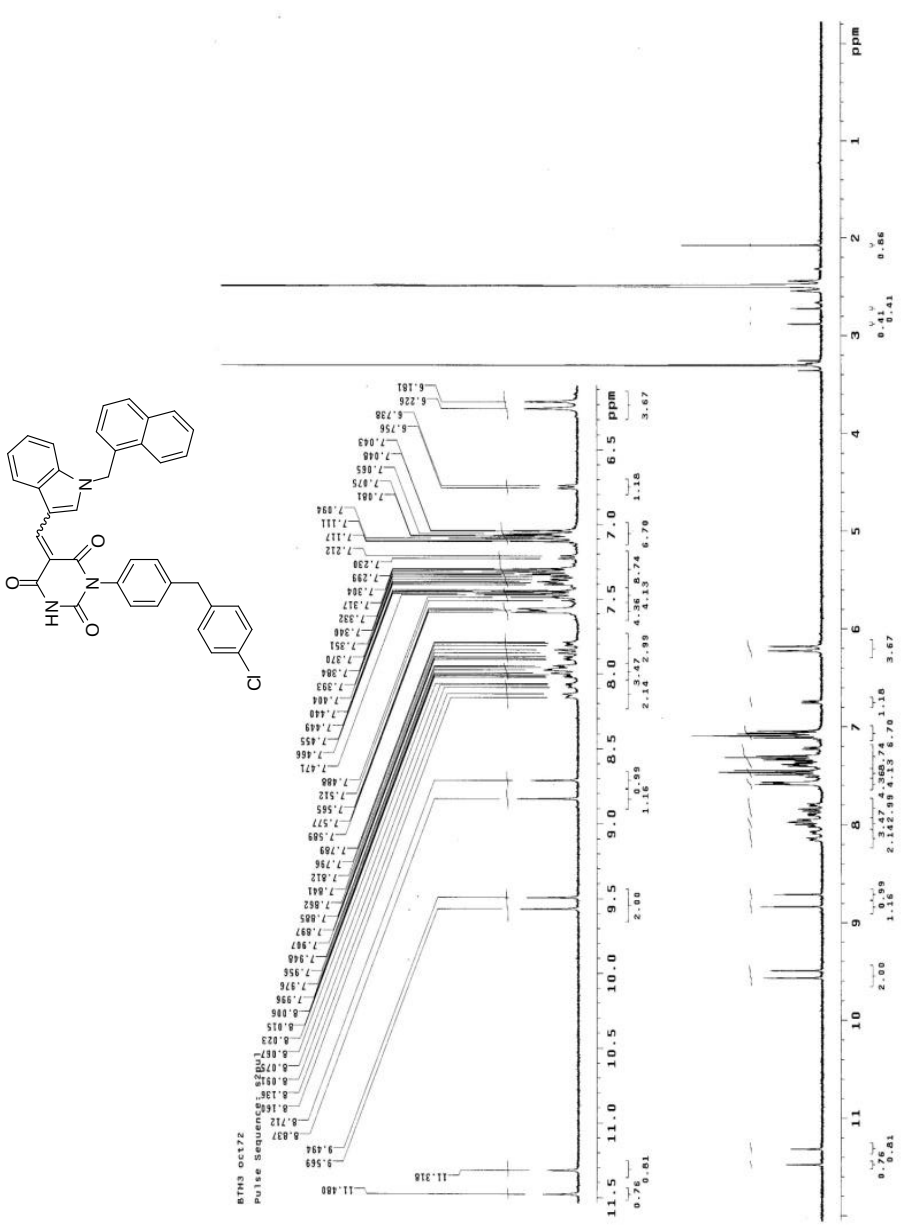

(Z)-1-(3,5-bis(trifluoromethyl)phenyl)-5-((1-(naphthalen-1-ylmethyl)-1H-indol-3-yl)methylene)pyrimidine-2,4,6(1H,3H,5H)-trione **(II-5o)**

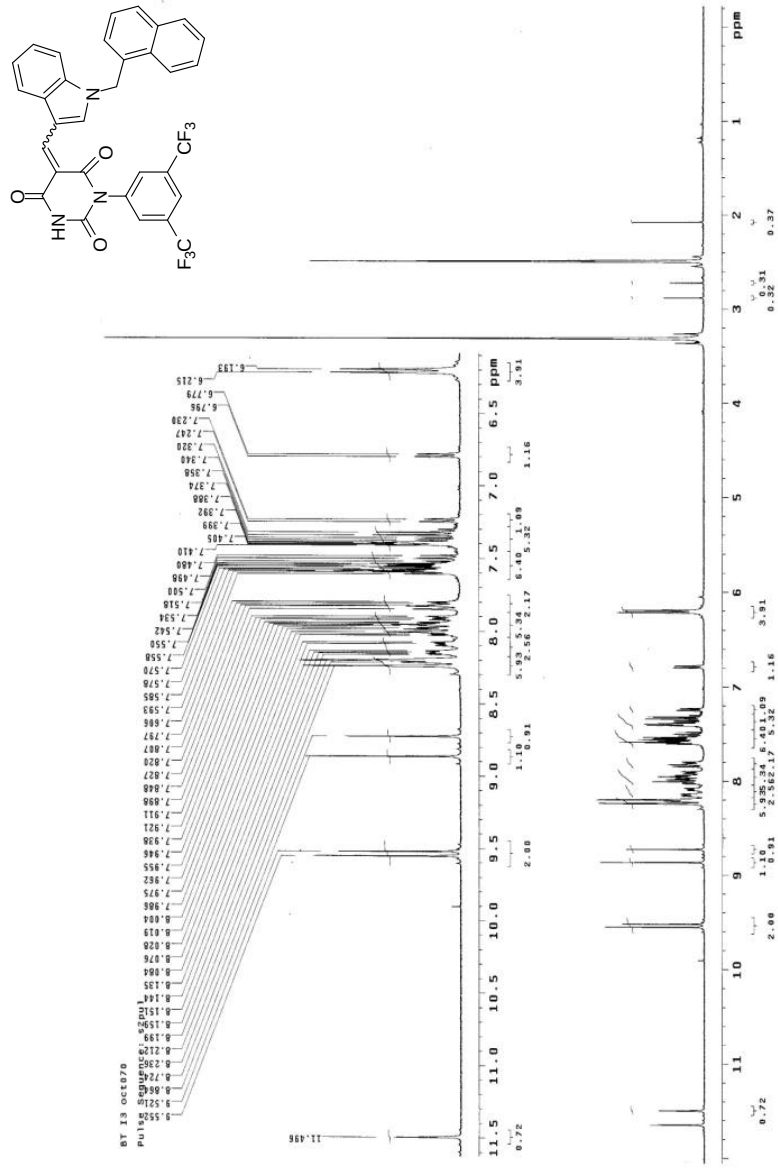

Appendix E. ^{1}H NMR of Napthyl derivatives

(4-methoxynaphthalen-1-yl)methanol **(II-6)**

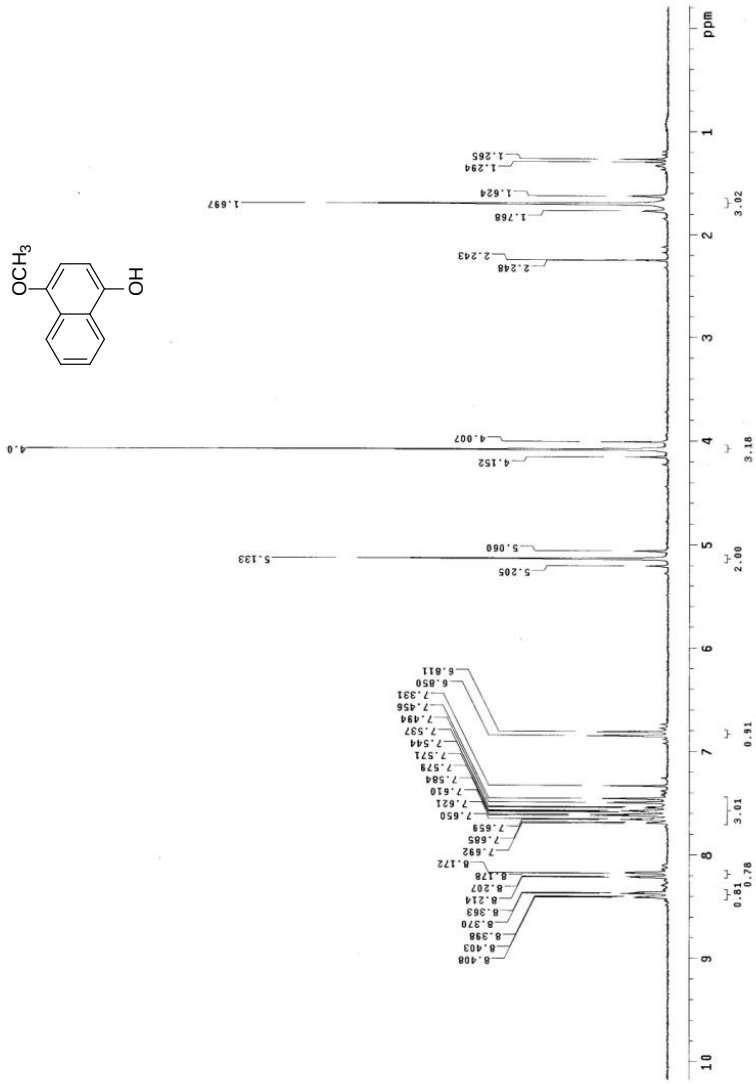

1-(bromomethyl)-4-methoxynaphthalene **(II-7)**

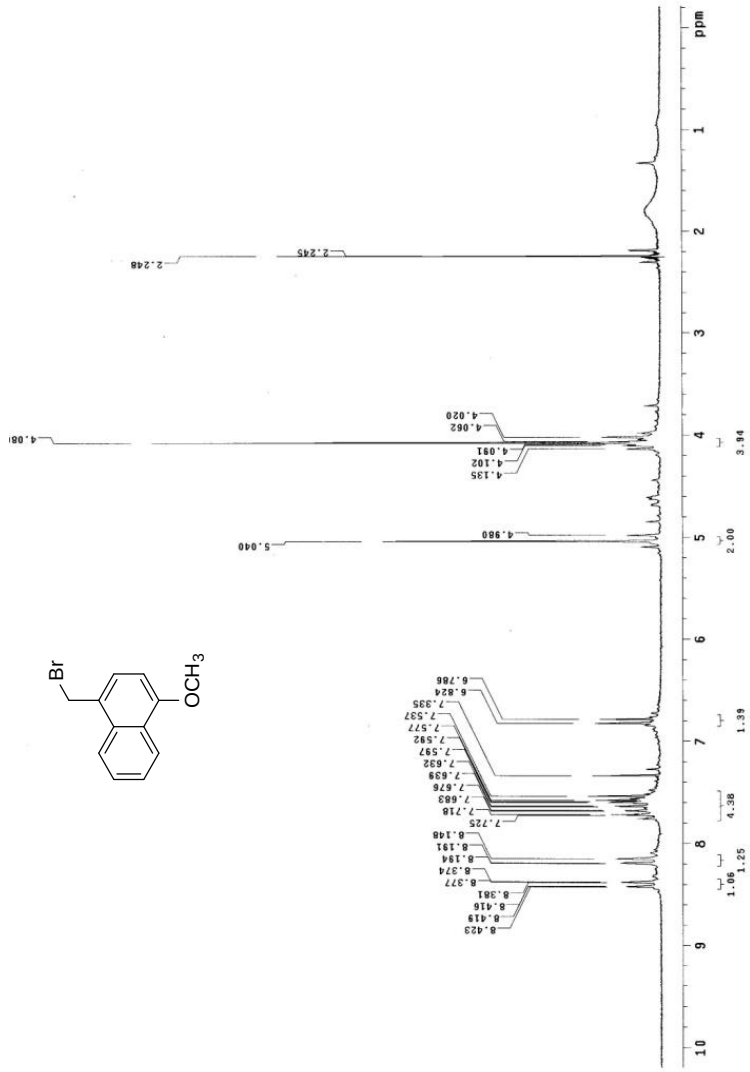

1-bromo-4-(bromomethyl)naphthalene **(II-8)**